

Zeitschrift: IABSE reports = Rapports AIPC = IVBH Berichte
Band: 59 (1990)

Rubrik: Theme D: Inspection and maintenance

Nutzungsbedingungen

Die ETH-Bibliothek ist die Anbieterin der digitalisierten Zeitschriften auf E-Periodica. Sie besitzt keine Urheberrechte an den Zeitschriften und ist nicht verantwortlich für deren Inhalte. Die Rechte liegen in der Regel bei den Herausgebern beziehungsweise den externen Rechteinhabern. Das Veröffentlichen von Bildern in Print- und Online-Publikationen sowie auf Social Media-Kanälen oder Webseiten ist nur mit vorheriger Genehmigung der Rechteinhaber erlaubt. [Mehr erfahren](#)

Conditions d'utilisation

L'ETH Library est le fournisseur des revues numérisées. Elle ne détient aucun droit d'auteur sur les revues et n'est pas responsable de leur contenu. En règle générale, les droits sont détenus par les éditeurs ou les détenteurs de droits externes. La reproduction d'images dans des publications imprimées ou en ligne ainsi que sur des canaux de médias sociaux ou des sites web n'est autorisée qu'avec l'accord préalable des détenteurs des droits. [En savoir plus](#)

Terms of use

The ETH Library is the provider of the digitised journals. It does not own any copyrights to the journals and is not responsible for their content. The rights usually lie with the publishers or the external rights holders. Publishing images in print and online publications, as well as on social media channels or websites, is only permitted with the prior consent of the rights holders. [Find out more](#)

Download PDF: 24.12.2025

ETH-Bibliothek Zürich, E-Periodica, <https://www.e-periodica.ch>



THEME D

Inspection and Maintenance

Inspection et maintenance

Überwachung und Unterhaltung

Leere Seite
Blank page
Page vide

Fatigue Crack Detection and Repair of Steel Bridge Structures

Détection de fissures de fatigue et réparation des structures de ponts en acier

Entdeckung von Ermüdungsrissen und Reparaturen an Stahlbrücken

John W. FISHER

Director
ATLSS, Lehigh Univ.
Bethlehem, PA, USA

Dr. Fisher, who is Director of the NSF ERC for Advanced Technology for Large Structural Systems, received his degrees from Washington University in St. Louis and Lehigh University. He was a Visiting Professor at the Swiss Federal Institute Lausanne in 1982 and was awarded Doctor Honoris Causa degree by EPFL in 1988. He is a member of the National Academy of Engineering.

Craig C. MENZEMER

ATLSS Scholar
Lehigh University
Bethlehem, PA, USA

Craig Menzemer obtained a Bachelor of Science Degree and Master of Science Degree in Civil Engineering from Lehigh University. He has been involved in construction management, stress analysis, product design and testing. Currently, Craig is employed by Alcoa and is also studying for a Doctor of Philosophy in Civil Engineering.

Ben T. YEN

Professor of Civil Eng.
Lehigh University
Bethlehem, PA, USA

Dr. Yen is a graduate of the National Taiwan University and received his Master of Science and Doctor of Philosophy degrees from Lehigh University. He specializes in structural engineering in the area of fatigue and fracture strength of structures and connections; buckling, strength and behavior of plate and box girders and curved bridge members, and inspection and retrofitting of bridges and structures.

SUMMARY

Repair of fatigue damaged bridge components depends on the cause and size of the cracks. Methods include peening, hole drilling, increasing the unsupported length of the web at some connections, attaching additional components at these connections and others. Two examples are given. One is an elevated highway bridge, with cracks at connections of cross girders to columns of bents and at ends of longitudinal girders. The other is a riveted truss bridge where cracks developed at hangers.

RÉSUMÉ

La réparation des éléments de pont ayant subi un dommage de fatigue dépend de la cause et de la dimension des fissures. Des méthodes possibles parmi d'autres sont le martelage, le percement d'un trou, l'augmentation de la longueur des couvre-joints, ou l'adjonction d'éléments de liaison supplémentaires. Deux exemples sont présentés. L'un concerne un pont d'autoroute contenant des fissures au droit des liaisons entre les traverses et les appuis, ainsi qu'aux extrémités des poutres longitudinales. L'autre exemple traite d'un pont à treillis riveté dans lequel des fissures se sont développées dans les montants.

ZUSAMMENFASSUNG

Reparaturmöglichkeiten von ermüdungsbedingten Schäden an Brückenelementen sind abhängig von deren Ursachen und Grösse. Mögliche Methoden sind unter anderen Hämmern, Bohren von Löchern, Verlängerung von Laschen oder Anbringung zusätzlicher Verbindungselemente. Zwei Beispiele werden vorgestellt: Eines stammt von einer Hochstrasse bei der an den Verbindungsstellen der Querträger mit den Stützen und an den Enden der Längsträger Risse auftraten. Das zweite Beispiel behandelt die in den Ständern einer genieteten Fachwerkbrücke aufgetretenen Risse.



1.0 INTRODUCTION

Localized failures have continued to develop in steel bridge components due to fatigue crack propagation which in some instances, has led to brittle fracture [1,2]. A majority of the fatigue cracks can be placed into one of two categories. The single largest category is a result of out-of-plane distortion in small, unstiffened segments of web plates. When distortion-induced cracking develops in bridge members, large numbers of cracks develop nearly simultaneously in the structure as the cyclic stress is high and the number of cycles needed to produce cracking is relatively small. Displacement induced cracking has developed in a wide variety of structures including suspension, two girder floor beam, multiple beam, tied arch, and box girder bridges. In general, the cracks form parallel to the primary stress field and are not detrimental to the performance of the structure provided they are discovered and retrofitted before turning perpendicular to the applied stresses.

The second largest category of fatigue damaged members and components comprises large initial defects or cracks. Defects in this category usually resulted from poor quality welds produced before nondestructive test methods were firmly established. In addition, a number of localized failures in this category developed because the groove welded component was considered a secondary member or attachment. As a result, weld quality criteria were not established and nondestructive test methods were not employed. Other details develop fatigue damage because of geometry or fabrication practice.

A majority of the remaining failures resulted from the use of low strength details that were not anticipated to have such a low fatigue strength at the time of the original design because of the limited experimental database that specification provisions were based.

2.0 REPAIR OF FATIGUE DAMAGED COMPONENTS

Any methodology used to repair fatigue damaged details is case specific and is generally dependent on the size and location of the crack(s) at the time of repair [3]. Obviously, this is highly dependent on both the inspection procedures and the ability to locate relatively small cracks. Apart from displacement-induced cracks, the majority of fatigue cracking has resulted from low strength details, or large initial defects, or geometric conditions which simulate crack-like conditions. Figure 1 illustrates the role played by both the initial defect size and stress concentration in the determination of the relative fatigue strength of various detail categories [4].

Various methods to retrofit or increase the fatigue resistance of welded details have been employed [5]. For cracks which have propagated from normal, in-plane design stress fields, peening can be a successful repair as long as the crack depth does not exceed the depth of the beneficial compressive residual stresses which result from the peening operation [6]. Laboratory studies have shown that a fatigue crack of up to 3 mm in cover-plated details can be arrested by peening provided the stress range does not exceed 41 MPa. Also peening has been most successful when conducted under a low minimum tensile stress or dead load. Finally, peening has been found to be a reliable solution when performed in the field and has been carried out on a number of detail types.

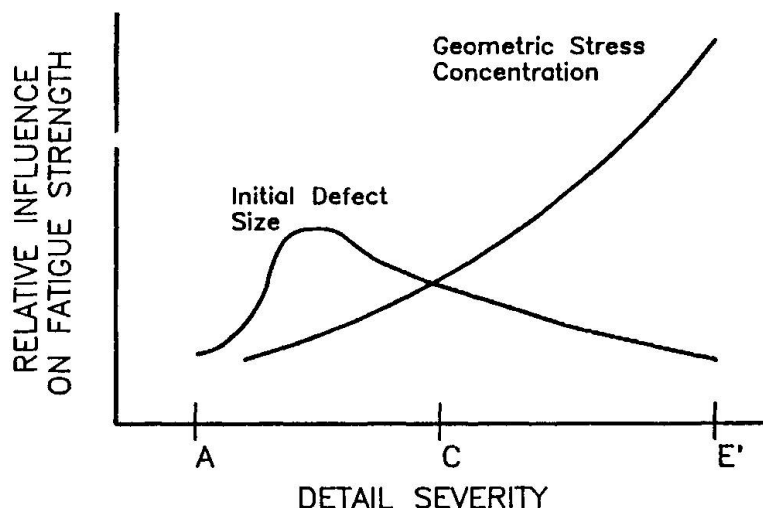


Fig. 1 Relationship Between Fatigue Strength, Detail Type and Defects

In situations where the crack has grown away from the influence of the stress concentration and is a through thickness crack, it may be successfully retrofitted with holes drilled at the crack tip [7]. Holes essentially blunt the tip of the crack, although they must be sized so as to satisfy

$$\Delta K / \sqrt{\rho} \leq A \sqrt{\sigma_y}$$

where ΔK = stress intensity range
 ρ = radius of the hole
 σ_y = yield stress of the steel
 A^y = coefficient - 10.5 for σ_y in MPa

The validity of this repair has been studied in the laboratory on full scale welded beams subjected to constant stress range cycle and variable amplitude loading up to 90 million cycles.

Distortion induced cracking may also be retrofitted by drilling holes, although laboratory tests have shown this to be ineffective when there are high levels of distortion [8]. For multiple girder structures, most displacement induced cracking occurs in the web gap region at the end of connection plates in the negative moment region [8]. Lengthening the web gap may be effective provided that the magnitude of the out-of-plane distortion does not increase as a result of reduced detail stiffness. The most effective, and by far most costly, eliminates the distortion through positive attachment of the connection plate to the girder flange.

In situations where extensive fatigue cracking has occurred, the only reliable technique is to provide a bolted splice or connection across the damaged area.

3.0 I-93 CENTRAL ARTERY

The Central Artery carries traffic through Boston, Massachusetts and surrounding communities. A viaduct structure, located in the Artery's northern area, consists of bilevel rigid steel frame bents which support a two girder floor-beam stringer system on each level. Columns of the rigid bents have box section while transverse beams have either box or I sections (Fig. 2). I-beam



to column connections contain closure plates fillet welded to the edges of the I section and column flanges (Fig. 3). Webs of the I beams are groove welded to the columns while beam flanges (both box and I) and box beam webs of the lower portion of the bents are connected via full penetration groove welds with back-up bars (Fig. 4).

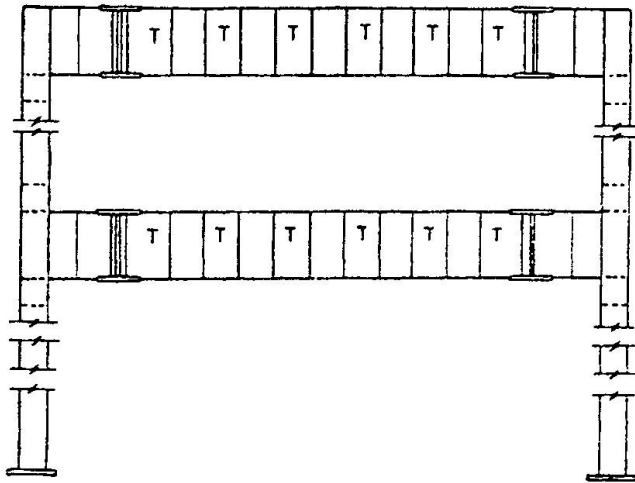


Fig. 2 Typical Bent Elevation

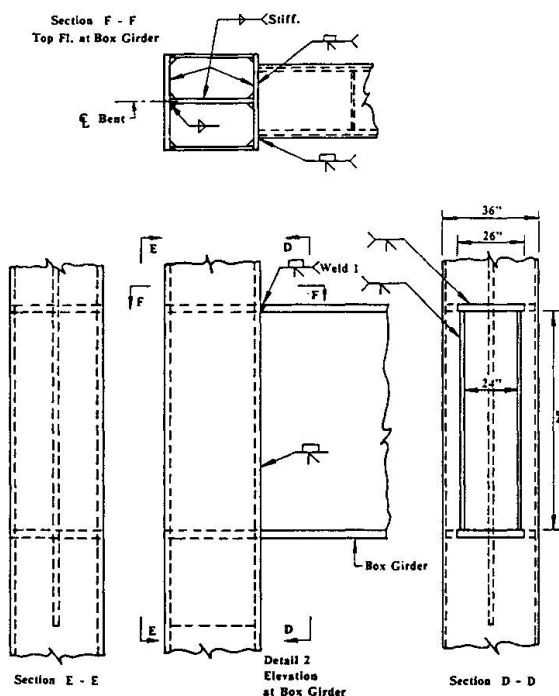


Fig. 4 Representative Box Beam to Column Connection

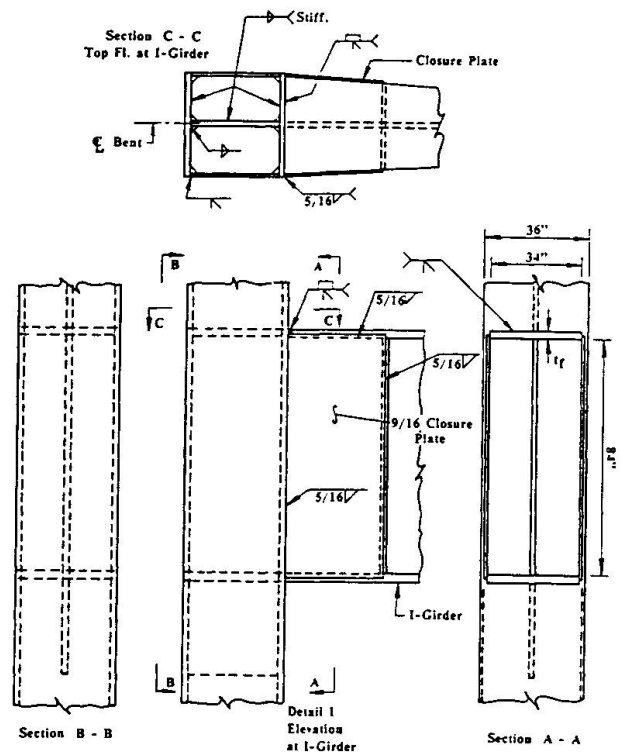


Fig. 3 Representative I-Beam to Column Connection

Beam flanges of the upper portion of the bent are continuous into the column. Cope openings in the box beam webs at the beam column connection points are covered with small plates which are fillet welded to the box beam webs [2].

For each of the two girder floorbeam systems, longitudinal girders and stringers form composite action with the reinforced concrete decks. Both top and bottom flanges of the longitudinal girders are coped by flame cutting to permit a bolted, double angle web connection with transverse beams of the bent. The connection angles are fitted to the top and bottom flanges of the transverse beams.

3.1 Inspection Results

Inspection of the structure revealed several areas which contained fatigue cracks. In addition, lateral displacement of several longitudinal girder bottom flanges was also observed. Fatigue cracks were found along the longitudinal girder web to flange weld at the flange terminations and vertical cracks were observed in the longitudinal girder webs at the reentrant corner of the bottom copes (Fig. 5). Cracking was occasionally observed along the bolt fixity line of the connection angles (Fig. 6).



Fig. 5 Vertical and Horizontal Fatigue Cracks at Bottom Web Cope

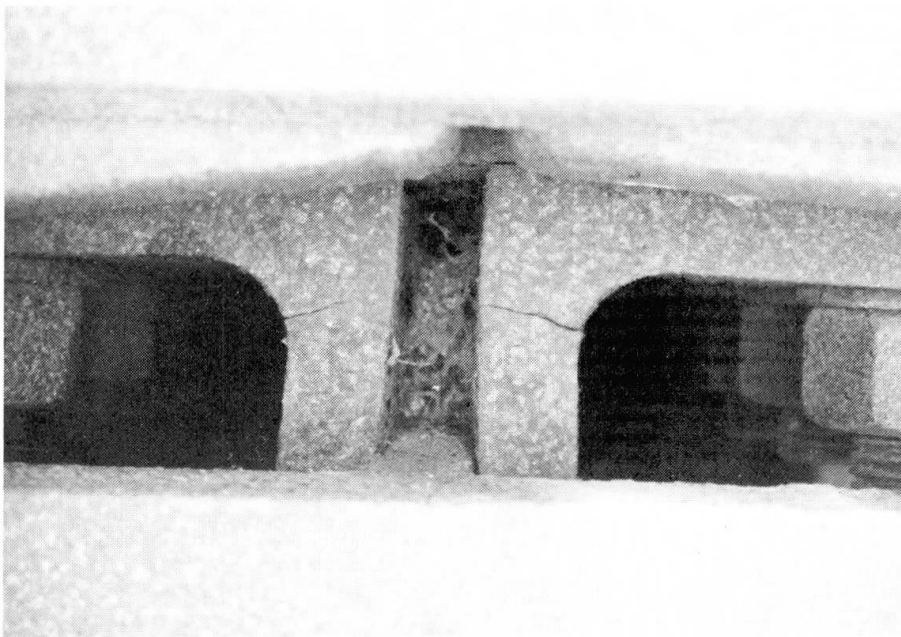


Fig. 6 Cross-Sectional View of Angle with Fatigue Cracks



Figure 7 shows cracks which extended several inches along the bottom end of the angle fillet, between the girder web and the transverse beam of the bents. The cracks were found only at locations where the longitudinal girder web was bolted full depth to the connection angles. Other locations where the girder web was not bolted full depth exhibited no evidence of cracking (Fig. 8).

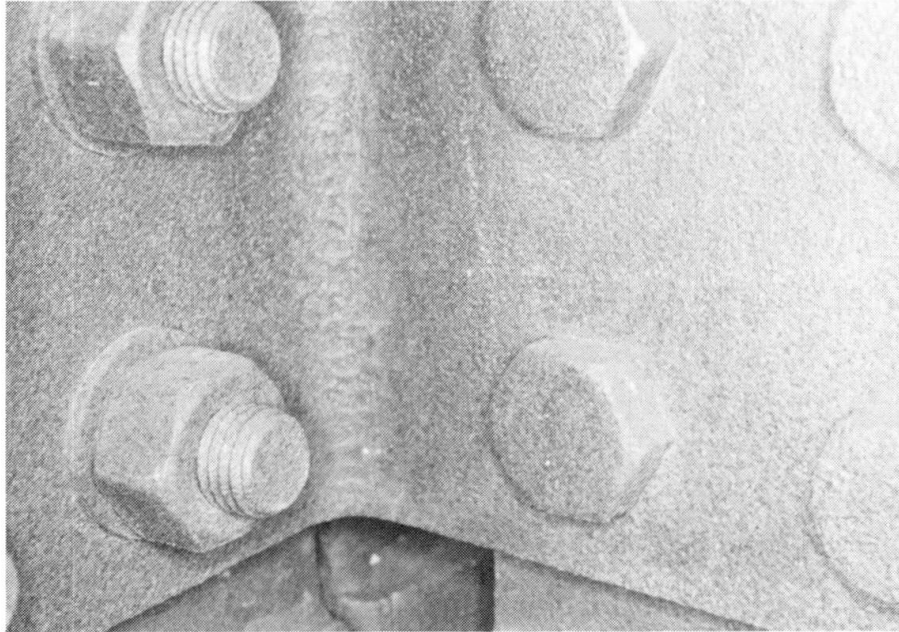


Fig. 7 Fatigue Crack in Longitudinal Girder-Beam (Bent) Angle Connection

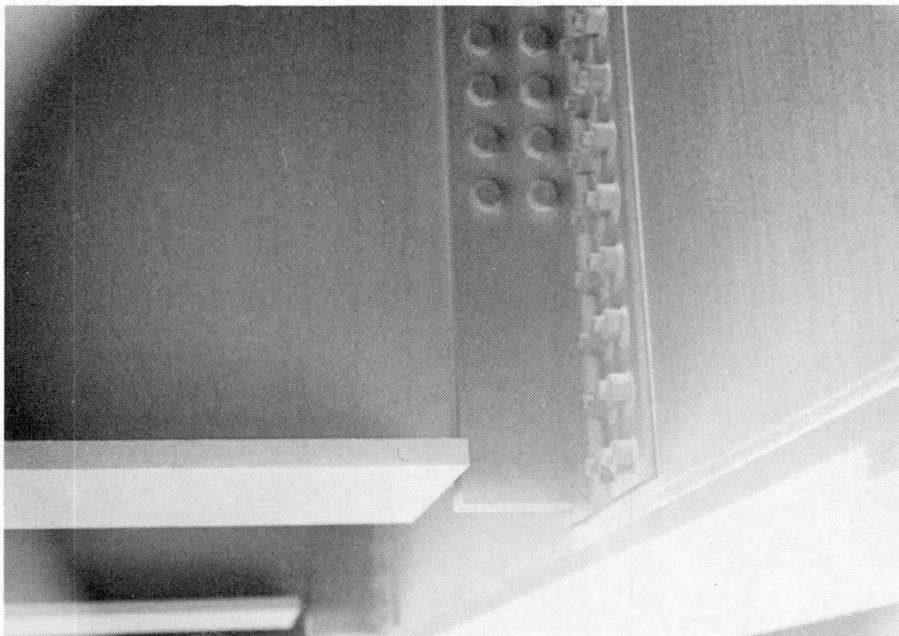


Fig. 8 Longitudinal Girder Not Bolted Full Depth to the Connection Angles

Inspection of the rigid frame bents revealed cracks in the fillet welds at several corner joints where transverse I-beam closure plates were jointed to the bent column flange. Grinding the fillet weld throat in the cracked corner region of the closure plates exposed the crack which had extended into the

groove weld connecting the top flange of transverse beam to the column. Further grinding exposed the crack which extended from the back-up bar halfway through the groove weld thickness. Other bents revealed cracks at the web cope closure plates of the transverse box beam (Fig. 9). Grinding the fillet weld throat into the beam flange exposed cracks extending from the back-up bar into the groove weld thickness.



Fig. 9 Cracks at the Cope Closure Plates of a Box Beam

3.2 Probable Causes of Failure

Coping by flame cutting the longitudinal girder and floorbeam webs resulted in high tensile residual stresses along the cut edge as well as at reentrant corner. In addition, coping greatly reduced the section modulus for in-plane bending and left an unstiffened segment of girder web between the flange terminations and the bolt fixity line of the longitudinal girders. At locations where the longitudinal girders were not bolted full depth to the connection angles, the girder web could rotate in plane without developing significant compressive forces in the lower portion of the girder. This resulted in no bottom flange lateral displacement, no web gap distortion, and no fatigue cracking in the web cope or connection angles. In locations where the girder was bolted full depth to the connection angles of the transverse beam, connection restraint resulted in lateral displacement of the bottom flange and web gap distortion from the compressive stresses in the web. Hence, fatigue cracks along the bottom edges of the connection angles were all displacement induced.

Connection geometry at the corner joints of the bent transverse beams produced a fabricated lack-of-fusion defect perpendicular to the primary stress field. Large initial defects and cracks are low fatigue resistant details, and with field measured stress range values exceeding the Category E fatigue limit of 31 MPa, crack growth would be expected. Measured differences in stress range between corners on the same transverse beam flange were observed and attributed to biaxial bending. Biaxial bending resulted from a combination of the vertical loading and longitudinal reaction and braking forces. Current design provisions do not take account of the longitudinal forces when evaluating fatigue resistance in these bent structures.



3.3 Recommended Retrofits

Retrofits recommended for fatigue cracking in the longitudinal girders included the drilling of holes to blunt the crack tips. Further retrofit was required to prevent the lateral displacement of the bottom flange and minimize web gap distortion. Otherwise, fatigue crack reinitiation from the retrofit holes and continued crack propagation along the bolt fixity line would result. Several rows of bolts were removed from the girder to transverse beam connection to reduce the compression in the web and help move the flange toward normal alignment. Angles were then bolted to the inside longitudinal girder web and flange and to the connection angle to prevent lateral motion of the bottom flange (Fig. 10) and to provide greater resistance to the end restraint.

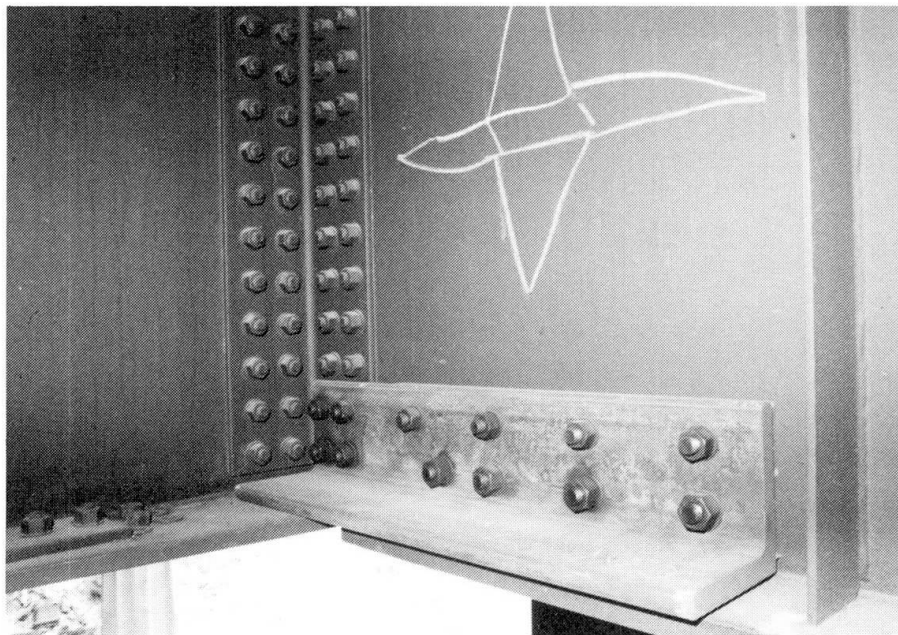


Fig. 10 Retrofit of a Longitudinal Girder Bottom Web Gap

Transfer of the live load forces from the beam top flange to the bent column had to be assured for an effective retrofit of the beam column connection of the bent. Short sections of wide flange shapes were modified by partial removal of the web and were bolted to the top flange of the lower beam and webs of the column (Fig. 11). If the fatigue cracks in the groove welds continued to propagate and eventually led to fracture of the top beam flange to column connection, the live load forces would be transferred via the bolted splice. In addition, the reinforcement provided more resistance to the longitudinal forces.

4.0 I-95 OVER THE SUSQUEHANNA RIVER

I-95 crosses the Susquehanna River in Maryland. The structure is a multiple span deck truss bridge whose members are either built-up riveted construction or rolled structural shapes. Transverse floorbeams and longitudinal stringers of the floor system are composite with the reinforced concrete deck. All of the floorbeams are supported by the top chord of the main deck trusses (Fig. 12). Suspended truss spans contain pin and hanger assemblies which consist of riveted box sections [2].

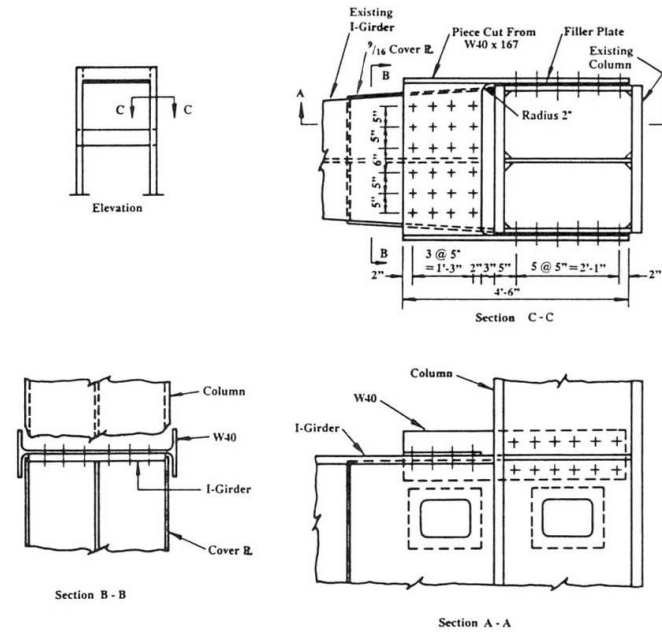


Fig. 11 Retrofit for an I Section Beam Column Connection

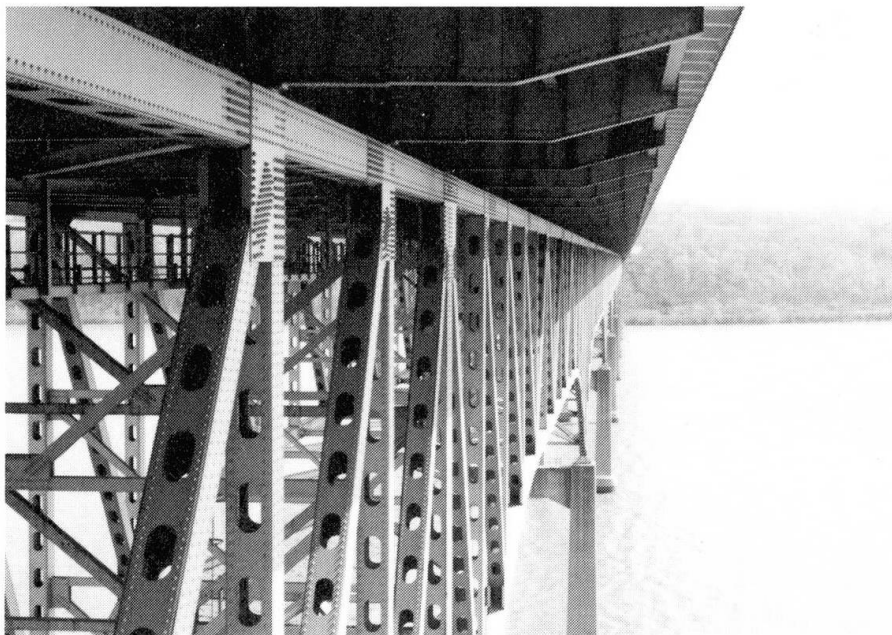


Fig. 12 Truss System of the Susquehanna River Bridge

4.1 Inspection Results and Field Measurements

Inspections of the structure revealed fatigue cracks emanating from the rivet holes in several hanger box sections (Fig. 13). In addition to the fatigue cracks, significant amounts of corrosion product was found between the corner angles and both web and flange plates of the hanger sections (Fig. 13). Environmental corrosion was also found between the gusset and hanger plate as well as on the gusset at the elevation of the pin connection (Fig. 14).

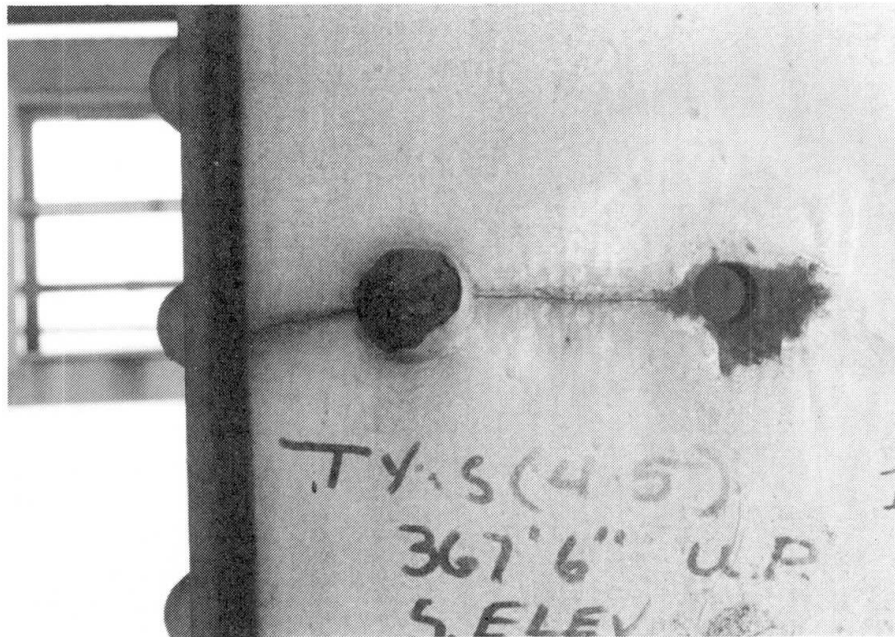


Fig. 13 Corrosion Between a Hanger Flange Plate and Interior Connection Angle and Web Crack from Rivet Hole

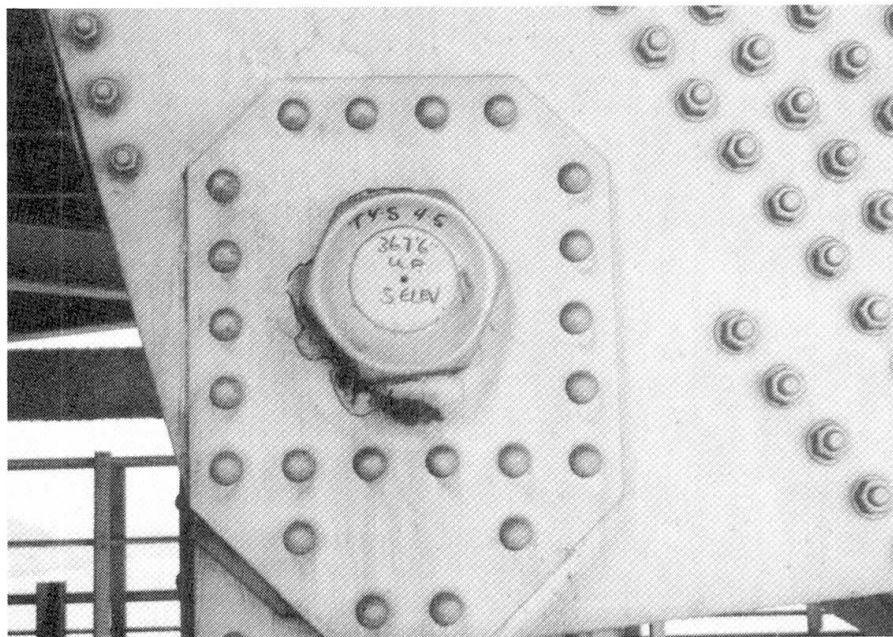


Fig. 14 Corrosion at Upper Pin

Several sets of field measurements were made on the structure between 1985 and 1987. Initial strain measurements were conducted on a single cracked hanger. Under normal traffic, small tension stress cycles developed in all the gages mounted on the hanger, with typical cyclic stress values of 10 MPa. In addition to the small tension cycles, both low level vibration of the hanger, and bending of the hanger web were observed. Unusual large dynamic responses periodically occurred in all gages mounted on the hanger and were on the order of the yield point (~ 250 MPa).

A subsequent set of field measurements were made after pins of the originally examined hanger were lubricated. For comparison, several other hangers were instrumented. At locations where pins had been lubricated, both the bending of the hanger webs and the large dynamic responses were minimized. Cracked hanger locations with the lubricated assemblies experienced a maximum stress range of 35 MPa. In contrast, unlubricated pin assemblies had hangers which experienced significant axial and bending stresses. Typical values varied up to 76 MPa.

Final field measurements were conducted after all pin assemblies had been lubricated. A maximum stress range of 30 MPa was observed for the original cracked hanger web while a cyclic stress of 55 MPa was recorded for a cracked hanger flange plate in a second location where only one of two pins was lubricated.

4.2 Probable Causes of Failure and Recommended Retrofits

The hanger connections are located directly below open roadway expansion joints which allows salt, water, and debris to fall and collect on the pin and hangers, thereby assisting and accelerating the corrosion process. Field inspections and strain measurements demonstrated that the development of corrosion caused pin restraint which, in turn, led to bending in the hangers. When the bending moment at the hanger joint was high enough to overcome the restraint, sudden release of the pin connection produced the dynamic action. Lubrication of the pins was effective in minimizing hanger bending and dynamic effects by reducing pin restraint and as such, was recommended as a routine maintenance practice. A longer term correction will require the redesign of the pin connection as well as effective control of water and debris by the elimination of open expansion joints.

Cracked hanger plates were temporarily retrofitted by the drilling of holes to blunt the crack tips. For the cracked hanger flange plates, the maximum measured stress range of 55 MPa exceeded the fatigue limit of 48 MPa for riveted members. Fatigue crack propagation is expected to continue in the flange plates. As a result, twice a year inspection of the hangers will be required, until the eventual replacement of the damaged hangers.

5.0 CONCLUSIONS

As replacement costs for highway bridges are often prohibitive, it is desirable to repair and retrofit existing structures to maximize the benefit from limited funds. A majority of fatigue damaged details can be repaired by drilling holes, weld toe peening, or bolting splices over damaged areas to strengthen the connection. In some instances, welding can be used, though care should be exercised so that low fatigue resistant details do not result. Once corrosion is identified as a problem, extensive repairs are often required. Development of corrosion monitors or sensors would greatly assist evaluation and monitoring in difficult to inspect areas of bridges to aid in the inspection and maintenance process.

Examination of the causes of fatigue cracking and corrosion, coupled with implementation of new design tools, code revisions, and effective technology transfer will help to minimize future structural deficiency problems. Simple, realistic models and analysis procedures for member interaction and connection



behavior are needed to reduce the occurrence of distortion induced fatigue problems. Identification of low fatigue resistant details and effective methods for detail classification would ease the burden on designers and limit the incidence of fatigue cracking.

REFERENCES

1. FISHER, J. W., *Fatigue and Fracture in Steel Bridges*, Wiley-Interscience, 1984.
2. FISHER, J. W., DEMERS, C., *A Survey of Localized Cracking in Steel Bridges 1981 to 1988*, Lehigh University, ATLSS Report No.89-01, 1989.
3. FISHER, J. W., PENSE, A. W., and YEN, B. T., *Retrofitting Fatigue Cracked Bridge Structures*, International Bridge Conference Proceedings, Pittsburgh, 1983.
4. Personal communication with Dr. Peter Keating, Texas A.& M.
5. FISHER, J. W., HAUSMANN, H., SULLIVAN, M. D., and PENSE, A. W., *Detection and Repair of Fatigue Damage in Welded Highway Bridges*, Transportation Research Board, NCHRP #206, 1979.
6. HAUSMANN, H., FISHER, J. W., and YEN, B. T., *Effect of Peening on Fatigue Life of Welded Details*, ASCE Proceedings, W. H. Munse Symposium on Behavior of Metal Structures - Research to Practice, 1983.
7. FISHER, J. W., BARTHELEMY, B. M., MERTZ, D. R., and EDINGER, J. A., *Fatigue Behavior of Full Scale Welded Bridge Attachments*, Transportation Research Board, NCHRP #227, 1980.
8. FISHER, J. W., and MERTZ, D. R., *Hundreds of Bridges - Thousands of Cracks*, ASCE - Civil Engineering, Vol. 5, No. 4, 1985.

Fatigue of Road Bridges

Résistance à la fatigue des ponts-routes

Ermüdungsfestigkeit von Strassenbrücken

Ferdinand TSCHEMMERNEGG

o. Univ. Prof.
University of Innsbruck
Innsbruck, Austria



Ferdinand Tschemmernegg, born 1939, received his doctoral degree at the technical University of Graz. He worked in the German steel industry and in South America in bridge building. Since 1980, he has been head of the Institute for Steel and Timber Structures at the University of Innsbruck, Austria.

SUMMARY

Fatigue load factors are derived from damage caused by fatigue and it is proposed that these factors should be described in terms of the number of load cycles for different details.

RÉSUMÉ

On montre de quelle façon les facteurs de charge de fatigue sont obtenus à partir des dommages en fatigue, et on propose que ces facteurs soient représentés en fonction du nombre de cycles de charge pour différents détails.

ZUSAMMENFASSUNG

Es wird gezeigt, wie aus Schadensfällen entsprechende Betriebslastfaktoren abgeleitet werden können. Ein Vorschlag wird gemacht, wie diese Faktoren für verschiedene Details je nach Anzahl der Lastwechsel gegliedert werden können.



1. PRELIMINARY REMARKS

Normally in road bridges a fatigue design is not necessary. But in the last years the volume of traffic grew very much and if at the same time the construction in view of fatigue is not well designed the fatigue problems come up in wind and torsional bracings, orthotropic plates (cross and longitudinal girders), transversal bracings and frames and expansion joints. If orthotropic plates are well designed there are no problems in fewer fatigues, but there are some problems today with the other secondary members. It is enjoyable that in the main structures of steel bridges no serious fatigue damages are known and damages in secondary members can be repaired relatively easy. From the known damages and damage analysis should be worked out systematically proposals for improving of the fatigue for this secondary members. In the following it will be tried to develop out of damages a simplified method for the fatigue design. At the present time because of lack of stress range spectras in the details because of lack of measurements the fatigue design according EC 3 [1] is very difficult.

2. STATE OF ART OF FATIGUE CODES IN AUSTRIA

In Austria at the time the fatigue design is regulated in Ö-Norm B 4600 part 3. The bases is the constant amplitude fatigue limit. In the meantime in Austria it was developed a new "guide line for fatigue design" [2] which follows the recommendations EKS-TC 6 and Eurocode 3. Parallel Austria is working on Ö-Norm B 4300 part 5, which also follows the european concept. With the guide line according [2] it is possible to use the european concept before the new Ö-Norm is ready. But the difficulty is, that if you use this concepts on the load side, realistic fatigue loads have to be known and here is a big lack. Using deterministic loads for fatigue designs is not allowed and in the road norms no load models are fixed for the fatigue loadings. In the Ö-Norm there is only the advice that the details should be constructive designed in a way that fatigue problems don't occure.

3. FATIGUE DESIGN FOR ROAD BRIDGES, ACCORDING EC 3

The EC 3 gives now a bases for fatigue design with variable amplitude design limit, but the results of such calculation are not controlled by measurements. It will be shown now which difficulties in applications of EC 3 concepts in road bridges occure, if the fatigue design for secondary members has to be done. In comparison to railway bridges the fatigue design of road bridges is more complicated because the trace is changing and so the affect of action is non linear to the action. Also much less measurements have to be done to road bridges in comparison to railway bridges. If you start the fatigue design according Eurocode, first the fatigue loading has to be settled, than the volume of the traffic (mean-daily-number of lorrys) and the design life has to be fixed. With a load model some loading events, for example pulk of lorrys or override-manoevres have to be defined. With this loading events in each detail a design stress spectrum has to be calculated which depends non linear from the action. Normally the stress spectrum is calculated for the hot-spot-point and it is to be decided which point is the hot-spot. For the stress spectrum also changing of traces, distance of lorrys and imperfections of the

$$\Delta\sigma_e = \left[\sum_i \Delta\sigma_i^3 \frac{n_i}{N_e} + \left(\frac{\gamma}{\Delta\sigma_{RD}} \right)^2 \cdot \sum_j \Delta\sigma_j^5 \frac{n_j}{N_e} \right]^{1/3} \quad (I)$$

$$\Delta\sigma_e = \left[\left(\frac{\Delta\sigma_{RD}}{\gamma} \right)^2 \cdot \sum_i \Delta\sigma_i^3 \frac{n_i}{N_e} + \sum_j \Delta\sigma_j^5 \frac{n_j}{N_e} \right]^{1/5} \quad (II)$$

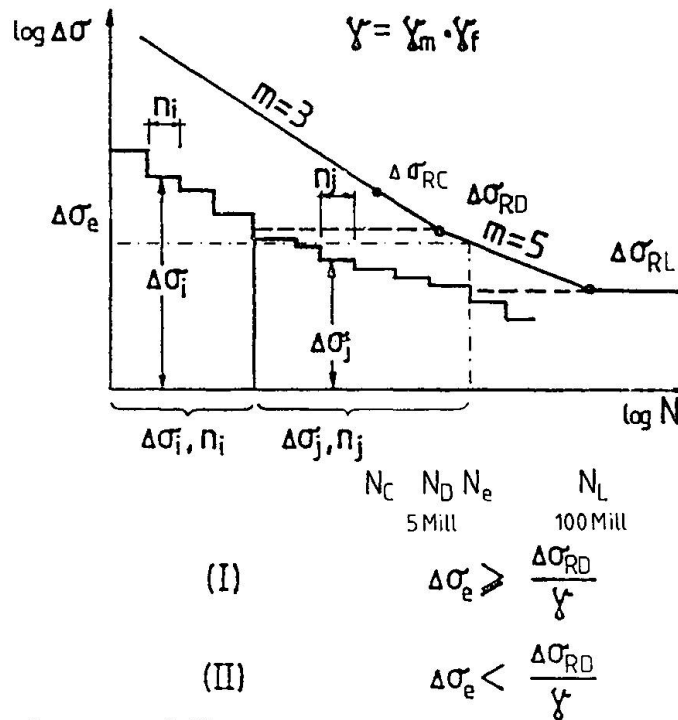


Fig. 1 Calculation of $\Delta\sigma_e$

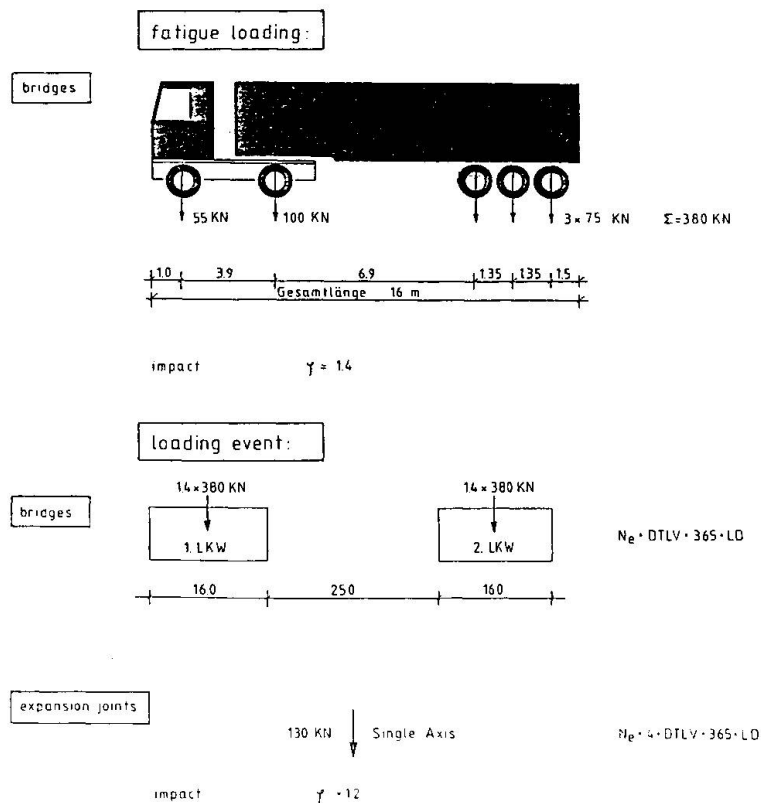


Fig. 2 Fatigue loading for bridges and expansion joints



road surface have to be fixed. In expansion joints the influence of the changing of the deflection, the dynamic stiffness of plastics and the difference of phase between vertical and horizontal forces have to be considered. With the worst loading conditions the maximum stresses and stress spectras the hot-spot-point have to be calculated. The next step is to decide the detail categorie using the Miner-summation to get equivalent constant amplitude stress range. According to the assumptions the result of the calculation, for example life time vary in a wide range, because small changing in stresses give a big change of life time. This is due to the logarithmic form of the fatigue strength curve. So the calculation gives only tendencies. Fig. 1 shows the fatigue sessment according EC 3. Computed stress spectras can not be controlled, they should be controlled by measurement. And here is a big lack of measurements.

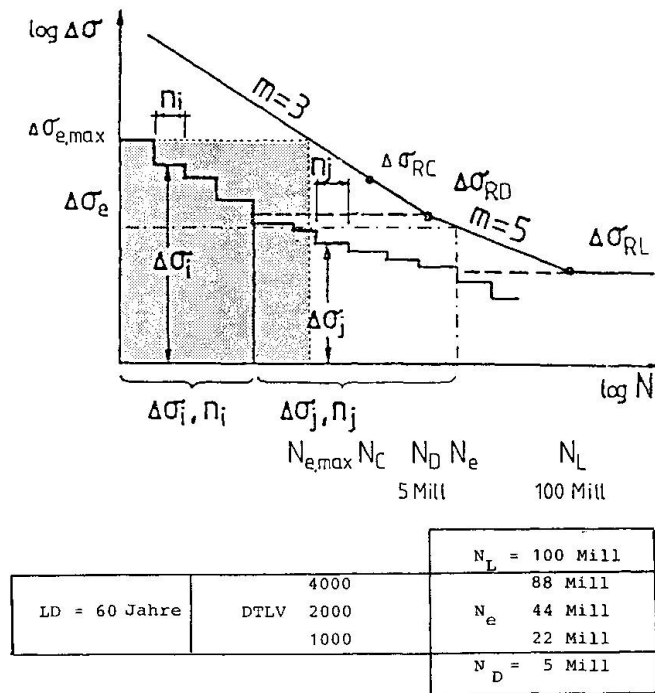
4. CALCULATION OF FATIGUE LOADING FACTORS FROM DAMAGES

In the following it will be shown how by systematic treatment of damage analysis fatigue load factors of road bridges can be gained. First a realistic fatigue loading has to be set up and the mean-daily-number of lorrys has to be known. In bridges the fatigue loading which is realistic is a lorry with 380 kN and on the expansion joints a single axis of 130 kN is the maximum possible loading for fatigues (Fig. 2). In the hot-spot-point where the damage occurred the maximum stress variation has to be calculated with this models. With the fatigue test the fatigue strength curve for the hot-spot-point has to be determined. Because now the life time and the maximum stress variation is known. The number $N_{e,max}$ of load cycles to damage with constant maximum amplitudes can be gained (Fig. 3). In this number all non linear influences are included out of observations of the damage and with this number it is possible to calculate a realistic fatigue load factor. The fatigue load factor can be calculated according equation (1):

$$\alpha = \frac{\Delta \sigma_e}{\Delta \sigma_{max}} = \left(\frac{N_{e,max}}{5 \cdot 10^6} \right)^{\frac{1}{3}} \cdot \left(\frac{5 \cdot 10^6}{N_e} \right)^{\frac{1}{5}} \quad (1)$$

where N_e the number of all load cycles during the life time is, This equation one get from the one step collective $\Delta \sigma_{max}$ and $N_{e,max}$ in comparison to the one step collective $\Delta \sigma_e$ and N_e according EC 3. With the observations according Fig. 4 and 5 [3,4] using the proposed method you get for a torsional bracing $\alpha = 0,63$ and for an expansion joint $\alpha = 0,34$ (Fig. 6). If the results are drawn in relation to the parameter $N_e / N_{e,max}$ you get Fig. 7. It shows that with growing number of load cycles the fatigue load factor is going down because of the fact that the propability of reaching the maximum stress variation goes down. Out of this it is proposed to give for different details different fatigue load factors, for example:

- details with low number of load cycles as torsion bracings and wind bracings, if they are acting in the main system
 - details with a middle number of load cycles as orthotropic plates, cross bracings and frames
 - details with high load cycle numbers as expansion joints.
- The fatigue load factors would be accordingly 0,65, 0,45 respectively 0,35.



$$\alpha = \frac{\Delta \sigma_e}{\Delta \sigma_{e,\max}} \cdot \left(\frac{N_{e,\max}}{5 \cdot 10^6} \right)^{1/3} \cdot \left(\frac{5 \cdot 10^6}{N_e} \right)^{1/5}$$

Fig. 3 Determination of $N_{e,\max}$

bracing:

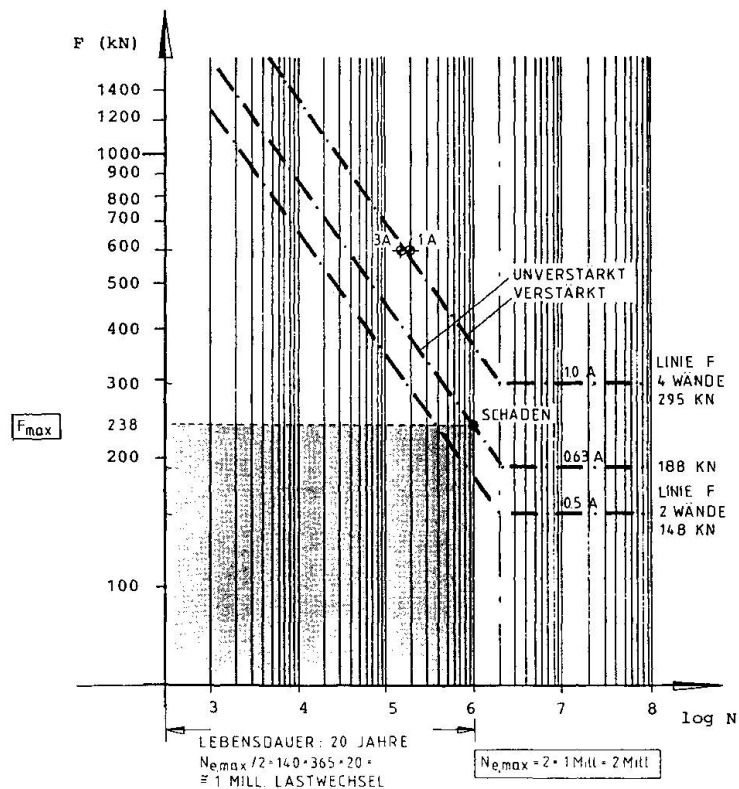


Fig. 4 Fatigue strength curve bracing



expansion joint:

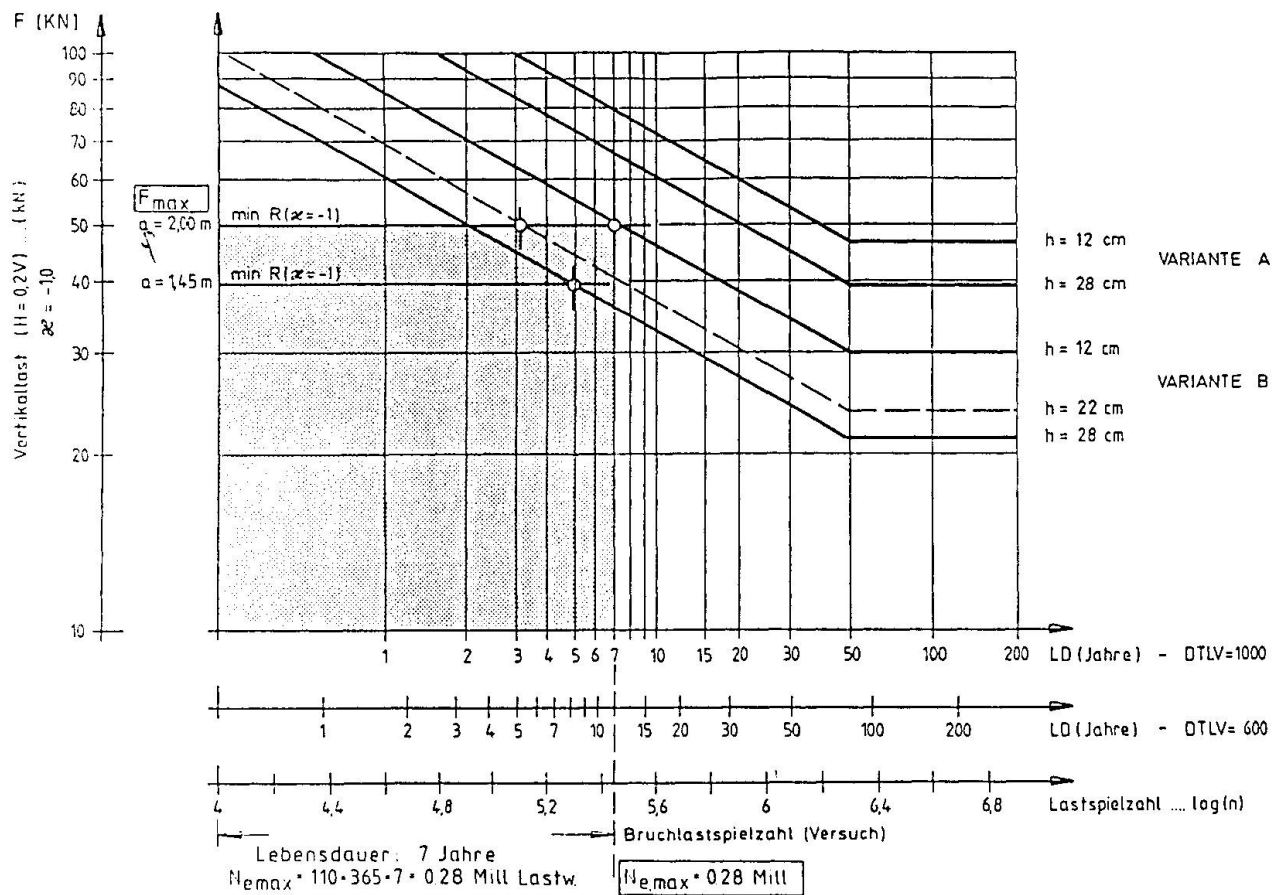


Fig. 5 Fatigue strength curve expansion joint

Lit.	[4]	[3]
member	bracing	expansion joint
LD Jahre	20	7
DTLV	1500	1000
N_e	$1500 \times 365 \times 20 = 11 \text{ Mill}$	$4 \times 1000 \times 365 \times 7 = 10 \text{ Mill}$
$N_{e,max}$	$20 \times 2 \times 140 \times 365 = 2 \text{ Mill}$	$7 \times 110 \times 365 = 0,28 \text{ Mill}$
α	0,63	0,34

Fig. 6 Determination of fatigue load factor α

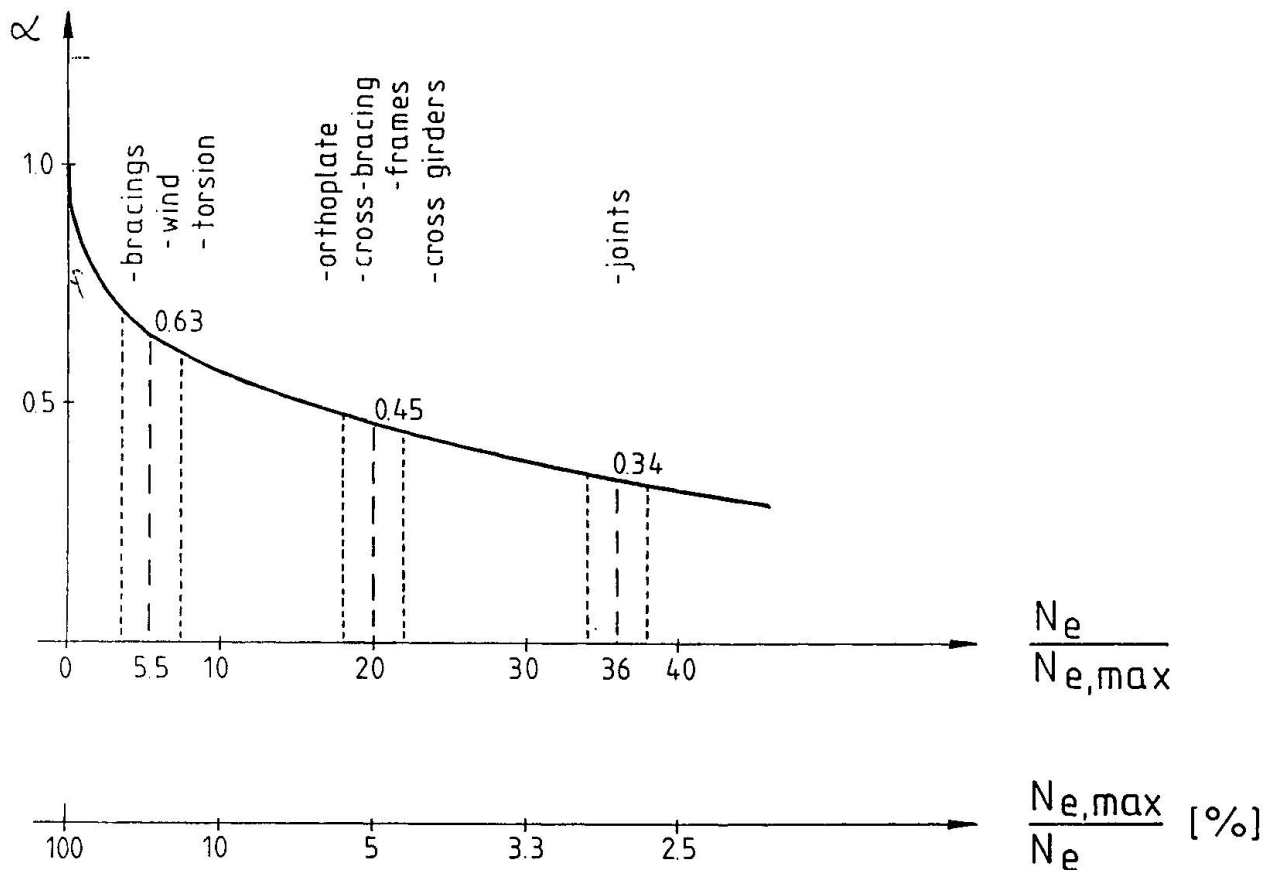


Fig. 7 Fatigue load factor for different details

Further research is necessary to verify this numbers. In any way it will be very helpful to give such fatigue load factors in EC 3 for different details to come to much easier fatigue assessment for secondary members of steel road bridges. Advantage is, that we are used to calculate maximum stresses and the fatigue tests have to be done at maximum stress variation. Further with the known fatigue load factors the remaining life time calculation is much easier and also results of computer simulation can be checked by this method.

References

- 1 Entwurf Eurocode 3, 1988
- 2 Richtlinie zur Berechnung ermüdungsbeanspruchter Konstruktionen aus Stahl, 1. Ausgabe, November 1988, Österreichischer Stahlbauverband, A-1130 Wien, Larohegasse 28
- 3 F. Tschemmernegg - Zur Bemessung von Fahrbahnübergängen, Bauingenieur 63 (1988), S. 455 - 461
- 4 F. Tschemmernegg/H.Passer/O. Neuner - Verbreiterung und Sanierung von Stahlbrücken, Stahlbau 58 (1989), Heft 10, S. 289 - 298

Leere Seite
Blank page
Page vide

Method to Back Decisions on Residual Safety of Bridges

Méthode pour la détermination de la sécurité restante des ponts existants

Methode zur Bestimmung der verbleibenden Sicherheit
von bestehenden Brücken

Winfried DAHL

Professor
Institute of Ferrous Metallurgy
Aachen, Fed. Rep. of Germany



Winfried Dahl, born 1928, received his degree in Physics at the Georgia-Augusta-University in Göttingen, FRG. Since 1969, he has been the head of the Institute of Ferrous Metallurgy at the TU Aachen.

Otfried SCHUMANN

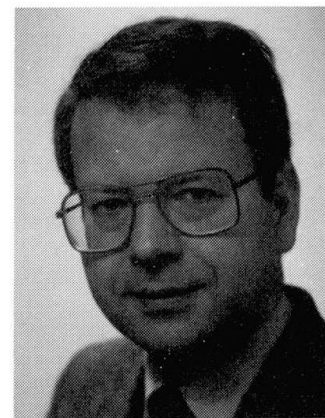
Civil Engineer
Dep. of Bridges and Constr. Eng.
Duisburg, Fed. Rep. of Germany



Dipl.-Ing. Otfried Schumann, born 1927, received his civil engineering degree at the Technical University of Berlin-Charlottenburg. Since 1977, he has been the head of the Dep. of Bridges and Construction Engineering of the town Duisburg.

Gerhard SEDLACEK

Professor
Inst. of Steel Construction
Aachen, Fed. Rep. of Germany



Gerhard Sedlacek, born 1939, obtained his PhD at the TU Berlin. After work in the steel construction industry, he became the head of a department of bridge building. Since 1976 he has been Professor of the Institute of Steel Construction of the TU Aachen.

SUMMARY

This paper demonstrates a fracture-mechanics based method to determine the safety of old steel bridges for modern traffic loading and to prepare an inspection programme which enables extended service life of bridges to be justified. The method is illustrated by means of a practical example.

RÉSUMÉ

Cet article présente une méthode basée sur la mécanique de la rupture, et qui permet de déterminer la sécurité d'anciens ponts en acier soumis aux charges du trafic moderne et de préparer un programme d'inspection qui permette d'assurer une prolongation de la durée de service des ponts. La méthode est illustrée à l'aide d'un exemple pratique.

ZUSAMMENFASSUNG

Der Beitrag zeigt eine auf der Bruchmechanik basierende Methode, die erlaubt, die Sicherheit alter Stahlbrücken abzuschätzen, die modernen Verkehrslasten unterworfen sind, sowie Inspektionsmassnahmen zu planen, mit deren Hilfe ein sicherer Betrieb garantiert werden kann. Die Methode wird an einem praktischen Beispiel dargestellt.



1. Introduction

A great part of existing steel bridges have been built in the last century, [fig. 1](#), and since then have undergone several phases of repair or strengthening after damages in the world wars or due to changes of service requirements.

For those bridges very often the question of the actual safety for modern traffic loads and the remaining service life is put forward.

This paper describes a procedure how the residual safety and service life of old steel bridges may be determined and how a basis may be established on which economic decisions for further strengthening or replacement by a new bridge may be taken.

The procedure is described by the example of an old roadway bridge, the Karl-Lehr-Bridge in Duisburg. It may however be applied to any other steel bridge.

2. Problem

The structural system and the cross-section of the Karl-Lehr-Bridge can be taken from [fig. 2](#). The bridge was built up in 1907 as a part of the Hohenzollern-Bridge over the river Rhein in Cologne and was blasted in the 2nd world war. After the war it was repaired and shipped on pontons to the harbour of Duisburg where it was installed for bridging a canal. In 1976 it got a new orthotropic deck to enhance the capacity to the loading class BKL 60 in DIN 1072.

In 1984 a tram on the bridge ran off the rails and hit a hanger, which exhibited cracks which were classified as "brittle". This behaviour alarmed the town authority that asked for an expertise that should answer the following questions:

1. Is the bridge sufficient safe for actual service conditions?
2. If so, what is the expected residual life and what are the requirements for inspection and maintenance to assure the expected residual life.

3. General conditions concerning "brittleness" and "ductility"

For answering the above mentioned questions a definition of different failure modes in view of "brittleness" and "ductility" is necessary.

The technical stress-strain curve obtained for tension coupon tests, see [fig. 3](#), reveals a maximum, which can be explained by the stability criterion

$$\delta R_t = A_m \cdot \delta \sigma_w + \sigma_w \cdot \delta A_m = 0$$

$$\text{hence } \frac{\delta A_m}{A_m} = - \frac{\delta \sigma_w}{\sigma_w}$$

where A_m is the actual cross sectional area
 σ_w is the true stress, taken from the true stress-strain curve in [fig. 4](#).

From [fig. 5](#) it can be derived that the elongation before reduction of area in the specimen is the reduced the curve the higher the yield strength of the material is.

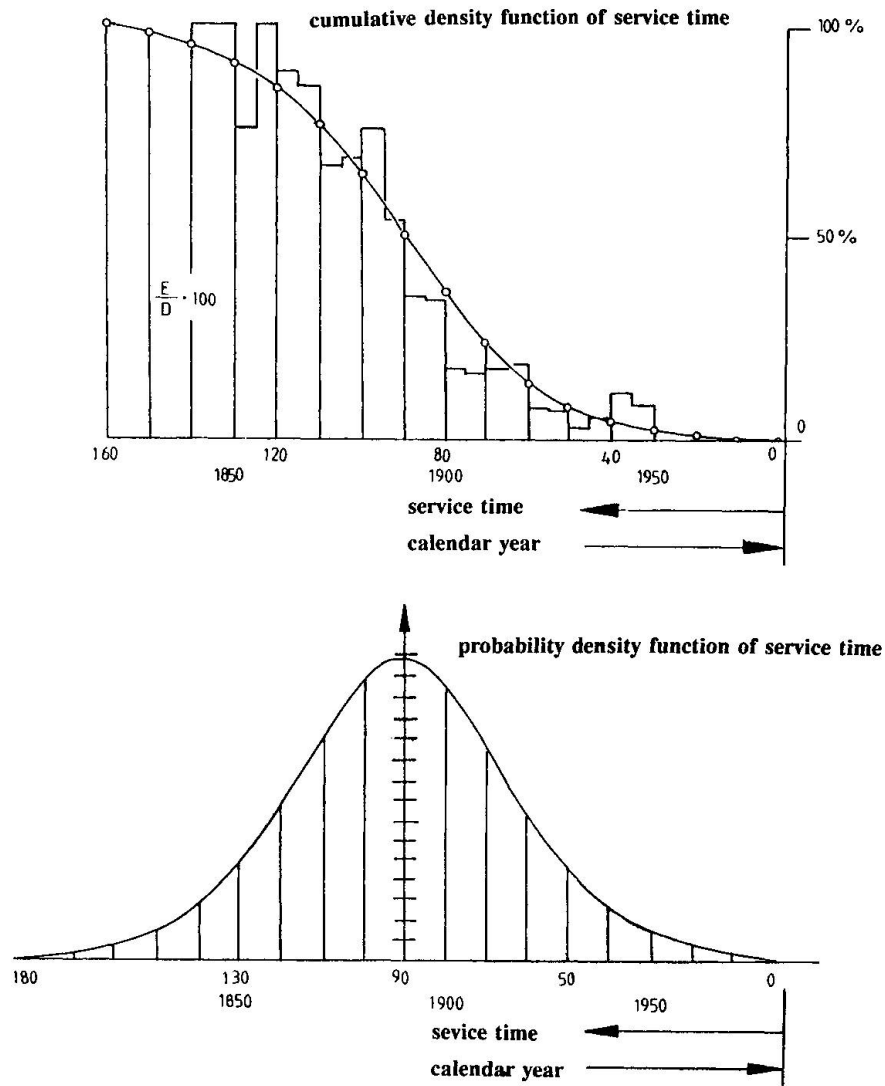


Figure 1: Distribution function of service time of existing railway bridges in steel

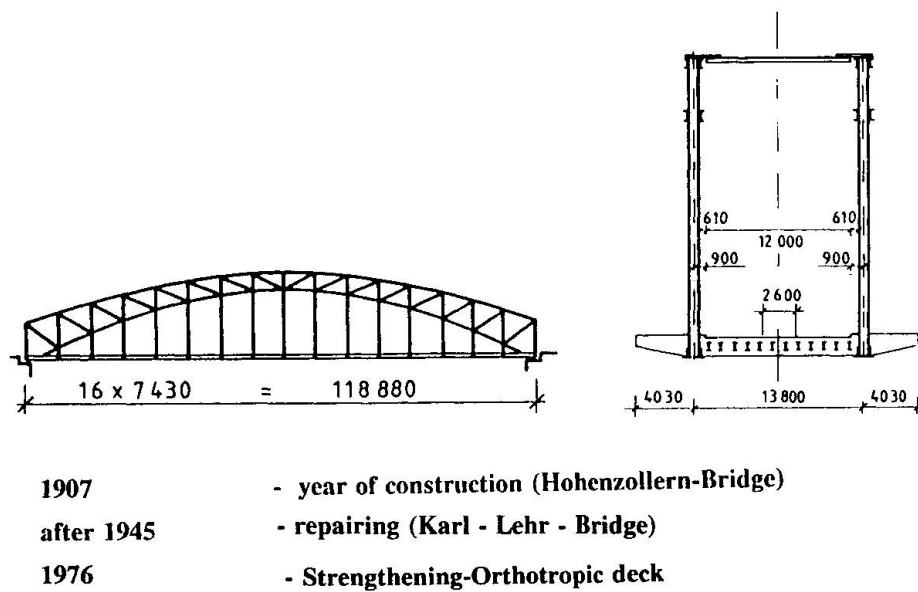


Figure 2: Structural system and cross-section of the Karl-Lehr-Bridge

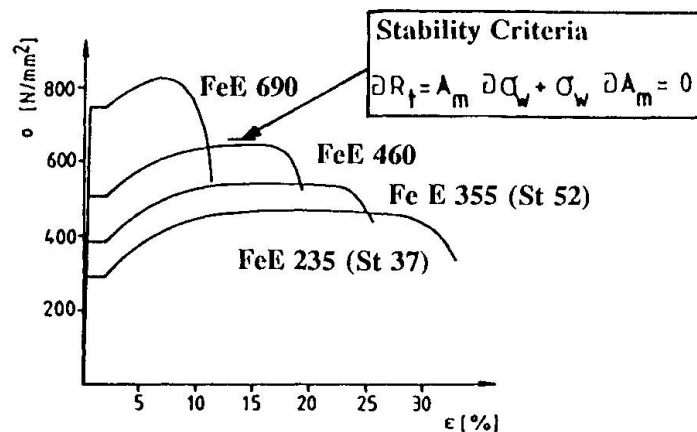


Figure 3: Technical stress-strain-curve

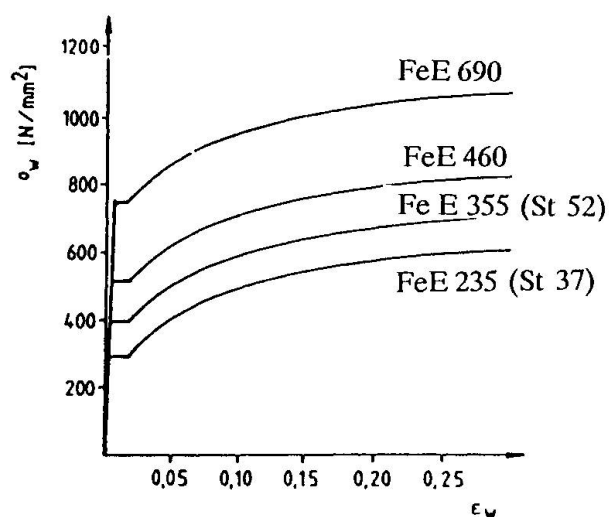


Figure 4: True stress-strain-curve

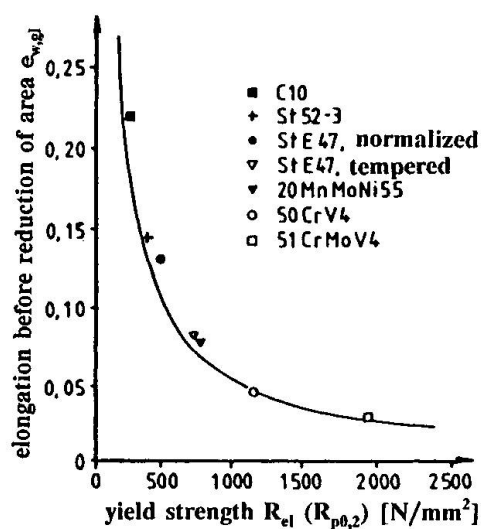


Figure 5: Elongation before reduction of the area $e_{w,gl}$ plotted versus yield strength R_{el}

A structural member may show different failure modes, which may be best distinguished for the example of a plate with a central crack in tension, fig. 6:

1. Unfavourable failure is exhibited when fracture occurs before net section yielding with only local yielding at the crack tips.

In this case all actual stresses in the net section comprising the stresses from external loads including notch effects, residual stresses and stresses due to other restraints have to be taken into account.

This failure mode commonly is called "brittle" failure.

2. If failure in structural applications occurs by fracture after net-section yielding, only the nominal stresses due to external loads in the net section are relevant, and notch effects, residual stresses and stresses due to other restraints may be neglected.

This and all following modes are called "ductile" failures.

3. Another ductile failure mode, that may be required for plastic zones in plastic hinges or dissipative zones in seismic design is achieved by fracture in the net section after gross-section yielding.

In this case the stresses from external loads only in the gross section are controlling the design of the member and the net section is capacity-designed.

The failure mode is mainly influenced by the material, the temperature, the loading rate and the shape of the structural member (state of stress).

For the safety assessment of old steel bridges of the kind of the Karl-Lehr-Bridge in general the first and the second mentioned failure modes are relevant, as the assessments have to be carried out for design situations with low temperatures and assumed cracks.

4. General procedure

The following steps are necessary to determine the actual safety and residual life of the structure.

1. Establishment of a failure scenario, where the consequences of failure of the different bridge elements for different design situations are investigated. Those bridge elements are identified as vital elements the failure of which would cause an immediate overall collapse.

For the Karl-Lehr-Bridge the vital element proved to be the tension tie, see fig. 7, as all other members are either redundant or stressed so little that they do not produce risks.

2. As far as the vital elements may fail by fracture due to tension loads, they are assessed in the following way:

- a) Several loading cases are determined with combinations of self weight, traffic loads including dynamic impact and temperature and with or without residual stresses and restraints depending on the expected failure mode.

For these loading cases and a crack situation in the vital element that is assumed such that the crack sizes just reach the size of detectability the applied fracture mechanics action effects in terms of J_{appl} , see chapter 5, is calculated.

- b) From miniaturized plate samples which are drilled from the vital elements at locations where they don't reduce the safety, the fracture mechanics material resistance in terms of J_{crit} for different temperatures is determined, fig. 8, which allow to carry out a safety check by

$$J_{appl} \leq J_{crit}$$

From this safety check and by varying the crack length assumptions a critical crack length can be determined which indicates what amount of crack extension beyond the size of



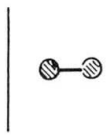
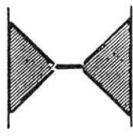
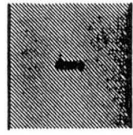
yielding pattern	failure mode	design values
	fracture before net-section yielding brittle	applied stress distribution in the net-section + residual stresses + restraints
	fracture after net-section yielding ductile	applied nominal stress distribution in the net-section
	fracture of the net-section after gross-section yielding ductile	applied nominal stress distribution in the net-section

Figure 6: Definition of failure modes and the applied design values of stresses dependant on the ductility level

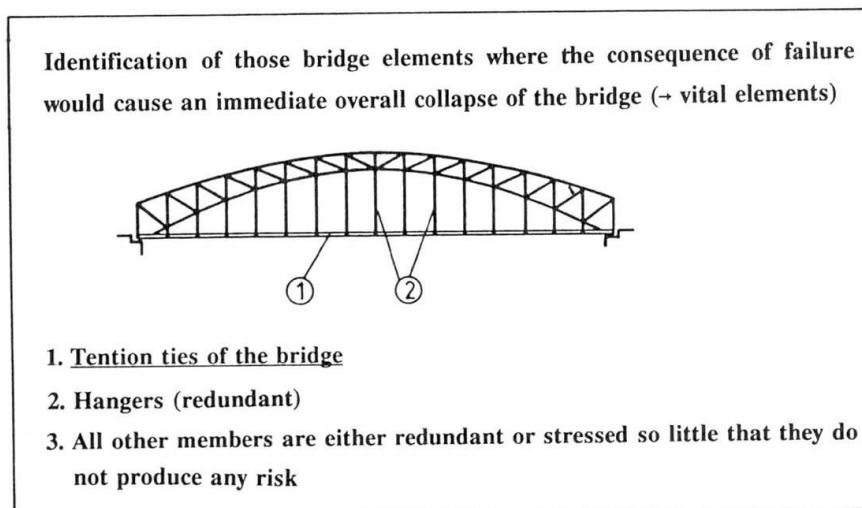


Figure 7: Vital elements of the Karl-Lehr-Bridge

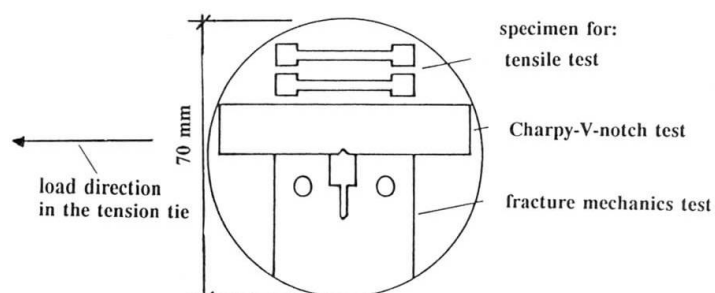


Figure 8: Miniaturized test element and available test specimens for different tests

detectability is tolerable.

3. From observations of the actual traffic situations on the bridge and extrapolation to future developments a fatigue load is defined which allows to determine the residual service time of the bridge on the basis of the crack propagation rate from the detectable crack to the critical crack size with a fracture mechanics model.

The procedure developed in [1] is illustrated in [fig. 9](#), in which the vital member resistance is plotted versus service life, due to fatigue induced crack propagation. It has been applied to different railway bridges, e.g. [2], [3].

The main advantages of this procedure are the following:

1. It can be demonstrated that cracks with detectable sizes can be accepted without catastrophic consequences and no collapse (without prewarning) may take place.

If this check is not positive, the member has to be strengthened with tough material or to be replaced before the next cold season (loss of toughness at low temperatures).

2. It can be demonstrated that the crack extension from the detectable crack size to the critical crack size takes sufficient time, to allow for economic intervals of inspection.

If this check is not positive a strengthening with tough material or a replacement should be considered.

3. In case of both checks being positive the inspections at safe intervals at the critical location of the vital elements will allow the following conclusions:

- As long as no cracks are observed, the structure is fit for use for at least the service period up to the next inspection.
- This statement can be repeated up to the inspection when first cracks are found.
- In case cracks are found there is sufficient time left to react by replacing the members or the total bridge.

5. Justification of the procedure

The procedure is based on the J-Integral [4],[5], [fig. 10](#)

$$J = \int_{\Gamma} \left(W \cdot \delta y - T \cdot \frac{\delta u}{\delta x} \cdot \delta s \right)$$

where

- W = Energy density
- T = Vector of stresses
- u = Vector of displacements
- Γ = Integration path around the crack tip
- δs = element of the integration path

The crack driving force in terms of the J-Integral J_{appl} can be calculated by FE-analysis with a grid of collapsed iso-parametric elements, [fig. 11](#).

The material toughness in terms of the J-Integral J_{crit} can be evaluated from the fracture mechanics test specimens, see [fig. 8](#) and can be interpreted as the energy which leads to crack tip opening just before crack extension, [fig. 12](#). This represents a conservative assumption for the ultimate limit state, because it neglects the reserves that may be produced by stable crack extension after initiation.

The critical material resistance values J_{crit} obtained from the small scale test specimens taken from the tension tie and tested at a temperature $T = -30^{\circ}\text{C}$ are plotted in [fig. 13](#), the lowest value found was 42

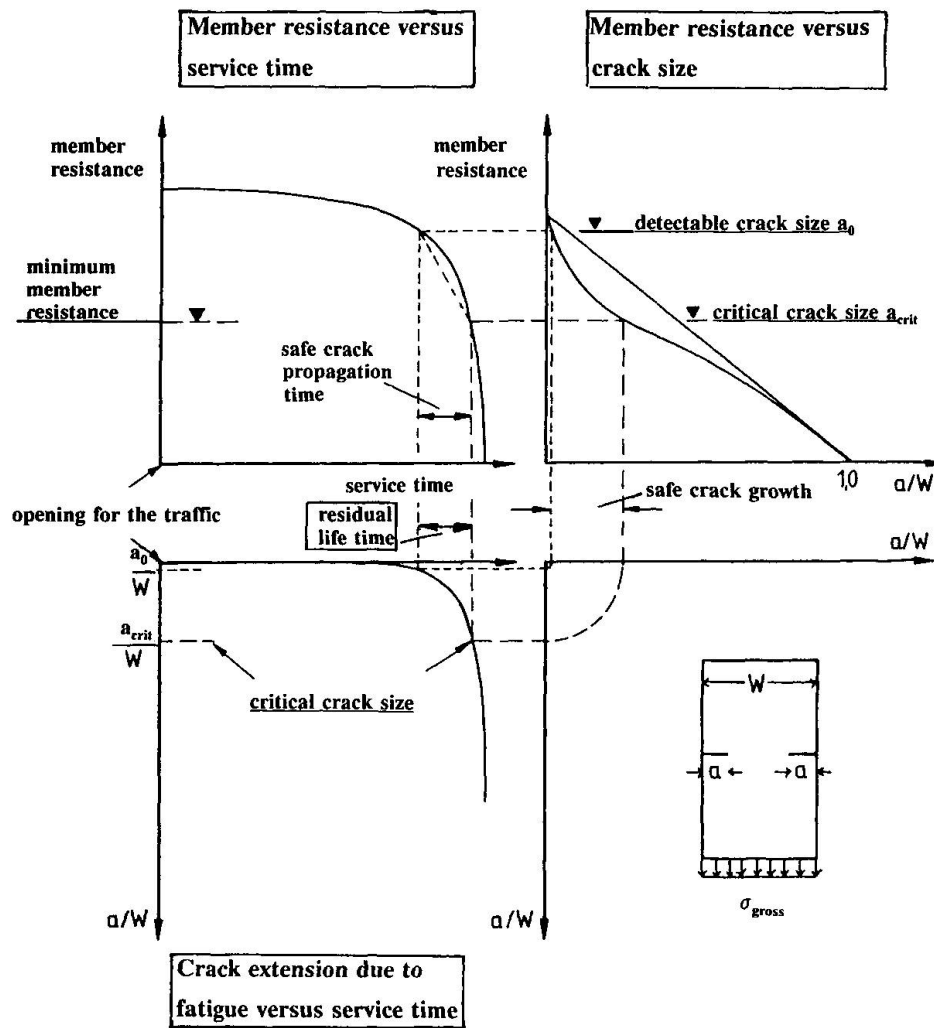


Figure 9: Relation between the member resistance and the crack sizes as a function of the service time

$$J = \int_{\Gamma} (W \cdot \delta y - T \cdot \frac{\delta u}{\delta x} \cdot \delta s)$$

Figure 10: Definition of the integration path for the J-Integral calculation

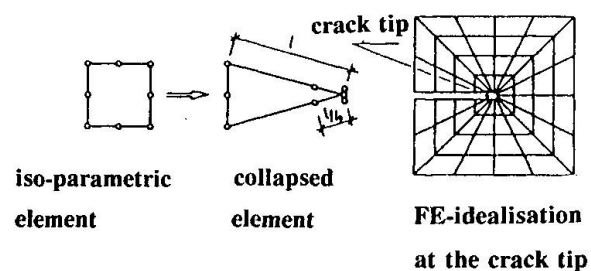


Figure 11: FE-elements and FE-grid for the calculation of J_{appl}

Load F

starting crack

formation of a plastic zone

rounding of the crack tip

formation- and growth of holes in the front of the crack tip

holes grow together

crack extension

Figure 10 is a graph showing the dependence of the critical current density J_c on the temperature T for the MgB₂/Ag system. The y-axis is labeled $J_c, J_c \text{ N/mm}$ and the x-axis is labeled temperature [°C]. The curve shows a peak at -30°C with a value of 95 N/mm, and a minimum at -20°C with a value of 42 N/mm. The critical current density is 29.4 N/mm at 0°C and 20°C.

The figure contains three technical drawings:

- Top Drawing:** A side view of a hanger holding two rows of samples. The total height is 200. The left row contains a "sample for Charpy-V-energy test" and a "sample for tension test". The right row contains two "1CT-10 sample"s. The width of the hanger is 100. The distance between the two rows of samples is 62.5.
- Bottom Left Drawing:** A circular cross-section of a "sample for Charpy-V-energy test". It shows a central notch and a "working edge" on the left.
- Bottom Middle Drawing:** A circular cross-section of a "1/2CT-10 sample". It shows a central notch.
- Bottom Right Drawing:** A circular cross-section of an "RCT sample". It shows a central notch and two circular features on either side. Dimensions include a total width of 55, a central width of 15, and a distance of 10 from the center to the edge of the circular features.

Test specimen taken from the hangers

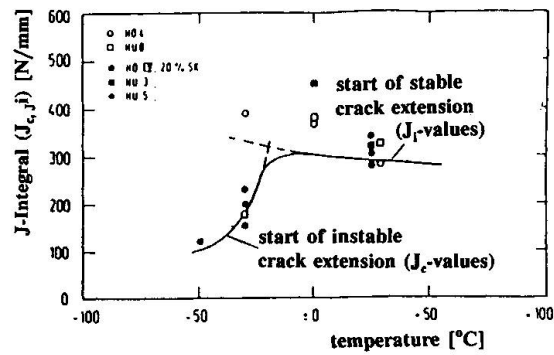


Figure 15: J-curve versus temperature

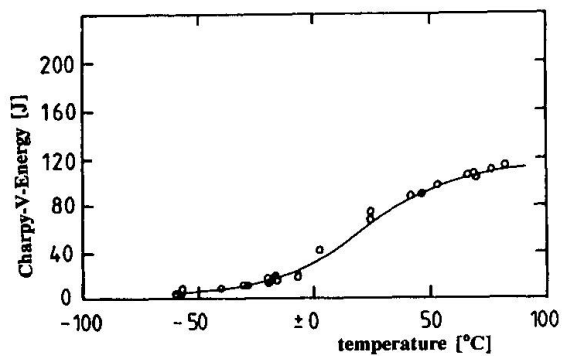


Figure 16: Charpy-V-energy-temperature curve

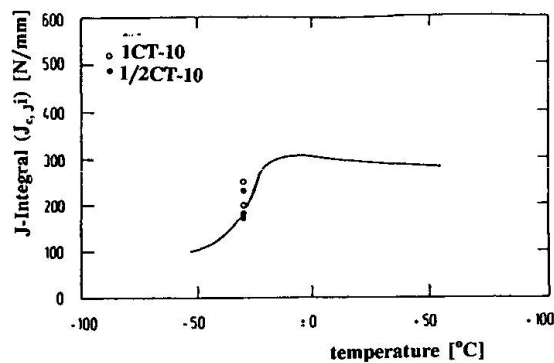


Figure 17: Comparison between 1CT-10 and 1/2CT-10 samples

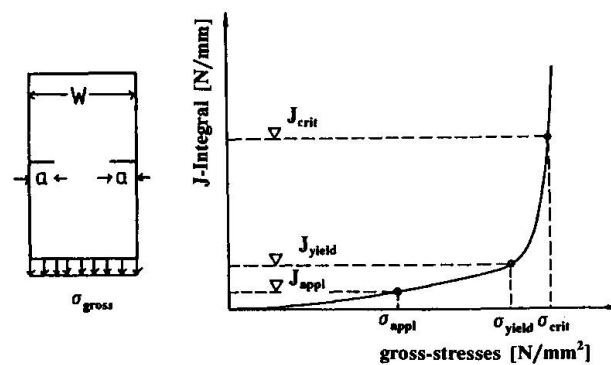


Figure 18: J_{appl} -curve

N/mm.

For the hangers of the bridge, which were not vital elements comparative tests could be made to determine possible scaling effects due to the miniaturized specimen and a correlation to the results of Charpy-V-energy tests if there are any. For this reason test specimens of different sizes were taken from the hangers, see [fig. 14](#). The 1CT-10 samples allowed to determine the J-Integral transition curve, [fig. 15](#), which gives no correlation to the Charpy-V-energy-temperature curve [fig. 16](#), which for safety assessments can only be used qualitatively.

A comparison between the results from 1CT-10 samples and 1/2CT-10 samples is given in [fig. 17](#). It demonstrated that the 1/2CT-10 samples give conservative data.

For a given structural member and a given crack location and crack size the curve of J_{app} versus the applied gross-stresses may be calculated if the true stress-strain curve of the material is known, [fig. 18](#). On this J_{app} -curve J_{yield} , where net section yielding is reached, and J_{crit} , where crack extension starts, are particular values. The case of brittle failure occurs if $J_{crit} < J_{yield}$, else net section yielding will occur before fracture is expected.

The reliability of the prediction of the ultimate resistance of structural members by the J-Integral method has been proved by a series of justification tests with big plates [6],[7].

6. Application and results of the procedure

[Fig. 19](#) demonstrates the cross section of the tension tie which is riveted, and three alternative models (I, II, III) for the fracture mechanics assessment of this tie.

In assuming that fatigue cracks would initiate in the parent metal under the heads of the rivets [8], a starting crack length is considered which represents the rivet hole plus two cracks at both sides of the rivet grown perpendicular to the direction of the applied stresses, that have reached the edge of the rivet head ($a = 21.5$ mm), [fig. 20](#).

For the given true stress-strain curve the J_{app} -curves for the models I, II, and III were calculated as plotted in [fig. 21](#) and model II was chosen as relevant.

In [fig. 22](#) several J_{app} -curves are given starting from the basic curve for $a = 21.5$ mm up to $a = 75$ mm.

The relevant load case was represented by a temperature of -30°C which was combined with the applied stress due to self weight and full traffic load as specified in DIN 1072. This gives a total gross stress $\sigma_{app} = 114$ N/mm² for the ductile failure mode and $\sigma_{app} = 234$ N/mm² for the brittle failure mode, where residual stresses have to be added.

The safety check has been made for the following cases, see [fig. 22](#):

1. For the minimum material value of $J_{crit} = 42$ N/mm the brittle failure mode is relevant and the tolerable crack length is $a = 34.5$ mm i.e. 13 mm crack growth beyond the edge of the rivet head.
2. In the second case, two of the four plates, that represent the tension tie, would fail, and the plates that survive would exhibit a material value $J_{crit} = 70$ N/mm, the behaviour of the latter could be classified as ductile failure mode and the applied stress they get would be 222 N/mm². For this case the tolerable crack length would be greater than $a = 34.5$ mm. So the first case with $a = 34.5$ mm is relevant.

The crack propagation calculation is based on measurements of the traffic situation to get the fatigue load; from these measurements the relevant damage-equivalent stress ranges were mainly caused by multiple traffic jams which yielded to $\Delta\sigma_e = 52.1$ N/mm² or $\Delta K_e = 460$ N/mm^{3/2} with a number of 10 cycles per day. This includes a dynamic impact factor $\psi = 1.20$ that was taken from the measurements as well. The "Paris"-coefficients were taken as given in [fig. 23](#).

The calculation of the crack extension yielded to the curves in [fig. 24](#), from which the limit curve in [fig. 25](#) could be derived.

Though the total procedure includes a set of conservative assumptions, the final proposal was not

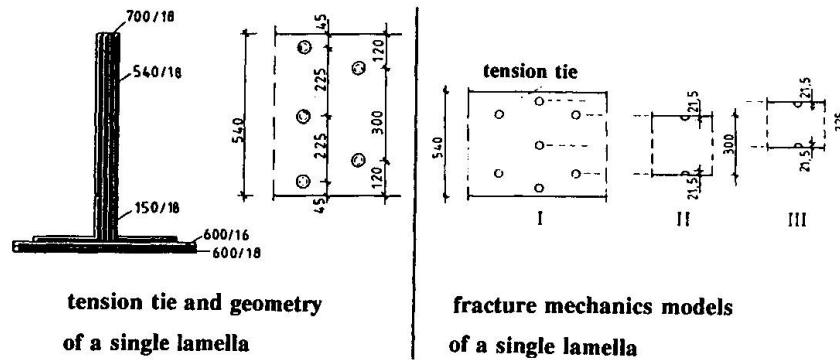


Figure 19: Cross section of the tension tie and three alternative models for the fracture mechanics assessment

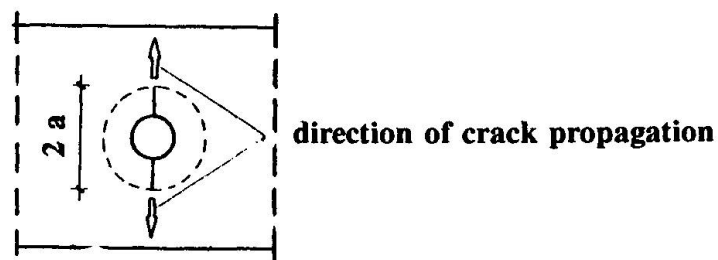


Figure 20: Definition of the starting crack size

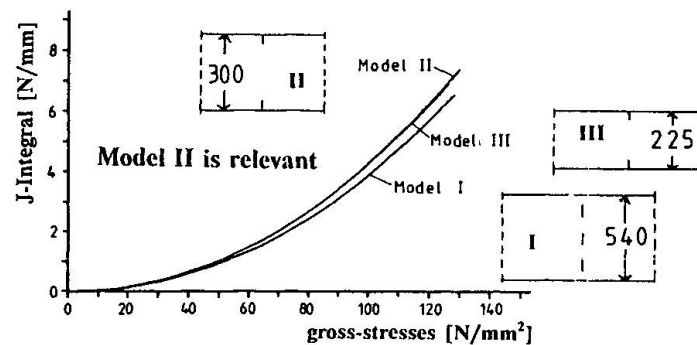


Figure 21: J_{appl} -curves for the fracture mechanical models I, II and III

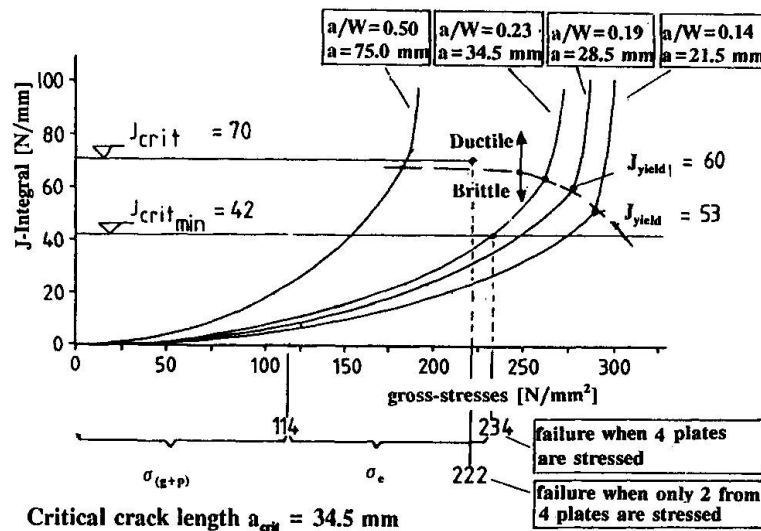


Figure 22: Determination of the critical crack size for the actual load situation

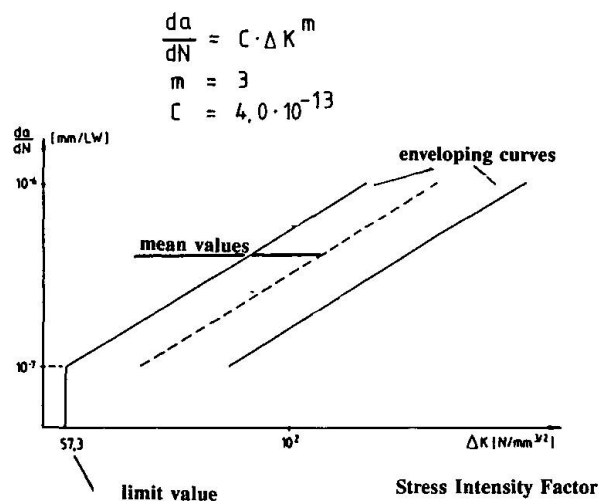


Figure 23: Determination of the crack propagation

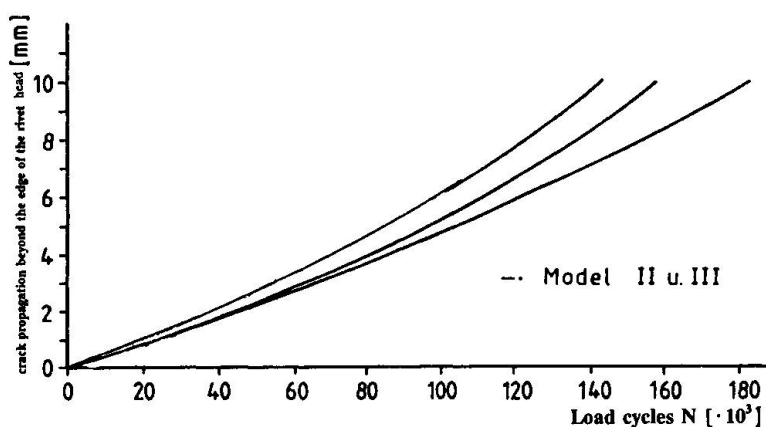


Figure 24: Crack propagation curve for the different fracture mechanical models

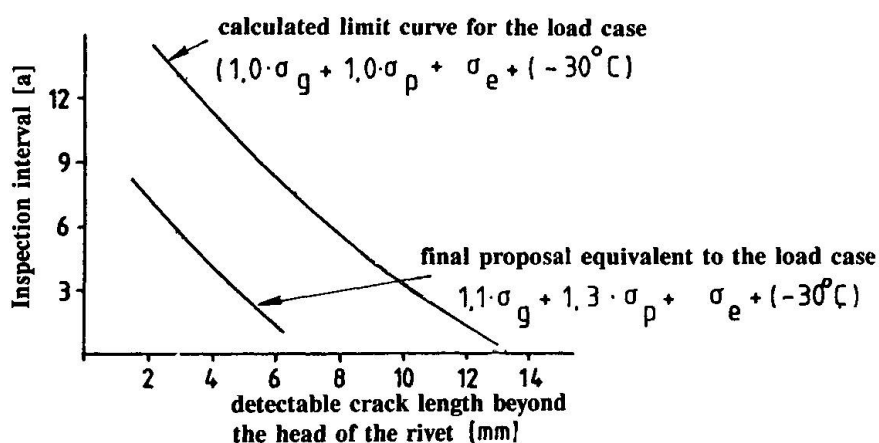


Figure 25: Crack propagation behaviour and inspection interval



based on the calculated limit curve but on a more conservative curve given in fig. 25. Details concerning the procedure can be found in [1].

The final result from all checks including the aforementioned fracture mechanics assessment was:

1. The bridge complies with the present design codes and is fit for the use with sufficient safety when no cracks at locations indicated in the crack control plan are found.
2. The inspection should be carried out every 1.5 years according to the crack control plan.
3. The bridge remains fit for the use with sufficient safety as long as no crack is detected during inspection and the loading conditions do not change significantly.

7. Conclusions

A fracture mechanics based procedure for the determination of the safety and the residual life of old steel bridges is presented, that avoids the uncertainties of predictions that are linked to S-N-curves.

The method has already been applied to railway and roadway bridges, to guyed masts and rotors and is considered as a useful tool together with other engineering judgments.

At present the method is being simplified and made more operational in order to be standardized in a code that could be used for the safety assessment of old steel bridges.

8. Acknowledgement

The afore mentioned work was mainly carried out by Dipl.-Ing. Johansson, member of the staff of Dipl.-Ing. Schumann, Dr.-Ing. W. Hesse and Dipl.-Ing. R. Hubo, Institute for Ferrous Metallurgy, Technical University Aachen and Dr.-Ing. J. Bild, Dipl.-Ing. H. Eisel and Dipl.-Ing. W. Hensen Institute for Steel Structures, Technical University Aachen.

The fruitful cooperation between the town authority in Duisburg and the institutes of the RWTH Aachen is highly appreciated.

9. References

1. BILD, J., Beitrag zur Anwendung der Bruchmechanik bei der Lösung von Sicherheitsproblemen im Stahlbau. Diss. RWTH Aachen, 1988.
2. DAHL, W., SEDLACEK, G., Untersuchungen zur Ermittlung der Sicherheit und Restnutzungsdauer der Karl-Lehr-Brücke in Duisburg. Expertise for the town Duisburg, 1986.
3. DAHL, W., SEDLACEK, G., Untersuchungen zur Ermittlung der Sicherheit und Restnutzungsdauer der Ackerfährbrücke in Duisburg. Expertise for the town Duisburg, 1986.
4. RICE, J.R. and TRACEY, D.M., J. Mech. Phys. Solids 17, pa. 201-217/1969.
5. CHEREPANOV, G.P., Crack propagation in continuous media. PMM Vol. 31, No. 3/1967, pa. 476-488.
6. DAHL, W., DORMAGEN, D., EHRHARDT, H., HESSE, W., TWICKLER, R., Anwendung bruchmechanischer Konzepte auf das Versagensverhalten von Großplatten. Nucl. Eng. and Design, Vol. 87/1985, pa. 83-88.
7. EHRHARDT, H., Untersuchungen zum Einfluß unterschiedlicher Fehlergeometrien auf das Versagensverhalten von Stahl auf der Grundlage von Großzugversuchen. Diss. RWTH Aachen, 1988.
8. BRÜHWEILER, E., ESSAIS DE FATIGUE SUR DES POUTRES A TRIPPLIS DOUBLE EN PER PUDDLE. Publication ICOM 159/1986.

Fatigue Reliability Updating Based on Inspection and Monitoring Results

Définition de la fiabilité à la fatigue basée sur les résultats d'inspection et de surveillance

Neubeurteilung der Ermüdungssicherheit aufgrund von Inspektions- und Überwachungsresultaten

Henrik O. MADSEN

Professor
Danish Engineering Academy
Lyngby, Denmark

Andrew G. TALLIN

Assist. Professor
Polytechnic University
Brooklyn, NY, USA

Henrik O. Madsen, born in 1953, received his M.Sc. and Ph.D. degrees from the Technical University of Denmark in 1976 and 1979, respectively. Following a period as research director at Det norske Veritas, he is since 1988 professor of structural mechanics. His main research interest is structural reliability analysis and its applications.

Andrew G. Tallin, born in 1954, received his B.Sc. and M.Sc. degrees from University of Manitoba, Winnipeg, Canada in 1978 and 1980, respectively, and his Ph.D. from Johns Hopkins University, Baltimore in 1985. Since 1984 he is assistant professor of civil engineering. His main research interests are structural reliability analysis and computer science.

SUMMARY

Probabilistic models for fatigue crack growth consider the uncertainty in loading, material properties initial flaw size, and model uncertainty in calculation of stress intensity factors. The reliability against a defined failure event can be computed. As in-service inspection or monitoring results become available, reliability can be updated. The analysis is particularly useful for maintenance planning.

RÉSUMÉ

Les modèles probabilistes de la propagation de fissure de fatigue tiennent compte de l'incertitude des charges, des propriétés du matériau, de la taille des défauts initiaux et des incertitudes dans les modèles du calcul des facteurs d'intensité de contraintes. La fiabilité peut être évaluée pour un certain mode de rupture défini. Si des résultats lors des inspections de service ou des surveillances sont disponibles, la fiabilité peut être mise à jour. Cette analyse est particulièrement utile pour un programme de maintenance.

ZUSAMMENFASSUNG

Wahrscheinlichkeitstheoretische Modelle für das Risswachstum berücksichtigen Unsicherheiten der Lastmodelle und der Materialeigenschaften sowie Ungewissheiten über die anfängliche Rissgrösse und die Berechnung der Spannungsintensitätsfaktoren. Die Ermüdungssicherheit kann in Abhängigkeit einer wohldefinierten Versagensart berechnet werden. Falls Resultate aus der Überwachung einer Brücke im Betriebszustand vorhanden sind, kann ihre Ermüdungssicherheit neu beurteilt werden. Die Untersuchung ist besonders im Hinblick auf die Planung der Unterhaltung der Brücke von Nutzen.



1. INTRODUCTION

About one third of all steel bridges in the US are fifty years old or more and many others are nearing that age [1]. Also in Europe are many steel bridges past or near their design life. As the number of bridges entering old age grows the need for inspection and maintenance becomes of increasing importance. At the same time the resources which can be allocated to the proper maintenance of bridges is shrinking. There is thus a great demand for methods which helps in allocating these resources in a manner which gives the highest overall utility. The paper reports on an application of probabilistic methods for such maintenance planning. The methods account explicitly for uncertainties in material properties, loading, initial flaw sizes, inspection methods and analysis models. Successful applications of the methodology are emerging in the offshore industry.

2. FATIGUE ANALYSIS

There are two common approaches to fatigue analysis of steel structures: the $S-N$ analysis mostly applied in design, and the fracture mechanics analysis mostly applied for structures in service. The $S-N$ approach relates the life time to the distribution of stress ranges at a fatigue critical point through the $S-N$ curve and the use of Miner's rule. This method has been used extensively in bridge fatigue studies, see e.g. [2,3]. Because $S-N$ analyses do not relate to a measurable indicator of damage, it is difficult to incorporate inspection observations into the fatigue analysis. On the other hand, monitoring information about the loads and load effects can be incorporated. The use of a linear elastic fracture mechanics (LEFM) model for fatigue crack growth allows information on the presence or size of observed cracks to be incorporated into descriptions of both failure and inspection events. The LEFM approach to fatigue analysis of steel bridges has been applied by a number of researchers, see e.g. [4,5].

The LEFM approach to fatigue crack growth relates the range in the stress intensity factor ΔK at the crack tip to the rate of crack growth da/dN by the equation suggested by Paris and Erdogan, [6]

$$\frac{da}{dN} = C (\Delta K)^m, \quad \Delta K > \Delta K_{thr}, \quad a(N=0) = a_0 \quad (1)$$

where C and m can be considered as material constants, ΔK_{thr} is a threshold value (in the following $\Delta K_{thr} = 0$), N is the number of stress cycles, and a_0 is the initial crack size. A crack initiation period is easily included in the analysis by changing the initial condition $a(0) = 0$ to $a(N_0) = 0$. A separate stochastic model for N_0 can then be formulated. Alternatively a_0 can be considered as an equivalent initial crack size as is commonly done for analysis of aircraft structures. To achieve a good correspondence with experimentally derived $S-N$ curves an initial crack depth of 0.1-0.2 mm must generally be assumed, [7].

A one-dimensional description of crack size is employed in Eq.(1), with a being the length of a through-crack or the depth of a surface crack. ΔK is expressed in LEFM as

$$\Delta K = Y(a) \sqrt{\pi a} S \quad (2)$$

where $Y(a)$ is the geometry function depending on the overall geometry of the joint including the presence and geometry of the weld, and S is the range of a far-field reference stress. For a surface crack the stress intensity factor is often written in the form suggested in [8]

$$K = (\sigma_t + H\sigma_b) \sqrt{\pi \frac{a}{Q}} F\left(\frac{a}{t}, \frac{a}{c}, \frac{c}{b}, \theta\right) \quad (3)$$

where σ_t and σ_b are remote tension and bending stresses, t is the wall thickness, c is the half crack length, b is the half-width of the cracked plate, θ is a parametric angle for the ellipse, H is a function depending on a/t , a/c and θ , and Q is the shape factor for an elliptical crack. A more direct treatment of crack growth with a two dimensional description of the crack is introduced through two coupled differential equations of the form as Eq.(1) describing the growth at the deepest point and at the surface, respectively. The shape of the crack is assumed to be semi-elliptical initially and to remain such. In the case of bridge girder details a number of stress intensity factors have been compiled in [9] for relevant AASHTO fatigue sensitive details.

For a stiffened bridge girder the growth of a crack can take place in four stages:

- from an initial defect to the penetration of the girder web
- along the stiffener-to-web weld to the tension flange
- through the flange until it is penetrated
- as a through-crack towards the ends of the flange until the total remaining intact cross section fails due to yielding.

In the first stage the crack is described as a surface crack and a two-dimensional crack description is employed. In the second stage with a through-crack, a one-dimensional description is used, in the third stage a two-dimensional description is again used, while a one-dimensional description is used in the fourth stage. The main part of the life time is spent in stage 1, but the other stages are of importance in connection with the possibility of crack detection before failure. In an experimental study, [7], on large scale plate girders, stage 1 amounted to 92% of the life time.

By combining Eqs.(1) and (2), the number of cycles N_1 to reach a crack size a in the first stage is

$$N_1 = \frac{1}{CS^m} \int_{a_0}^a \frac{dx}{Y(x)^m (\sqrt{\pi x})^m} \quad (5)$$

where $\overline{S^m}$ is the average value of the m th power of the stress ranges. The number of cycles before the crack has extended through the thickness of the web is determined with a equal to the thickness. The number of cycles N_2-N_4 in stages 2-4 are determined similarly, when a suitable initial condition is applied for each stage. The failure criterion becomes

$$M = N_1 + N_2 + N_3 + N_4 - vT \leq 0 \quad (6)$$

where v is the frequency of load cycles, and T is the considered time period. M is called the safety margin.

3. RELIABILITY ANALYSIS

Many of the parameters entering the analysis can not be assessed with certainty, and in fact large uncertainties are present for some parameters. It is of importance to account for these uncertainties, and probabilistic methods provide tools for this. Each parameter is described as a random variable of a certain distribution type and with a mean value and coefficient of variation. The probability that the failure criterion in Eq.(6) is exceeded can then be computed, e.g by first- or second-order reliability methods (FORM and SORM), [10]. These methods are particularly useful as they are directly based on an available deterministic description of crack growth, they are fast, and besides a reliability measure they as a by-product provide importance factors for each source of uncertainty and sensitivity factors for each input parameter. It is thus directly clear which of the uncertainty sources are of highest importance, and without a re-analysis it is possible to give the change in reliability from a change in a deterministic design parameter or a statistical input parameter. FORM and SORM methods are easily extended to compute the probability and sensitivity factors for a parallel system $\{M_1 \leq 0 \cap M_2 \leq 0 \cap \dots \cap M_k \leq 0\}$. The reliability is generally expressed in terms of the reliability index β , which is defined as

$$\beta = -\Phi^{-1}(P_F) = -\Phi^{-1}(P(M \leq 0)) \quad (7)$$

where the failure probability P_F is the probability for the event defined in Eq.(6), and $\Phi(\cdot)$ is the standard normal distribution function.

4. INSPECTION RESULTS, EVENT MARGINS AND RELIABILITY UPDATING

The influence of in-service inspection results is introduced in the reliability analysis. Let an inspection be performed at time T_1 and a crack size A_1 be measured.

$$a(T_1) = A_1 \quad (8)$$

A_1 is generally random due to measurement error and/or due to uncertainties in the interpretation of a



measured signal as a crack length. Measurements of the type in Eq.(8) can be envisaged for several times. For the j th measurement an event margin H_j can be defined similarly to Eq.(5) as, [11]

$$H_j = \int_{a_0}^{A_j} \frac{da}{Y(a)^m (\sqrt{\pi a})^m} - C \bar{S}^m v T_j = 0 \quad (9)$$

This event margin is zero due to Eq.(8).

A second type of inspection result is that no crack is detected. For an inspection at a time T_i this implies

$$a(T_i) \leq A_d \quad (10)$$

expressing that the crack size is smaller than the smallest detectable crack size A_d . A_d is generally random since a detectable crack is only detected with a certain probability depending on the crack size and on the inspection method. The distribution for A_d is provided through the probability of detection curve (pod curve) for which experimental results exist for various inspection methods. Figure 1 shows experimental data and a pod curve for magnetic particle inspection (MPI).

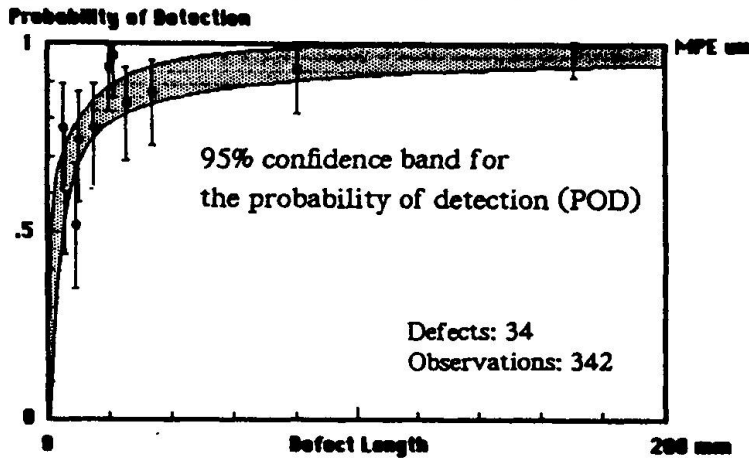


Fig. 1 Inspection reliability for MPI

Information of the type in Eq.(10) can also be envisaged for several times. For the i th measurement of the form in Eq.(10), an event margin H_i can be defined as, [11]

$$H_i = \int_{a_0}^{A_d} \frac{da}{Y(a)^m (\sqrt{\pi a})^m} - C \bar{S}^m v T_i \quad (11)$$

This event margin is negative when a crack is detected and positive when no crack is detected.

With one performed inspection where no crack is detected, the updated failure probability is

$$P(M \leq 0 | H_i \geq 0) = \frac{P(M \leq 0 \cap H_i \geq 0)}{P(H_i \geq 0)} \quad (12)$$

Evaluation of the reliability of a parallel system (numerator) and a component (denominator) are thus required, and a FORM or SORM analysis can be directly applied.

With one inspection result of the type in Eq.(8) the updated failure probability is

$$P(M \leq 0 | H_j = 0) = \frac{\frac{\partial}{\partial x} P(M \leq 0 \cap H_j \leq x)}{\frac{\partial}{\partial x} P(H_j \leq x)} \quad (13)$$

where the derivatives are computed at $x=0$. An evaluation of the sensitivity factor for a parallel system (numerator) and a component (denominator) are thus required, and a FORM or SORM analysis can be

directly applied. The analysis is easily generalized to simultaneous consideration of several inspection results.

The interest is now on updating after repair and it is assumed that a repair takes place at time T_{rep} when a crack size a_{rep} is observed. An event margin H_{rep} is defined as

$$H_{rep} = \int_{a_0}^{a_{rep}} \frac{da}{Y(a)^m (\sqrt{\pi a})^m} - C \bar{S}^m \sqrt{v} T_{rep} = 0 \quad (14)$$

The crack size present after repair and a possible inspection is a random variable a_{new} and the material properties after repair are m and C_{new} . The safety margin after repair is M_{new}

$$M_{new} = \int_{a_{new}}^{a_c} \frac{da}{Y(a)^m (\sqrt{\pi a})^m} - C_{new} \bar{S}^m \sqrt{v} (T - T_{rep}) \quad (15)$$

where a_c is the critical size. The updated failure probability is

$$P(M_{new} \leq 0 | H_{rep} = 0) = \frac{\frac{\partial}{\partial x} P(M_{new} \leq 0 \cap H_{rep} \leq x)}{\frac{\partial}{\partial x} P(H_{rep} \leq x)} \quad (16)$$

where the derivatives are computed at $x=0$.

4.1 Example 1 - Cover plate

A 32 mm welded cover plate terminus (AASHTO category E, [12]) on a plate girder has been analysed. This cover plate is similar to the cover plates which were observed to develop cracks after only 12 years of service on the Yellow Mill Pond Bridge in Connecticut [9]. Table 1 shows the distributions for each of the random variables used in the reliability analysis and the subsequent updating. Failure was defined as the development of a through crack longer than 220 mm. Inspection times were chosen as the times when the reliability index fell below the value 2.0, i.e. when the failure probability in the period from the latest inspection became larger than 2.3%.

Quantity	Distribution
Effective stress (\bar{S}^m) ^{1/m}	Normal, $\mu=9.6$ MPa, COV=20%
Material constant C	Lognormal, $\mu=1.3 \cdot 10^{-8}$ MPa \sqrt{m} , COV=7%
Material constant m	Normal, $\mu=3.2$, COV=2%
Correlation coefficient $\ln C$ and m	$\rho=-0.97$
Initial crack size a_0	Lognormal, $\mu=0.05$ mm, COV=11%
Number of trucks per day	Normal, $\mu=5700$, COV=10%
Fixed values	
Final crack size	110 mm
Crack aspect ratio	0.25
Thickness of cover plate	32 mm
Thickness of flange	32 mm
Width of flange	420 mm
Thickness of web	19.3 mm
Weld size	12.7 mm

Table 1: Yellow Mill Pond Bridge Data

Figure 2 shows the reliability index as a function of service time with no inspection (curve marked limit state). The figure also shows curves obtained by updating following inspections after 24, 33, and 40 years of service. It has been assumed that none of these inspections reveal a crack. The effect of updating is

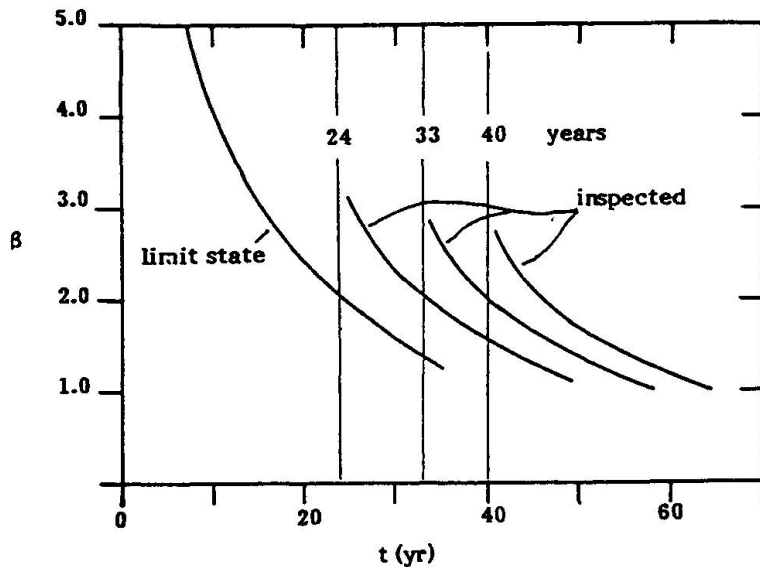


Fig. 2 Updated reliabilities for the Yellow Mill Pond Bridge.

important, but not as large as found in previous studies for offshore structures, see e.g. [11]. The main reason for this is the different behavior of the geometry function for a cover plate and a tubular joint with a high degree of local bending stresses.

The reliability of the inspection method has been expressed by an exponential pod curve

$$p(c) = F_c(c) = 1 - \exp(-c/8.9), \quad c \text{ in mm} \quad (17)$$

Such a quality is probably too optimistic for bridge inspection. With this inspection quality the probability of detecting a crack at the first inspection after 24 years is 30%. Because the crack growth rate is much higher for larger cracks, a decrease in the inspection quality (i.e. an increase in the smallest detectable crack size) causes the time between inspections to decrease and the necessary amount of inspection to increase.

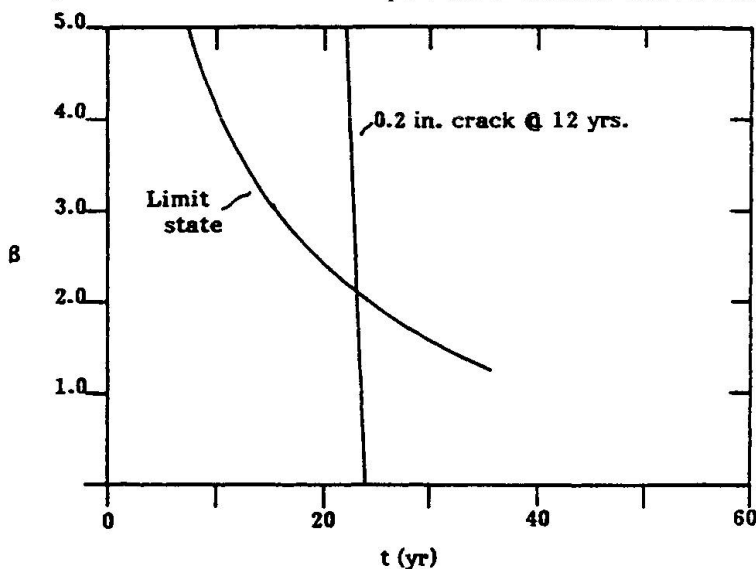


Fig. 3 Updated reliabilities for the Yellow Mill Pond Bridge when a 5 mm crack was found in the first inspection after 12 years of service.

Figure 3 shows results obtained when it is assumed that a crack of 5 mm is detected in the first inspection after 12 years of service. The reliability immediately after the inspection is elevated as the crack still has some distance to grow before failure. The drop in reliability with time is, however, very fast and a repair should be performed within a short period of time.

4.2 Example 2 - Rolled Beam

A W30×360 rolled section has been analysed at several levels of applied stress range and for a single inspection where no crack was detected. The failure criterion was the development of an edge crack of 64 mm in the flange. As in the case of the cover plate the inspection time was selected at the point where the reliability falls below the level $\beta=2.0$. Table 2 gives the applied input data, and Fig. 4 shows the reliability index for both the inspected and non-inspected detail. The inspection at 17 years lifts the reliability immediately after the inspection. The reliability level, however, soon approaches the level for the non-inspected situation and a second inspection is necessary after a few years.

Quantity	Distribution
Effective stress $(S^m)^{1/m}$	Normal, $\mu=68.9$ MPa, COV=20%
Material constant C	Lognormal, $\mu=1.3 \cdot 10^{-8}$ MPa \sqrt{m} , COV=7%
Material constant m	Normal, $\mu=3.2$, COV=2%
Correlation coefficient $\ln C$ and m	$\rho=-0.97$
Initial crack size a_0	Lognormal, $\mu=0.03$ mm, COV=48%
Number of trucks per day	Normal, $\mu=500$, COV=10%
Fixed values	
Final crack size	64 mm
Crack aspect ratio	0.67
Thickness of cover plate	43 mm
Thickness of flange	32 mm
Width of flange	423 mm
Thickness of web	24 mm

Table 2: Rolled Beam W36×360 Data

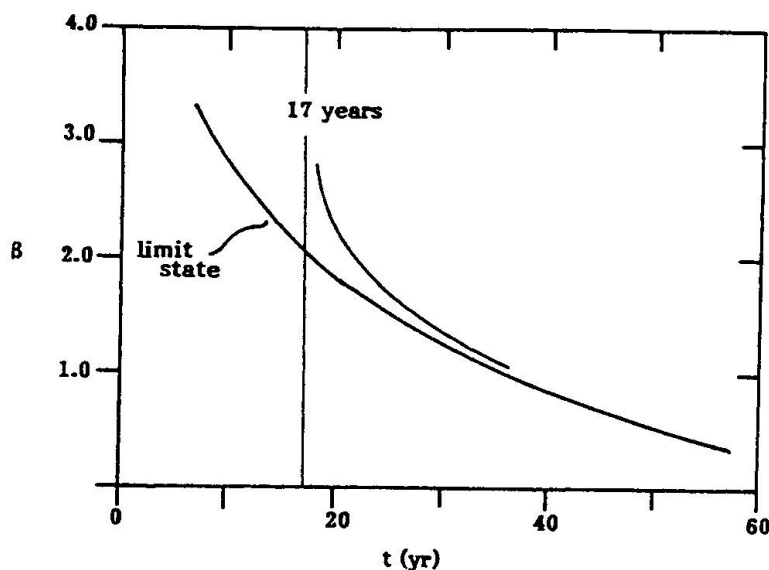


Fig. 4 Updated reliabilities for a W30×360 rolled section.

5. MAINTENANCE OPTIMIZATION

The examples have operated with a threshold value of $\beta=2$ from one inspection to the next. Such a limiting value could be specified in codes. Alternatively one can perform a formal cost optimization, minimizing the total cost of design and inspection and the expected cost of repair and failure. Such an optimization is illustrated in [13] for four different repair strategies. The optimization results in an optimal value for element thickness, inspection times and qualities and a limiting crack size for choice of repair method.



6. CONCLUSIONS

The method of reliability updating described here can be used to estimate reliabilities for fatigue sensitive details conditioned on the results of inspections which result in either no crack detection or detection and possibly also repair of a crack. Because the LEFM based fatigue analysis relates physical quantities such as crack size and stress range, the method of updating estimated reliabilities using LEFM is straight forward.

The examples showed the limited effectiveness of even fairly high quality inspections of details for which a short fatigue life had been observed. Because the inspection quality used for bridges is such that only rather large cracks are detected, the effect on the estimated reliability of an inspection which detects no damage is limited to a fairly short time after the inspection. The gain in reliability is shorter than experienced for analysis of offshore jacket structures.

The example of the inspection resulting in a crack detection gave updated reliabilities which quickly fell off following the discovery of the crack. In such a case, the rate of decrease of the estimated reliability can be used to determine the available time for repair in order to maintain an acceptable level of safety.

Acknowledgement

The work was supported in part by the research program "Reliability of Building Structures" sponsored by the Danish Technical Research Council.

REFERENCES

1. GALAMBOS, C.F., Bridge Design, Maintenance and Management. Public Roads, Vol. 50, No. 4, 1987.
2. MOSES, F., Probabilistic Load Modelling for Bridge Fatigue Studies. Proceedings, IABSE Colloquium on Fatigue of Steel and Concrete Structures, Lausanne, Switzerland, 1982.
3. NYMAN, W. and MOSES, F., Calibration of Bridge Fatigue Design Model. Journal of Structural Engineering, ASCE, Vol. 111, No. 6, 1985.
4. FISHER, J., Fatigue and Fracture in Steel Bridges - Case Studies. John Wiley & Sons Inc., New York, 1984.
5. YAZDANI, N. and ALBRECHT, P., Risk Analysis of Fatigue Failure of Highway Steel Bridges, Journal of Structural Engineering, ASCE, Vol. 113, No.3, 1987.
6. PARIS, P. and ERDOGAN, F., A Critical Analysis of Crack Propagation Laws. Journal of Basic Engineering, ASME, Vol.85, 1963.
7. WESSEL, H.-J. and MOAN, T., Fracture Mechanics Analysis of Fatigue in Plate Girders. Proceedings, 13th IABSE Congress, Helsinki, 1988.
8. NEWMAN, J.C. and RAJU, I.S., An Empirical Stress Intensity Factor Equation for the Surface Crack. Engineering Fracture Mechanics, Vol. 15, No. 1-2, pp. 185-192, 1981.
9. ALBRECHT, P. and YAZDANI, N., Risk Analysis of Extending the Service Life of Steel Bridges. Maryland Dept. of Transp. Report No. FHWA/MD-84/01, 1986.
10. MADSEN, H.O., KRENK, S. and LIND, N.C., Methods of Structural Safety. Prentice-Hall Inc., Englewood Cliffs, NJ, 1986.
11. MADSEN, H.O., TALLIN, A.G., SKJONG, R. and KIRKEMO, F., Probabilistic Fatigue Crack Growth Analysis of Offshore Structures with Reliability Updating. Proceedings, Marine Structural Reliability Symposium, SNAME, Arlington, VA, 1987.
12. AASHTO, Standard Specifications for Highway Bridges. 12 th Ed., American Association of State Highway and Transportation Officials, Washington, D.C., 1977.
13. MADSEN, H.O. and SORENSEN, J.D., Probability-Based Optimization of Fatigue Design, Inspection and Maintenance. Proceedings, Integrity of Structures Symposium, Glasgow, 1990.

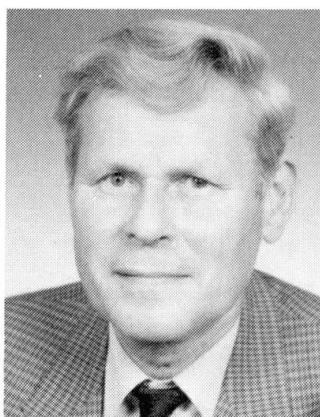
Determination of Inspection Intervals for Riveted Structures

Détermination des intervalles d'inspection pour des constructions rivetées

Bestimmung von Inspektionsintervallen für genietete Konstruktionen

H.M.C.M. van MAARSCHALKERWAART

Eng.
Netherlands Railways
Utrecht, The Netherlands



Mr. van Maarschalkerwaart, born 1927, joined the Netherlands Railways in 1948 and was, until the end of 1989, involved in the design of steel railway bridges. Over the last 10 years, he has been head of the Section for Design and Maintenance of Steel Bridges and a member of the Sub-Committee for Bridges of the UIC.

SUMMARY

Fatigue life calculations of bridges sometimes result in the conclusion that there is no remaining life while in reality, no cracks are observed. Assuming that small cracks emanating from rivet holes are present, an attempt is made to determine the length of inspection intervals in order to detect the assumed cracks before they grow to a critical size. Crack extension has been investigated using fracture mechanics methods and particularly, the severity of edge cracks is pointed out. Results of fatigue crack growth calculations are compared with available test data.

RÉSUMÉ

Les calculs de la durée de vie des ponts aboutissent parfois à la conclusion qu'il n'existe aucune durée de vie restante, alors qu'en réalité aucune fissure n'a pu être détectée. Sous l'hypothèse qu'il existe des petites fissures provenant des trous des rivets, une tentative de détermination de la durée des intervalles d'inspection est faite dans le but de détecter les fissures possibles avant qu'elles n'atteignent une dimension critique. La propagation de la fissure a été analysée à l'aide des méthodes de la mécanique de la rupture, et plus particulièrement en mettant l'accent sur la sévérité des fissures de bord. Les résultats des calculs de la propagation de fissures de fatigue sont comparés avec les résultats d'essai à disposition.

ZUSAMMENFASSUNG

Oft folgt aus der Berechnung der Ermüdungslebensdauer einer Brücke, dass deren Restlebensdauer erschöpft ist, obwohl am Objekt selbst noch keine Risse beobachtet werden können. Vorausgesetzt kleine, von Nietlöchern ausgehende Risse vorhanden sind, wird versucht, die Länge der Inspektionsintervalle so zu bestimmen, dass diese Risse entdeckt werden können, bevor sie eine kritische Grösse erreichen. Mit Hilfe bruchmechanischer Berechnungsmethoden wird die Rissausbreitung untersucht. Auf die Gefährlichkeit wird besonders von Kantenrissen hingewiesen. Die Rissausbreitungsberechnungen werden mit Versuchsergebnissen verglichen.



1. INTRODUCTION

Judging old bridges it may occur that fatigue life calculations result in the conclusion that a bridge has exceeded its theoretical fatigue life.

Even when conservative assumptions are corrected by results of stress measurements there may be situations of a calculated negative life while in reality in a bridge no cracks are present. This situation especially can occur when little is known about previous loading and safe assumptions have to be made for that. In such cases bridges have to be inspected frequently.

Starting from an actual situation that no cracks have been found, but assuming a certain crack length in the most critical bridge elements, it is tried in this paper to define the length of inspection intervals within which the assumed crack does not grow to a critical size.

For that, fracture mechanics methods may be helpful. While in early times many bridges have been built as riveted structures, fatigue crack propagation behaviour of these structures forms an important aspect judging the reliability.

2. FATIGUE CRACK GROWTH OF WROUGHT IRON AND EARLY MILD STEEL

In order to determine a safe inspection interval one needs information about crack propagation.

The crack growth rate da/dN is described by the Paris power law.

$$\frac{da}{dN} = C \cdot \Delta K^m \quad (1)$$

where ΔK is the range of the stress intensity factor. C and m are constants. To define the crack growth rate, fatigue crack growth tests were carried out with center-cracked specimens of early steel.

Figure 1 shows the results presented as a relationship between the crack growth rate, da/dN , and the range of the stress intensity factor ΔK .

Adopting for the constant m the value $m = 3$, for the constant C was found $C = 4 \cdot 10^{-13}$ for the upper bound, and $C = 1 \cdot 10^{-13}$ for the lower bound.

Fatigue crack growth tests were also carried out with specimens made of wrought iron. The results are shown in figure 2.

It can be seen from this figure that there is a great scatter. At lower values of ΔK the crack growth is slower than that of early steel.

At higher values of ΔK the maximum magnitudes of the crack growth rate are close to the upper bound of early steel.

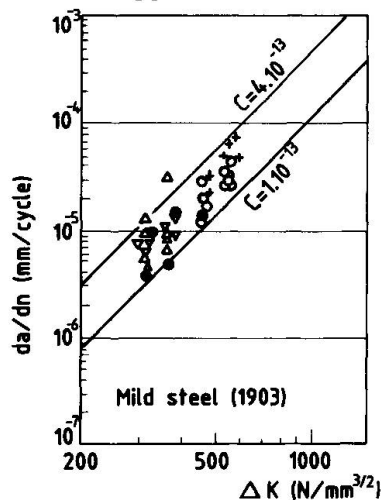


Fig 1 Relationship between crack growth rate da/dN and ΔK of early mild steel.

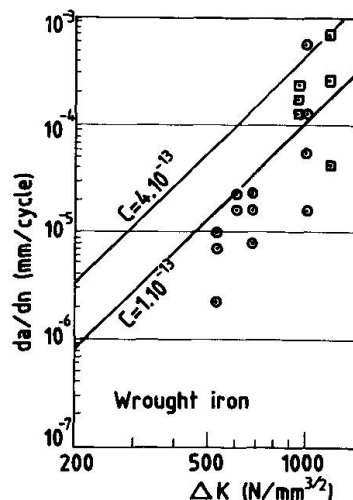


Fig 2 Relationship between crack growth rate da/dN and ΔK of wrought iron.

3. FATIGUE CRACK PROPAGATION ANALYSIS OF RIVETED COMPONENTS USING FRACTURE MECHANICS

3.1 Fatigue crack growth of several configurations

Fatigue cracks in riveted structures generally emanate from rivet holes at stages most subjected to tension.

However in the case of sections deteriorated by corrosion, cracks can develop at edges with reduced area. In particular also components subjected to tension are sensitive for that.

In the present study the effect of force redistribution to other section components during crack extension is neglected.

The conservative assumption is made that, having a built up member, all parts simultaneous start to crack at the same location, at both sides of a hole, and redundancy is not taken in account.

In order to evaluate fatigue-crack growth of several configurations numerical analysis were carried out using equation (1) with values of $C = 4 \cdot 10^{-13}$ and $m = 3$.

As constant amplitude loading a stress range of $\Delta \sigma = 75 \text{ N/mm}^2$ (gross section) was chosen.

For the initial crack at the hole two opposing cracks with a size of $a = 16 \text{ mm}$ were assumed, being a situation of appear of the crack just beyond the rivet head.

Cracks at rivet holes nearest to the edge of members were assumed to be most severe (excentric crack in a plate).

To determine the influence of the edge distance of the rivets, in one example the edge distance was varied.

To define the values of ΔK the correction factors $F(a)$ for excentric cracks were taken from literature [1].

The results of the calculations are shown in figure 3. The extension of the cracks is plotted against the number of cycles.

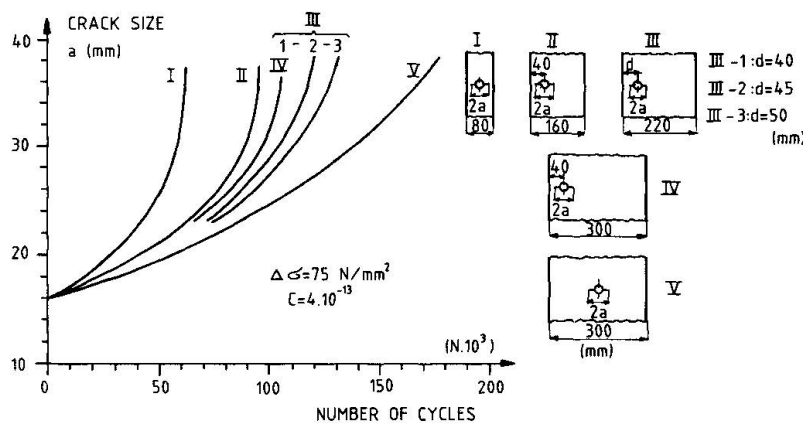


Fig. 3 Crack growth curves of several configurations. Cracks emanating from unloaded rivet holes.

To represent situations of cracks developing at edges affected by corrosion, or to evaluate cases when cracks emanating from rivet holes have reached edges, numerical analyses were also carried out for the chosen configurations assuming edge cracks.

The results are shown in figure 4.

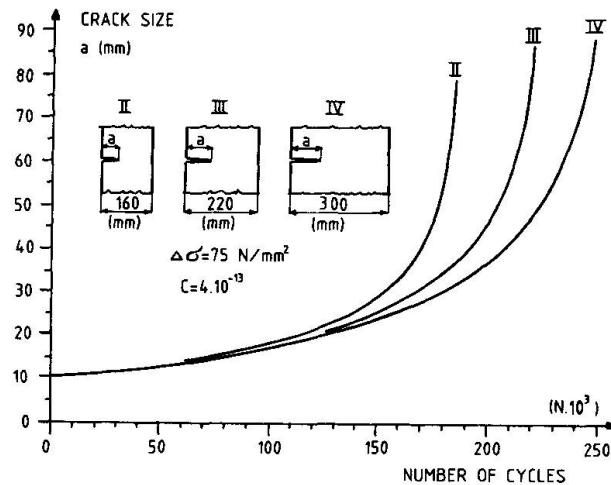


Fig. 4 Crack growth curves of several configurations. Edge cracks.

3.2 Influence of loaded rivets on crack growth

In the preceding part crack growth has been evaluated in riveted components having rivets with a function of only clamping.

In cases of shear forces or connections, rivets transmit load, and pressure on the holes is involved.

The case of a crack with internal pressure is described in literature [1].

The stress intensity factor for a finite plate with a loaded rivet hole can be obtained by superposition of the stress intensity factor of a plate with a crack and the stress intensity factor of a plate with a hole with internal pressure and two cracks [2].

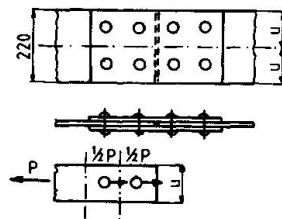


Fig. 5 Configuration of the investigated example with loaded rivets.

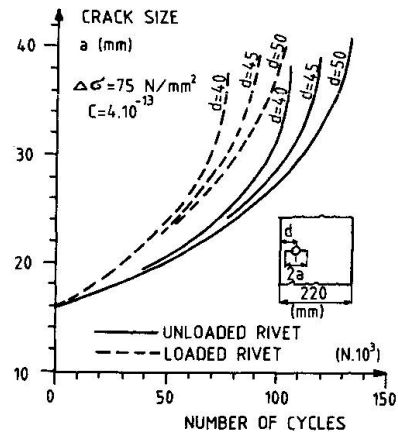


Fig. 6 Crack growth curves. Comparison between loaded and unloaded rivets. Influence of different edge distances.

To show the influence of the pressure on a rivet hole an example of a fracture mechanics calculation is given for a configuration with a width of 220 mm (fig. 5).

The conservative assumption is made that, dividing the component in gage strips, there are two rivets in a line, and one rivet transmits half the load, while in the strip itself half the load is present already.

The results of this calculation are shown in fig. 6.

3.3 Examination of fracture mechanics analysis

As can be seen in the figures 3, 4 and 6 the computed crack propagating life, starting from the initial crack size $a_i = 16$ mm, is relatively short.

Reaching the edge the crack size becomes critical. Increase of edge distance shows an increase of the number of cycles previous to reach the critical crack size.

When the crack has grown to the edge, there is a transition of the crack geometry into an edge crack.

Considering an edge crack with a size of about 80 mm, it can be seen from figure 4 that in this stage the remaining life is very short.

For lower or higher stress ranges the critical crack size has the same value, only the number of cycles to reach the critical crack size differs.

4. DETERMINATION OF INSPECTION INTERVALS

Determining inspection intervals it is important to know how long it will take the crack to grow from the minimum detectable size to the critical size.

Experience [3] has indicated that performing a visual inspection with the aid of a magnifying glass and good illumination, cracks can be detected when they appear about 10 mm beyond the rivet head.

Such a crack means a size of about $a = 26$ mm.

To evaluate an inspection interval a crack propagation of $a_i = 28$ mm to $a_j = 33$ mm is assumed. That includes a possible crack extension during the inspection interval of 5 mm.

Fracture mechanics calculations have shown that dependent on the width of the components and the edge distance of the rivets, crack sizes of $a = 35$ mm to $a = 40$ mm become critical.

It has to be pointed out that when cracks of such sizes in reality are found in primary members, repair or replacement of a bridge has to be considered.

Numerical integration of the crack growth rate description between the two crack sizes results into a SN-curve for a crack, propagating from $a_i = 28$ mm to $a_j = 33$ mm. For the constant C the value $C = 4 \cdot 10^{-13}$ is used.

$$N = \int_{a_i}^{a_j} \frac{da}{C \cdot \Delta K^3} \quad (2)$$

where $\Delta K = F(a) \cdot \Delta \sigma \cdot \sqrt{\pi a}$

$F(a)$ is a geometric correction factor.

For several configurations SN-curves are presented in figure 7, indicated by the value $\Delta \sigma$ (gross section) at $N = 2 \cdot 10^6$ cycles and a slope $m = 3$.

A fatigue limit is disregarded.





		UNLOADED RIVETS						LOADED RIVETS						
		W mm	80	160	220	220	220	300	80	160	220	220	220	300
		d mm	40	40	40	45	50	40	40	40	40	45	50	40
		$\Delta\sigma_{2.10^6}$ (N/mm ²) $a_i=28-a_f=33$ mm						$\Delta\sigma_{2.10^6}$ (N/mm ²) $a_i=28-a_f=33$ mm						
		11	13	14	15	15	14	11	13	13	14	15	13	

Fig. 7 SN-curves crack growth $a_i = 28$ to $a_j = 33$ mm for several configurations of riveted structures (mild steel).

To determine the fatigue crack propagating life, growing the crack between the two crack sizes, a representative stress spectrum with variable amplitude and a number of cycles n_s , is transformed into a spectrum with an equivalent stress range $\Delta\sigma_e$ of constant amplitude and the same number of cycles n_s , causing the same damage.

$$\Delta\sigma_e = \left[\frac{\sum n_i \cdot \Delta\sigma_i^3}{n_s} \right]^{1/3} \quad (3)$$

Using the SN-curve for the crack extension of 5 mm and the equivalent stress range $\Delta\sigma_e$ (gross section), the propagating life N can be computed.

Now the inspection interval ΔT_i has to be estimated as:

$$\Delta T_i = \frac{N}{n_s} \quad (4)$$

Only cracks visible from outside can be detected by a visual inspection. At splices internal cracks cannot be detected visually before reaching the edge and then they are unstable.

In such cases it is necessary to apply radiographic inspection methods.

5. NUMERICAL EXAMPLE

Suppose a riveted railway bridge with a span of 10 m has been in service for about 85 years.

Recalculation with the UIC-loading included dynamic increment results in a stress range $\Delta\sigma_{UIC} = 125$ N/mm² (net section).

The measured stress range spectrum yields to an equivalent stress range $\Delta\sigma_e = 25$ N/mm² (gross section) and a number of cycles $n_s = 8,9 \cdot 10^5$ per year.

Using the evaluated SN-curve with $\Delta\sigma = 15$ N/mm² at $N = 2 \cdot 10^6$ cycles and $m = 3$, the propagating life N for $\Delta\sigma_e = 25$ N/mm² is computed at $N = 4,33 \cdot 10^5$ cycles. The inspection interval is estimated at:

$$\Delta T_i = \frac{N}{n_s} = \frac{4,33 \cdot 10^5}{8,9 \cdot 10^5} = 0,5 \text{ year}$$

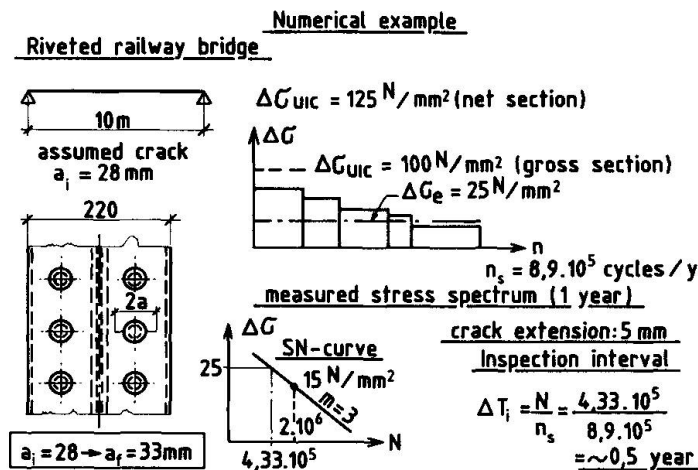


Fig. 8 Example determination inspection interval of a riveted railway bridge.

6. EVALUATION METHOD OF PREDICTION

6.1 Influence way of the crack growth

The presented method of determination inspection intervals for riveted structures is based on the assumption that cracks grow at the same time from both sides of a hole, and increase at each side with 5 mm.

Observing crack growth in practice [3], it can be seen that cracks many times emanate at first from one side of a hole, extend to the edge, and then start to grow, or increase in growing, at the other side of the hole.

The question can be posed whether the presented method is too conservative or not.

Therefore the results of the fracture mechanics analysis of one of the examples, shown in figure 3, are compared with the results of an analysis like that for the situation of an asymmetrical crack growth.

The example has been chosen of the plate with a width of $W = 220$ mm and a hole of 20 mm diameter, center 45 mm from the edge.

It is assumed that cracks with a size of 13 mm beyond the rivet head are present, being the initial crack size used for the presented method of determination inspection intervals.

Again the constant amplitude loading with a stress range $\Delta\sigma = 75$ N/mm² is chosen.

Three cases of crack growth are compared:

- symmetrical crack growth.
- asymmetrical crack growth, with cracks on both sides of the hole, but one of which hidden by the rivet head.
- asymmetrical crack growth, starting from one side of the hole, growing up to the edge, and then arrested in the hole.

The results of the fracture mechanics calculations are shown in figure 10.

To have an idea of the number of cycles to start the arrested crack, the data concerning the relationship between $\Delta K/\sqrt{\rho}$ and the number of cycles to reinitiation, known from literature [4], [5] and [6], have been used. (ρ is the radius of the hole).



This relationship is transformed into an SN-curve for the considered configuration.

The relationship $\Delta K/\sqrt{\rho}$ versus fatigue life and the SN-curve derived from that are plotted in figure 9.

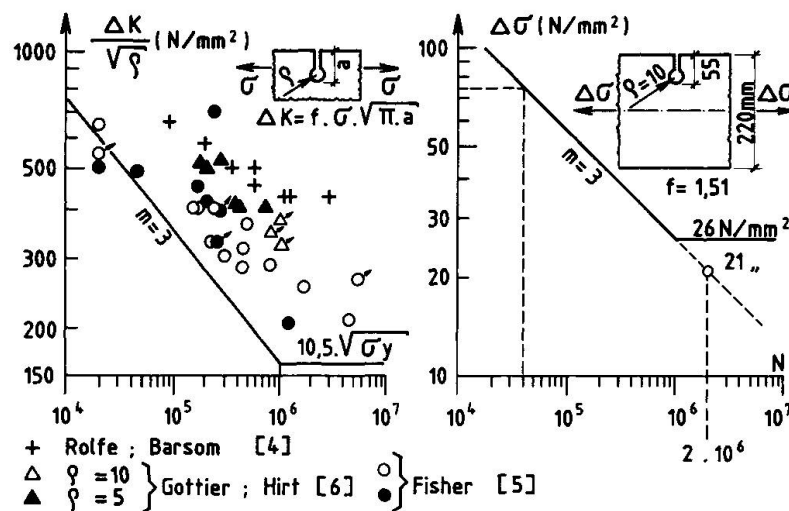


Fig. 9 Relationship $\Delta K/\sqrt{\rho}$ versus fatigue life, and SN-curve of crack initiation.

It can be seen from figure 10 that asymmetrical crack growth is more favourable concerning fatigue life than the assumed pattern of crack growth adopted for the determination of inspection intervals.

However small fatigue cracks easily can be overlooked, and then cracks may emanate up to the edge before detecting.

In that situation also the asymmetrical cracks are close to the critical size.

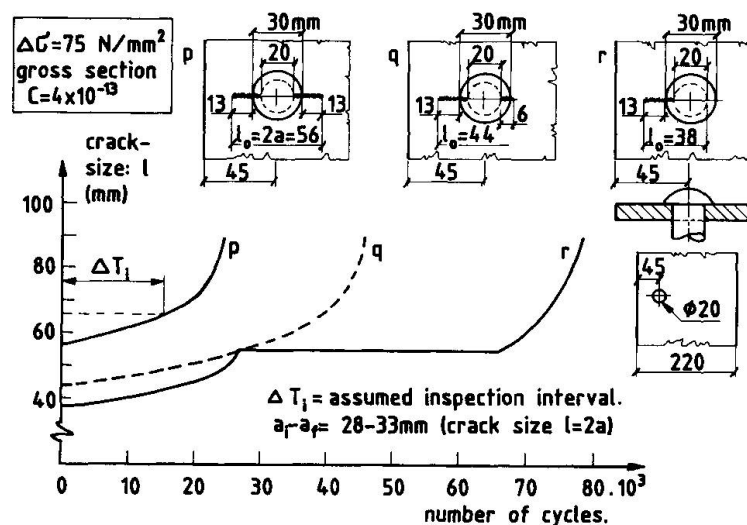


Fig. 10 Comparison influence of different ways of crack growth behaviour on fatigue life.

Even the arrested asymmetrical cracks may be close to that, while no body can see how far the initiation has proceed; unless it is sure that during the former inspection such a crack was not present. It can be seen from figure 10 that, in cases of crack growth up to the edge, the presented method of determination inspection intervals may provide a certain period in which measures can be taken just after the moment that the crack has reached the edge.

6.2 Influence value of the constant C

Variation of the crack growth constant C in the Paris equation (1) has a linear effect on the results of the calculation of the number of cycles in an inspection interval.

In this paper for the upper bound a value $C = 4 \cdot 10^{-13}$ was adopted, using units of mm for the crack size, and $N/mm^{3/2}$ for ΔK .

Figure 11 shows the influence of ranging the constants from $C = 4 \cdot 10^{-13}$ to $C = 2 \cdot 10^{-13}$, and gives a comparison with the results of a crack growth investigation during a fatigue test [3], carried out by ICOM, after growing the crack up to the edge.

The result of the calculation of the inspection interval is also given in this figure.

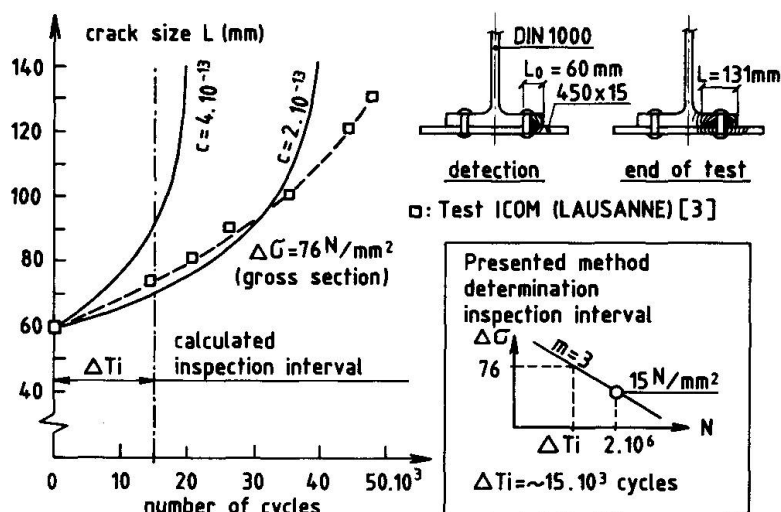


Fig. 11 Influence change of the constant C. Comparison theoretical crack growth with test results.

7. CONCLUDING REMARKS

Only cracks visible from outside can be detected by a visual inspection. In cases of splices radiographic inspection methods are necessary.

It has to be pointed out that when cracks become visible from outside, in general, the remaining life is very short.

Keeping in mind that in practice symmetric crack growth seems to be improbable, the conclusion could be that the presented method, based on the assumption of a crack extension of 5 mm at both sides of a rivet, may be conservative.



On the other hand small cracks easily can be overlooked and have grown already up to the edge before detecting.

Fracture mechanics calculations show that for the situation of asymmetric crack growth up to the edge the presented method may provide an inspection interval of sufficient length.

It has to be mentioned that a possible redundancy of a structure may be a very important factor in judging.

REFERENCES

1. ROOKE, D.P. and CARTWRIGHT, D.J.
Compendium of Stress Intensity Factors London, Her Majesty's Stationary Office (1976) London.
2. BROEK, D.
Elementary Engineering Fracture Mechanics.
Leiden, Noordhoff International Publishing (1974).
3. RABEMANANTSOA, H. and HIRT, M.A.
Comportement à la Fatigue de Profiles Lamines avec Semelles de Renfort Rivetées.
Rapport ICOM 133 (1984) Ecole Polytechnique Federale de Lausanne.
4. ROLFE, S.T. and BARSOM, J.M.
Fracture and Fatigue Control in Structures.
Prentice-Hall, Inc. 1977.
5. FISHER, J.W., MERTZ, D. and EDINGER, J.
Fatigue Resistance and Repair of Full-scale Welded Web Attachments.
Colloque International sur la Gestion des Ouvrages d'Art. Vol. 2 Ed. ENPC 1981.
6. GOTTIER, M. and HIRT, M.A.
Das Ermüdungsverhalten einer Eisenbahnbrücke.
Bauingenieur 58 (1983) p. 243-249.

Recording of Stresscollectives of a Steel Bridge

Observation des collectifs de contraintes d'un pont en acier

Erfassung von Spannungskollektiven einer Stahlbrücke

Werner BAUMGÄRTNER

Dr.-Eng.
Techn. Univ. of Munich
Munich, Fed. Rep. of Germany



Werner Baumgärtner, born 1944, received his engineering degree at the Technical University of Munich and then worked in construction offices involved in bridges and buildings. Since 1972 he has been employed by the Technical University of Munich and works in the field of structural mechanics, especially dynamics.

SUMMARY

Due to the decreasing costs of microelectronic devices in the field of measurement, it has become possible to install permanent measurement systems in structures. Indicators related to fatigue can be developed, using the hysteresis-counting-method and hypotheses of damage accumulation. These indicators give a more realistic estimation of the load history and of changes in a structure.

RÉSUMÉ

Du fait de la diminution du prix des dispositifs micro-électroniques de mesure, il devient désormais économique d'installer des systèmes de mesure permanents dans les ouvrages. Grâce à l'analyse continue de ces mesures, il est possible d'obtenir des valeurs caractéristiques relatives à la fatigue en tenant compte de la méthode de comptage des hystérèses et de l'hypothèse de cumul du dommage. Ces valeurs fournissent une estimation plus réaliste de l'historique des charges et des modifications dans la structure.

ZUSAMMENFASSUNG

Die zunehmend preisgünstigen mikroelektronischen Bausteine im Bereich der Messtechnik ermöglichen die ständige Installation von wirtschaftlichen Messsystemen an Bauwerken. Bei einer kontinuierlichen Auswertung der Messdaten unter Berücksichtigung der Spannungshysteresen-Zählmethode und von Schadensakkumulationshypothesen lassen sich anschauliche, ermüdungsrelevante Indikatoren ermitteln. Diese werden zu wirklichkeitsnahen Einschätzungen von Belastungsgeschichten und Strukturveränderungen genutzt.



1. INTRODUCTION

Steel constructions with severe changes in the load, such as bridges, masts and cranes have to be analysed with respect to fatigue strength. In the planning stage assumptions have to be made for the load and for the structure. The maximum stress of the connecting element between the main girder and the traverse stiffening as shown in fig. 1 can be determined with a relatively high reliability. The stress-collective, however, which is a basic assumption to calculate the fatigue strength, can be estimated only approximately. The reason for this are influences such as the quantity and load spectra of the traffic, the roughness of the bridge-surface and the dynamic reaction of the coupled system composed of structure and moving vehicle.

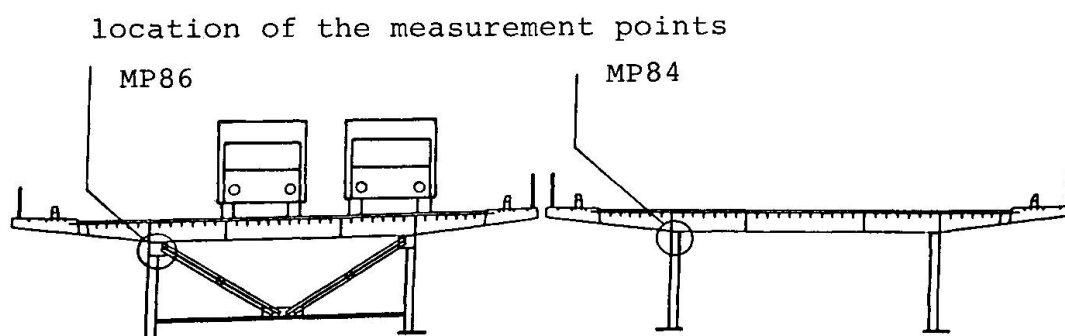


Figure 1: Cross-section of a steel bridge with transverse bracing

The surveillance of road bridges in the Federal Republic of Germany is done by inspections according to the code DIN 1076 "Ingenieurbauwerke im Zuge von Straßen und Wegen". The intention of this paper is to show how to support these inspections by the determination of indicators based on permanent measurements. The proposed procedure uses counted hysteresis-loops to provide information concerning the traffic and the structure.

Due to the decreasing costs of microelectronic devices such as processors, analogue-digital-converters and storage elements, it becomes economical to install permanent working measurement systems in constructions. The permanent observation based on measured data is already in use in special constructions such as off-shore platforms. By standardising the measuring unit and the service programs, it would be possible to observe a certain amount of constructions with respect to stress. In order to avoid a flood of data, indicators have to be determined so that changes can be detected easily. The idea of a consistent observation of structures in use is being more frequently discussed in public, e.g. at the symposium of the IABSE 1989 in Lisbon "Reliability of structures"/3/ or in the area of quality control/5/.

2. DERIVATION OF AN INDICATOR RELATING TO FATIGUE STRENGTH

The best way to estimate a construction with respect to its dynamic reaction or its fatigue-relevant behaviour is the analysis based on parameters obtained by parametric identification of the finished construction. Experience shows this method is restricted because of the great effort and the limited accuracy of the results received for the substructures for which fatigue strength is dominant.

2.1 Reducing of measurement data with the HCM-algorithm

A relatively good estimate of the dynamic behaviour of the stress of a substructure can be obtained by permanent observation of the strains with attached strain gauges. Using several measurement points in the area of the connection between the transverse bracing and the main girder the dynamic behaviour of this substructure can be described rather well. With a chosen sample frequency of 400 Hz one measurement point yields $1.44 \cdot 10^6$ values in an hour.

When fatigue strength monitoring of a structure is the main topic data reduction can be obtained by using the hysteresis counting method (HCM) /1/. With a division in 64 classes of the stress cycle parameters, namely the stress range and the mean value, a reduction factor of 350 for the storage can be reached. The original record for a time period was therefore replaced by a hysteresis matrix. The fatigue-relevant effect caused by traffic can be observed with the help of the stored matrix. Derived stress collectives (stress range spectra) include the effects of traffic and the real reaction of the structure and are very useful for checking the assumptions made in the stage of design.

2.2 Further reduction of data with damage accumulation hypotheses

Through an installation of a bigger amount of measurement points and a longer time period for measurement, it makes sense to store indicators which comprise a further data reduction. With respect to a fatigue-relevant consideration, we use damage accumulation hypotheses. The increment in the damage for a time step is named indicator S , the accumulated value is named ΔS .

With this method the hysteresis matrices are available in short time increments of about 2 minutes and therefore also nonlinear accumulation hypotheses can be used, which estimate the load history in a more realistic way.

For test purposes 8 different hypotheses are used simultaneously. There is a detailed description given in /7/. The hypotheses H6 and H8 are linear according to the specifications of the Deutsche Bundesbahn DS804 and the code EC3 of the European community.

The hypothesis H7 takes into account the decrease of the constant amplitude fatigue limit with the increase of the damage according to Haibach /4/ and Reppermund /8/. This hypothesis is therefore nonlinear.

Taking into account different detail categories along with the different damage hypotheses leads to an additional variation of the indicator S . Using all together 30 variations of S the need for storage is further reduced by a factor of 120.

The temporal development of the indicators S and ΔS shows the effect caused by the traffic in a clear way and can be evaluated numerically (see fig.5).



3. PERFORMANCE OF THE MEASUREMENT

For use in the laboratory and in a construction (see part 4 of this paper) a measurement assembly was established consisting of plain microelectronic elements. The design takes into account the fact that we want to operate with self-developed programs on the measured data during the running measurement. An additional advantage for a custom made measurement assembly is the reasonable price.

Purchaseable measurement units which can provide hystereses matrices in a permanent way are used in airplane and motor car construction. Applications in the field of civil engineering are not known to us.

3.1 Hardware

To perform measurements a personal computer was used with an installed analogue-digital converter unit. The evaluation was also performed with a personal computer.

3.2 Measurement software

Menu-driven preliminary programs compute facts for the calibration, provide data for the chosen accumulation hypotheses and the detail categories and ask for parameters such as sampling frequency, time increments for storing the indicators and the number of the classes for the HCM.

During the measurement the digital signals are analyzed continuously by the HCM-algorithm and the results are stored in matrices. The installed configuration can serve 4 channels with a sample frequency of 400 Hz. The greatest number of classes for storing the hysteresis cycles is 64x64.

In short time steps the program computes the indicators DS with respect to 8 different accumulation hypotheses. After chosen time periods, e.g. 1 hour, the indicators S and the accumulated hystereses matrices were stored, as well as the highest and lowest values of the stress. Based on the stored extreme values of the stress, the greatest loads within each time period can be identified with an accuracy of 10 seconds.

3.3 Evaluation software

To convert the stored data to other formats, to display them graphically (see fig. 4) and to store them in a data bank, a menu-driven service program system was developed. With these programs it becomes possible to check measurement results immediately after measurement.

For longer observations it seems sufficient for most of the measurement points to store only the indicators S and the extreme values of the stress. According to information from the "Oberste Baubehörde Bayerns" this volume of data can be stored within the data bank for the existing buildings.

4. APPLICATION TO A STEEL HIGHWAY BRIDGE

4.1 Struktur

During an inspection of a steel highway bridge crossing the Danube river cracks were detected (see fig. 1). In order to design a rehabilitation concept measurements using strain gauges were performed. The aim of a special measurement task was to investigate the stress collectives for different points of the structure and to compare them at different times.

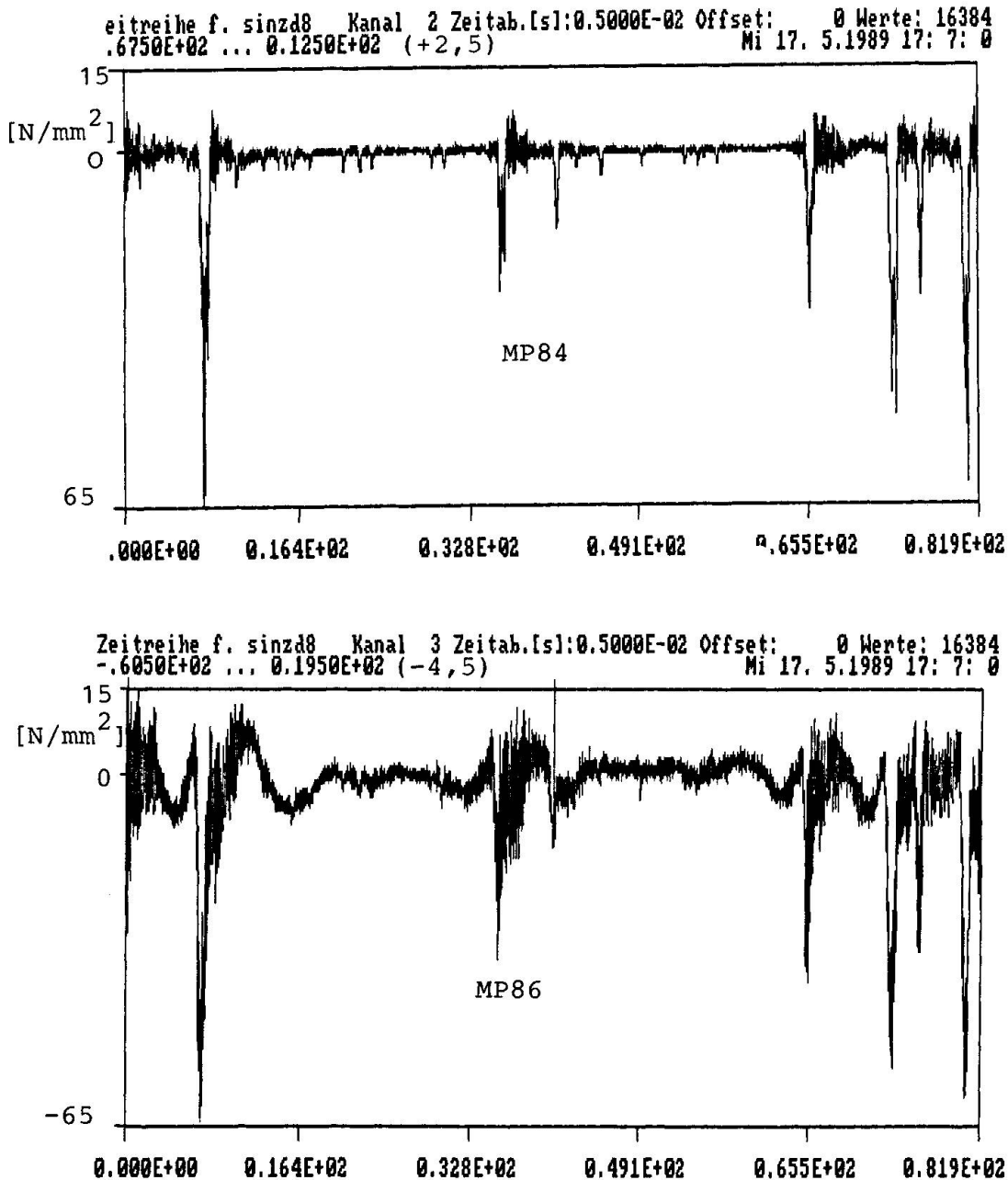


Figure 2: Stress records of MP84 and MP86



4.2 Results of the dynamic measurement

In the spring of 1989 measurements were performed for several days. Before and after the measurements with the HCM-concept the strain in time was recorded for control purposes. Figure 2 shows parts of 2 typical records. After the measuring points in the direction of the traffic were separated by only 3 meters and simultaneously measured, the same traffic load can be assumed. Whereas the maximum value for the compressive stress in both records is nearly the same, the record of point MP86 is more turbulent.

4.3 Stress collectives (stress range spectra)

During the measurements which lasted several days, the hysteresis matrices were stored after each hour, along with the extrem values of the stress and the times of their appearance. Measured stress collectives which are not yet normalized are presented in figure 3. The full lines represent a measurement lasting 96 hours, the dotted lines represent another measurement lasting 61 hours. The comparison of the measurement points shows a higher portion of greater stress values in the curve for the point MP86.

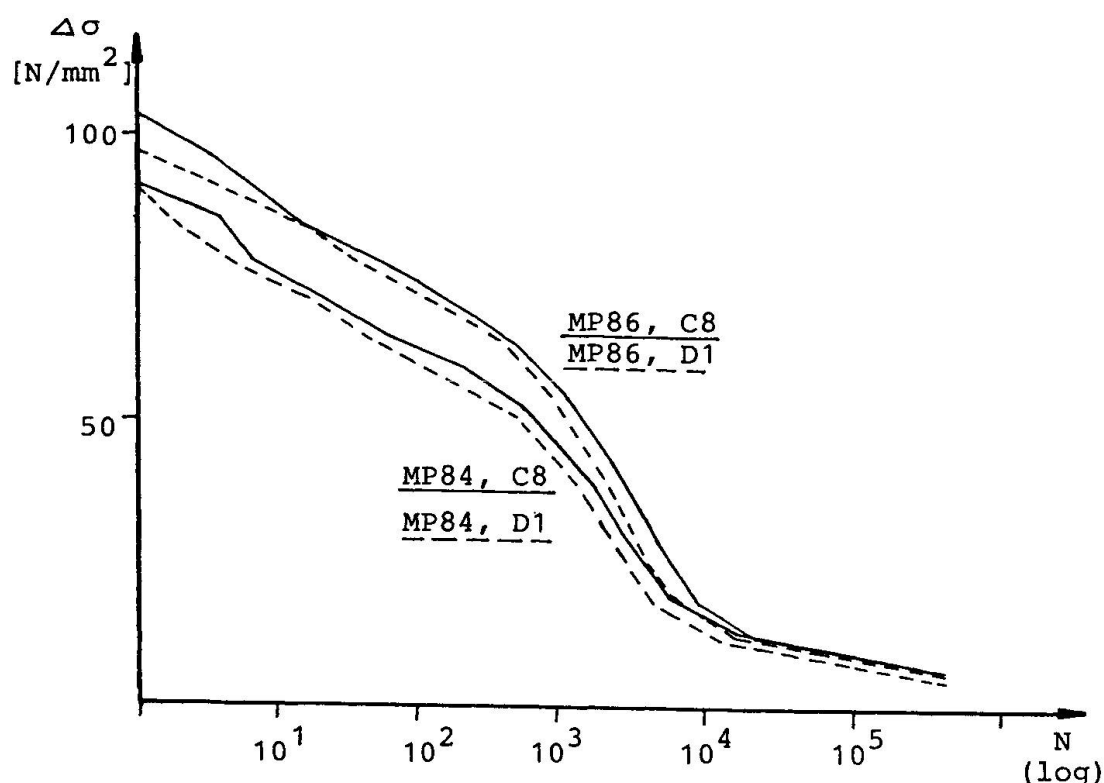


Figure 3: Stress collectives

4.4 Indicators S and ΔS

For a numerical and a clearly arranged evaluation of the stress of the measurement points, the indicators as described in section 2 are very suitable. As to be seen in figure 4, the curves belonging

to different damage accumulation hypotheses are qualitatively rather similar for a short time interval. An average detail category was chosen for the presented results. The stress values of the measuring points without a traffic load was not known and assumed to be zero.

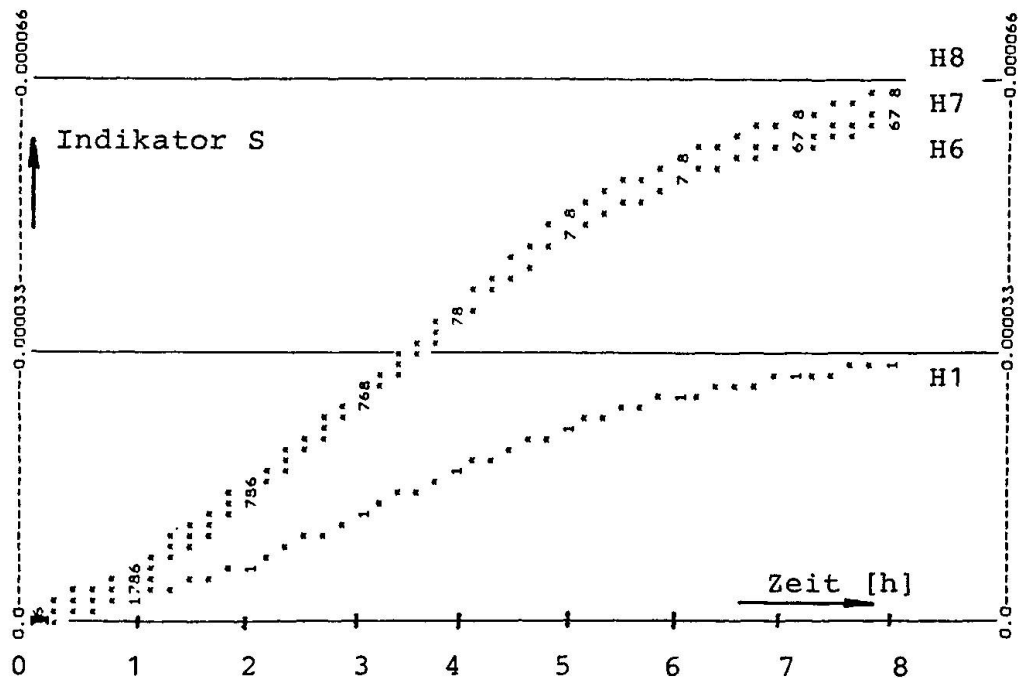


Figure 4: Curves of S for different accumulation hypotheses

Figure 5 presents the indicators S and DS resulting from a measurement starting on May 14. In the night of the 15th to the 16th a sudden increase was detected. An important reason for that could be the ban of trucks during the Pentecostal holidays till the 15th. The loading of the bridge can be estimated very clearly by the indicator ΔS . The other measurement points and the other accumulation hypotheses showed similar results.

The comparison of the fatigue strength of the measured elements of the structure represented by MP84 and MP86 using the indicator S yields the following data:

measurement of	MP 64	MP86
May 10 to 14; 96 hours	100%	293%
May 14 to 17; 61 hours	100%	305%

Although the maximum compressive stress of MP84 and MP86 was very similar, the fatigue strength according to the presented measurement differs by the factor 3.

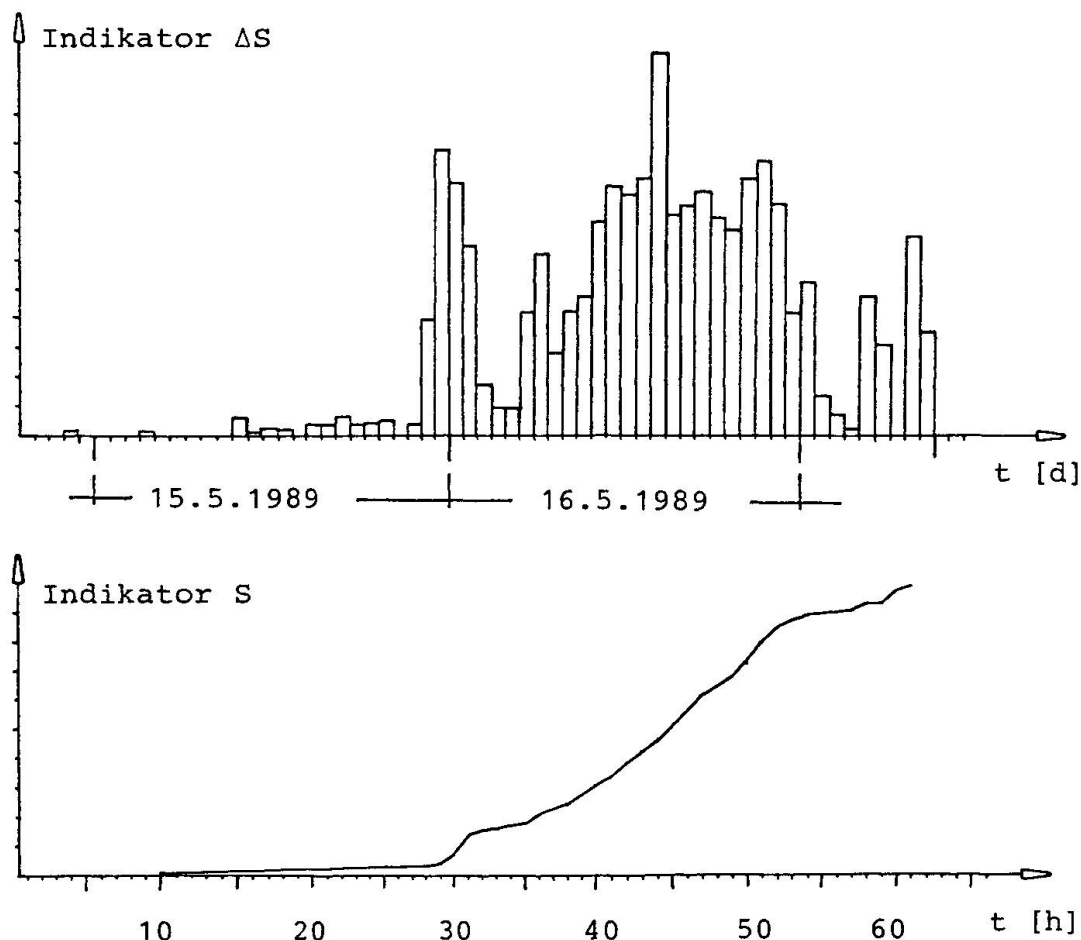


Figure 5: Indicators ΔS and S (61 hours)

4.5 Evaluation of the measurement results

On the basis of the above explanations, it can be said that measurements covering a long time period can lead to a better estimate of the loading due to traffic with respect to fatigue strength. Quantitative statements, based on traffic load models and a dynamic analysis of a structure can be effectively added. These ideas can indicate which construction parts need more or less inspection.

5. FINAL REMARKS

The method presented here is not restricted to steel constructions, but can also be used for the observation and inspection of concrete structures. An important consideration here is the selection of adequate sensors, for which are new economical developments.

With the increasing variety and reduction in cost of microelectronic components in the area of measurements and data analysis, permanently installed measurement systems can be used in a greater number of structures. These systems can contribute to an estimate of the state of the structure without damaging it and therefore to

quality control.

The following is a summary of some advantages resulting from the permanent observation of the stress of a construction:

- Large discrepancies between the calculated stress and actual stress as well as major defects can be detected in an early stage.
- A control for the stress collective used in design is given.
- Changes and damages of the observed elements of the structure can be detected by comparing the measurement results with reference values.
- The loading of the structure as a result of traffic and the changes of the traffic in the course of time can be quantified. These results of the permanent measurement can be partly transferred to other bridges in the same highway.
- Data concerning the stress cycles are available for a later assessment of the structure with respect to rehabilitation or changes in traffic patterns.
- For future constructions updated data concerning the stress collectives is available.
- Nonlinear damage accumulation hypotheses can be tested under realistic stress histories in comparison to more conventional ones.

REFERENCES

1. CLORMANN U.H., SEEGER T., Rainflow-HCM; Ein Zählverfahren für Betriebsfestigkeitsnachweise auf werkstoffmechanischer Grundlage. Der Stahlbau, 3/1986.
2. FRANKE L., Schadensakkumulationsregel für dynamisch beanspruchte Werkstoffe und Bauteile. Der Bauingenieur 60(1985).
3. IVBH-Symposium, Dauerhaftigkeit der Bauwerke. Lissabon 1989.
4. HAIBACH E., Modifizierte lineare Schadensakkumulations-Hypothese zur Berücksichtigung des Dauerfestigkeitsabfalls bei fortschreitender Schädigung. Techn. Mitt. Nr. 50/70 des Lab. f. Betriebsfestigkeit, Darmstadt 1970.
5. MAIDL B., VON GERSUM F., Qualitätssicherung im Bauwesen, ein Thema, dem wir uns stellen müssen. Bauingenieur 64 (1989).
6. REPPERMUND K., Probabilistischer Betriebsfestigkeitsnachweis unter Berücksichtigung eines progressiven Dauerfestigkeitsabfalls mit zunehmender Schädigung. Diss. Hochschule der Bundeswehr, München 1984.
7. WAUBKE H., Kontinuierliche Erfassung von Schwingungsbeanspruchungen mit paralleler Ermüdungsbewertung unter Berücksichtigung von nichtlinearen Schadensakkumulationshypothesen. Dipl.Arbeit Nr. 29, Lehrstuhl für Baumechanik, München 1988.

Leere Seite
Blank page
Page vide

Life Extension of Steel-Girder Bridges on the Tomei Expressway

Prolongation de la durée de vie de ponts en acier de l'autoroute Tomei

Lebensdauerverlängerung von Stahlbrücken der Tomei-Schnellstrasse

Chitoshi MIKI

Associate Professor
Tokyo Institute of Technology
Tokyo, Japan

Seiji OHKAWA

Manager of maintenance
Japan Highway Public Corporation
Kawasaki, Japan

Hiroyuki TAKENOUCHI

Research Chief
Constr. Methods Res. Inst.
Fuji, Japan

Nobutoshi MASUDA

Associate Professor
Musashi Inst. of Technology
Tokyo, Japan

SUMMARY

Some steel bridges on Tomei Expressway have experienced distortion-induced fatigue cracking. Fatigue cracking, stress measurement, retro-fitting methods and structural improvements, performed for life extension of this highway, are described in this paper.

RÉSUMÉ

Quelques ponts en acier de l'autoroute Tomei (Japon) ont montré des fissures de fatigue dues à la torsion. Cet article présente les caractéristiques de ces fissures de fatigue, les mesures des contraintes, les procédés de réparation ainsi que les améliorations structurales réalisées dans le but de prolonger la durée de vie de cette autoroute.

ZUSAMMENFASSUNG

Einige Stahlbrücken der Tomei-Schnellstrasse erlitten verformungsinduzierte Ermüdungsrisse. In dieser Abhandlung werden die Eigenheiten solcher Risse, Spannungsmessungen, Reparaturmethoden sowie strukturelle Verbesserungen beschrieben, wie sie im Hinblick auf eine Lebensdauerverlängerung dieser Schnellstrasse durchgeführt wurden.



1. INTRODUCTION

The Tomei Expressway [National Expressway No. 1] is a vital arterial road running through the center of the economic activity belt of Japan extending from Tokyo to Nagoya to Osaka [Fig. 1]. The full length of this road was completed and opened to traffic in February 1969 and it has been in service now for approximately 20 years. From around 1980, fatigue damage began to be discovered in steel girders.

This report is on typical fatigue damage which have occurred on steel plate-girder bridges of the Tomei Expressway. The results of field investigations made concerning fatigue cracks produced in the cross bracing connection, studies of the causes of occurrence, and examination of retrofitting methods are reported. The facts that retrofitting work must be done while open to traffic as much as practicable because of the importance of this expressway with no alternative expressway available, and that the places requiring retrofitting comprise a huge number are features of this rehabilitation project.

2. OUTLINE OF BRIDGE STRUCTURES ON TOMEI EXPRESSWAY

There are 112 plate-girder bridges (composite and non-composite) on the part of the Tomei Expressway under the authority of the Tokyo First Operating Bureau of the Japan Highway Public Corporation. Of these, approximately 58 percent are quadruple-main-girder bridges, 37 percent are triple-main-girder bridges, and the remainder small numbers of quintuple-main-girder and sextuple-main-girder bridges. The spacings of main girders are 3400 mm for approximately 70 percent of the quadruple-main-girder bridges and 4000 mm for approximately 80 percent of the triple-main-girder bridges. These plate-girder bridges all have reinforced concrete deck slabs, the thicknesses of which are 180 to 200 mm for triple-main-girder bridges with 190 mm in the majority of cases, while for quadruple-main-girder bridges they are 170 to 190 mm with 170 mm making up the greater part. In all of the bridges damage began to occur in the reinforced concrete deck slabs four to five years after being put into service, and stringers for supporting deck slabs are being added starting in order from bridges in the poorest conditions.

Fig. 2 shows the transitions in the volume of traffic on the Tomei Expressway.

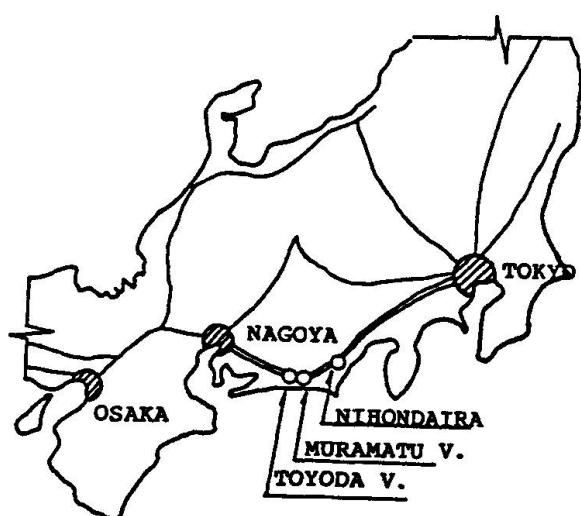


Fig. 1 Central Japan and Tomei Expressway

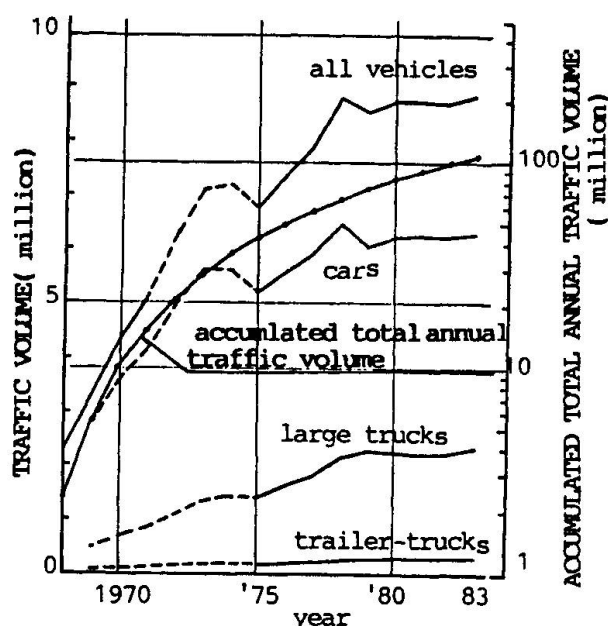


Fig. 2 Traffic Volume on Tomei Expressway

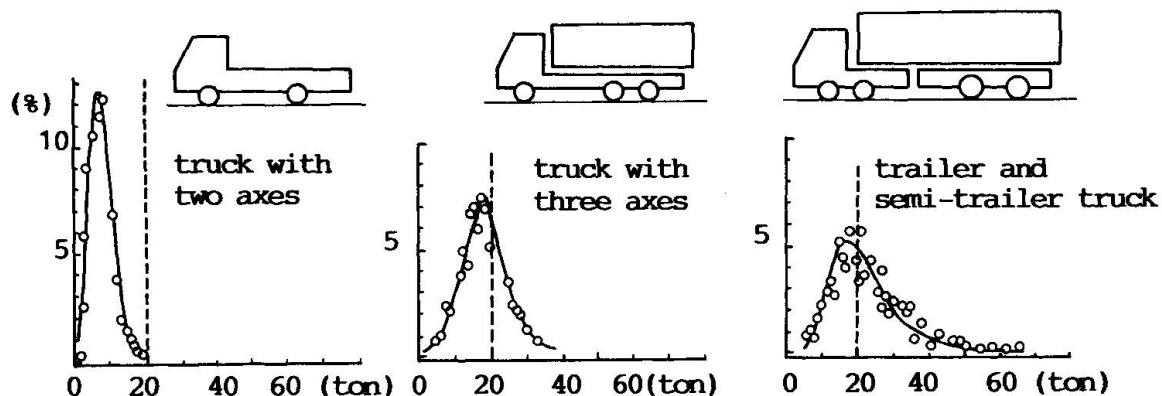


Fig. 3 Weight distributions of trucks measured at Nihondaira

The daily volume in one direction is approximately 50,000 vehicles, with about 30 percent being of large size. Scales are installed in the main traffic lanes at Nihon Daira of the Tomei Expressway. Fig.3 shows the truck weight distribution measured by these scales and it can be seen that substantial numbers of large-sized vehicles in overloaded condition are traveling on the expressway [1].

3. FATIGUE DAMAGE

Various investigations were made on two viaducts (Toyoda Viaduct and Muramatsu Viaduct) on the Tomei Expressway. The reasons for selecting these two viaducts were that they are a triple-main-girder bridge (Toyoda Viaduct) and a quadruple-main-girder bridge (Muramatsu Viaduct) which are types existing in large numbers on this expressway, they are bridges on which stringer additions were made at an early stage for strengthening the deck slab (Toyoda Viaduct) and on which additions are to be made hereafter (Muramatsu Viaduct), and they are comparatively close to Nihon Daira where vehicle weight measurements are being periodically made.

Fig. 4 shows the modes of fatigue cracks occurring at these parts and the respective identification marks given them. Vertical stiffeners are joined to top flanges and webs by fillet welds, and fatigue cracks have formed at various parts of these welds. Fatigue cracks have also formed at riveted joints for attaching cross bracing to vertical stiffeners and at cut-away portions of top flanges of top members of cross bracing.

Fig. 5 shows a part of the results of inspections on Toyoda Viaduct carried out in 1985, expressed as sums of the lengths of all fatigue cracks at various locations. The features of fatigue damage on this bridge are listed below.

- Cracks were formed at 200 locations out of the 240 locations in all excluding locations on bearing points.
- Type A cracks occurred at 198 out of the 200 locations and Type B cracks at 2 locations.
- Type C and Type D cracks occurred along with Type A and Type B cracks.
- Damage was more prominent the closer to the middle of a span and did not occur on a bearing.
- Of the three main girders damage was prominent at outer girders.

Approximately the same results were seen on Muramatsu Viaduct, but the following were tendencies differing from Toyoda Viaduct.

- Crack dimensions were comparatively small.
- Numerous Type A cracks were thought to have been initiated from the roots of fillet welds.

-

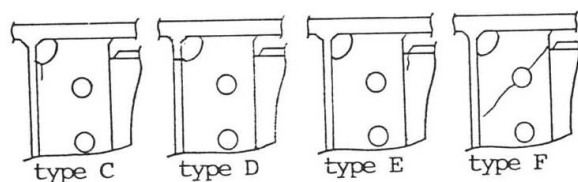
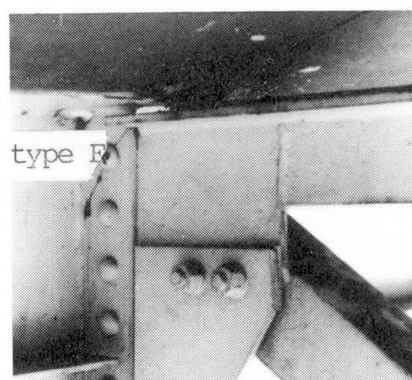
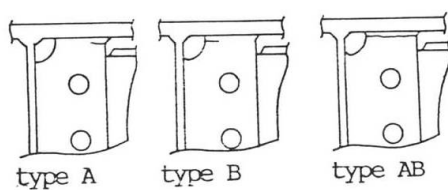
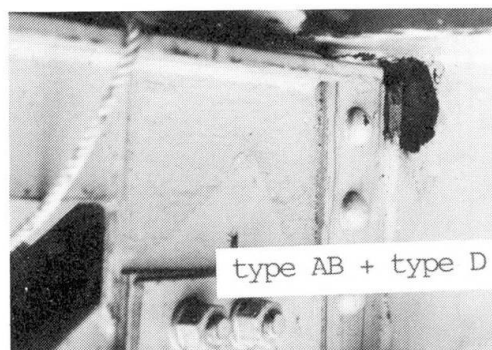


Figure 5 consists of several components illustrating inspection results on the Toyoda Viaduct in 1985:

- 3D Bar Chart:** A perspective view of the viaduct deck showing the sum of crack lengths (mm) at various locations. The locations are labeled L1, L2, L3, L4 along the length and P1, P2, P3, P4, P5, P6 across the width. A scale bar indicates 10mm.
- 2D Bar Charts:** Two bar charts showing the sum of crack lengths (mm) for the eastbound and westbound directions. The locations are labeled L1, L2, L3, L4. The y-axis for the eastbound chart ranges from 0 to 1500 mm, and for the westbound chart from 0 to 400 mm.
- Location Diagrams:**
 - A diagram showing the location of cross girders (a, b, c, c, b, a) and the location of cross girder (L1, L2, L3, L4).
 - A diagram showing the location of cross girder (L1, L2, L3, L4) and the location of cross girder (L1, L2, L3, L4).
- Orientation:** Arrows indicate the direction towards NAGOYA and TOKYO.

Fig. 5 Inspection results on Toyoda Viaduct,
sums of crack length(in 1985)

4. STRESS MEASUREMENT OF DAMAGED BRIDGES UNDER ACTUAL TRAFFIC LOAD

A series of field measurements on stress and deflection of actual bridges was carried out.

The measurements were made for the following two purposes:

(1) Purpose 1: To clarify structural characteristics

Load, deflection and stress are measured simultaneously and the relations between the loading conditions and stress responses at various details of the bridge structure are analyzed. This is important for investigating the causes of fatigue damage and finding the most suitable repair methods.

(2) Purpose 2: To obtain data for fatigue life estimation

Stress at the exact point concerned is continuously measured for certain period of time under ordinary service conditions. Direct evaluations are made on fatigue damage and remaining fatigue life by stress histogram analysis of the measured data.

One of the main features of the stress measurements in this study is that the on-site measurements of actual bridges in service were carried out without disturbing ordinary traffic flow. The measured items and locations for Toyoda Viaduct of Tomei Expressway are shown in Fig. 6.

For the Purpose 1 measurements, a newly developed automatic vehicle detector and computer controlled measuring system were utilized[2]. This system enables the simultaneous measurements of stresses and deflections in accordance with passing vehicle information such as passing time and lane, vehicle speed, length and interval.

Fig. 7 is an example of measured influence lines at various measuring points. The pattern of vehicle detector output indicates that these data were obtained when a truck passed through on the passing lane.

For the Purpose 2 measurements, an automatic stress histogram analyzer [histogram recorder] was utilized. Fig. 8 is an example of the output of stress histogram analysis. The same data were analyzed in two ways, by the level-crossing method and the rain-flow method. From the field stress measurements described here, it was found that the fatigue strengths of fillet welds between stiffeners and top flanges of cross bracing connections are not high enough for

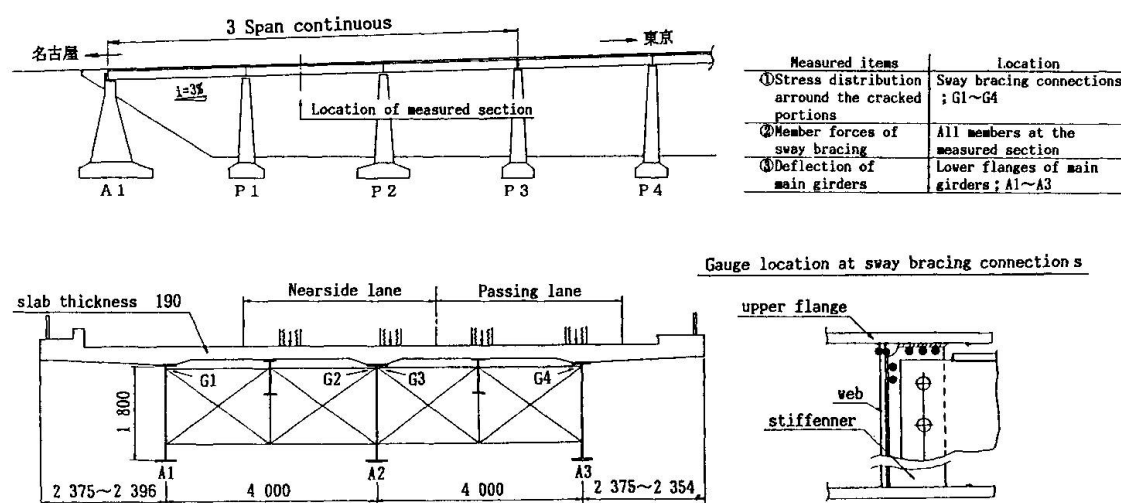


Fig. 6 Measuring plan for Toyoda Viaduct

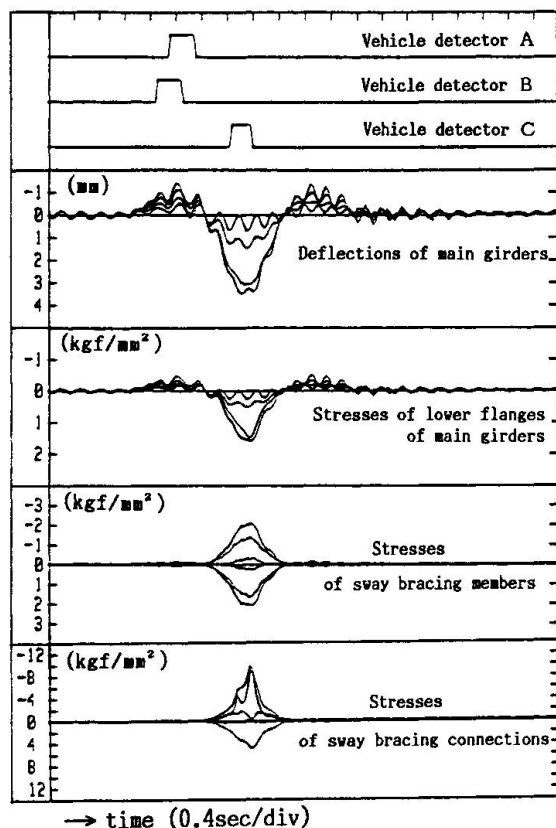


Fig. 7 Examples of measured influence lines

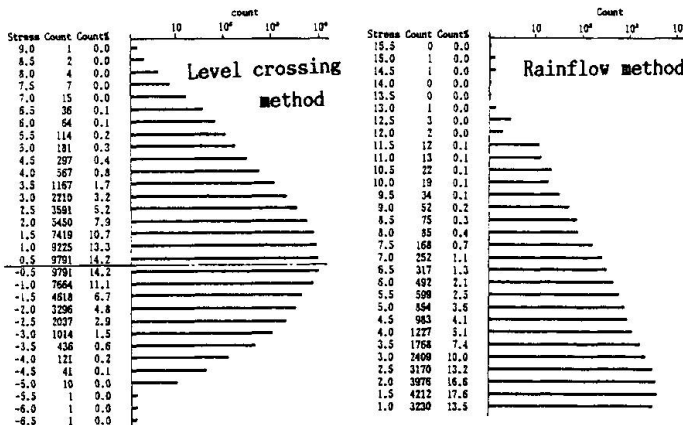


Fig. 8 Examples of Stress counting

the repeated stresses induced by relative vertical deflections between adjacent main girders and by deflections of concrete slabs.

5. RETROFITTING METHODS FOR FATIGUE CRACKS

Two kinds of retrofitting methods are conceivable for the prevention and repair of fatigue cracks:

- (1) Lowering stress occurring at a crack location.
- (2) Increasing fatigue strength of joint.

In this study, however, "increasing fatigue strength of joint" was taken for the first step, and increasing weld size and finishing toes with TIG dressing was proposed as one of the most suitable repair methods. The repairing effect was examined by fatigue tests and fatigue life analyses [3].

In the fatigue tests, three kinds of specimens were tested, AS-WELD, GRINDING and TIG specimens. The AS-WELD specimens were reproductions of fillet welds of the damaged portions. The GRINDING specimens are welded by full penetration welding and their weld toes were finished by grinder. The TIG specimens had an additional pass of fillet welding on top after welding in the same way as the AS-WELD specimens, and the toes were finished smooth by TIG dressing. Macro-etch-examinations of the welds are shown in Fig. 9.

Fatigue test results are shown in Fig. 10 with the design allowable S-N curves in the Design Standards for Steel Railway Bridges [4]. From Fig. 10, AS-WELD specimens results can be classified as Class D and it can be improved to be Class A by one pass of reinforcement welding and TIG dressing, or to be Class B by grinding. An approximate evaluation of the fatigue life remaining after repairs was made based on the fatigue test result and the actual load condition.

Considering the make-up ratio of vehicles, approximately 30 million large vehicles had passed in each direction during the 16 years from the time of opening in 1968 to 1983, when the damage was found. And 2.5 million large vehicles had passed in each direction annually during 1978 to 1983.

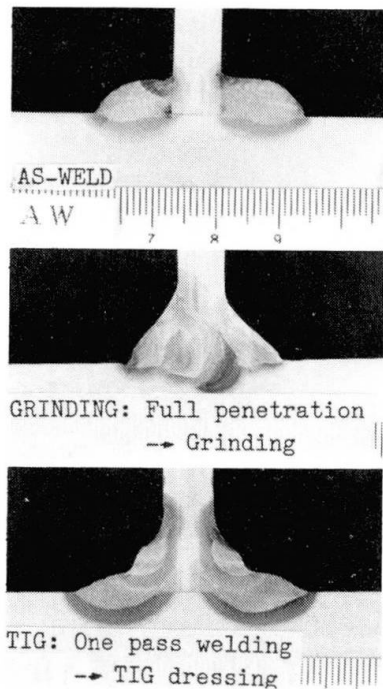


Fig. 9 Macro-Etch results of specimen

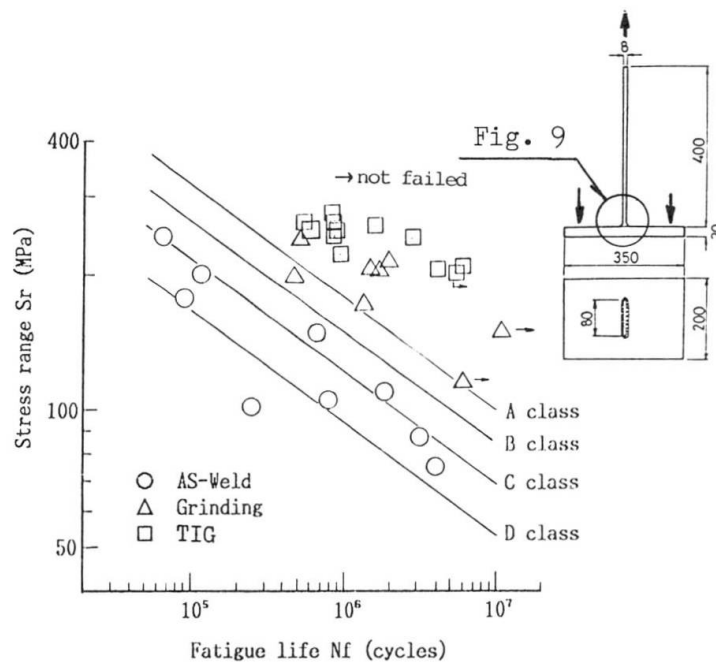


Fig. 10 Fatigue test results

When improvement has been done from Class D up to Class A, the remaining fatigue life will be

$$\left(\frac{15.3}{8.05} \right)^4 \times \frac{3 \times 10^7}{2.5 \times 10^6} = 157 \text{ years}$$

When improvement has been done from Class D up to Class B, the remaining fatigue life will be

$$\left(\frac{12.75}{8.05} \right)^4 \times \frac{3 \times 10^7}{2.5 \times 10^6} = 76 \text{ years}$$

where 15.3 kgf/mm², 12.75 kgf/mm², and 8.05 kgf/mm² are allowable stress range for Class A, B and D respectively.

The abovementioned evaluation shows that ample remaining fatigue life can be obtained by the repair method proposed here.

6. ANALYTICAL INVESTIGATIONS ON THE EFFECTS OF STRUCTURAL CHANGES AND CONSIDERATIONS FOR STRUCTURAL IMPROVEMENTS

The influences of structural changes aiming to prevent occurrence or growth of slab cracking on fatigue damage of transverse stiffeners are studied through numerical analyses.

The following countermeasures for the fatigue damage of transverse stiffeners may also be considered such as: introduction of floor beams with high stiffness at span centers in order to achieve more effective transverse load distribution together with the elimination of all or a part of cross bracing members, which are considered to be the sources of the fatigue damage; or conversely, addition of cross bracings between existing ones in order to reduce maximum member forces in cross bracings. The effects of these measures are also analytically examined.

6.1 Analytical Model [5]

The entire bridge under consideration is modeled as a stiffened plate, as shown in Fig. 11, where reinforced concrete floor slabs are modeled by thin plate



elements, main girders by offset beam elements, and cross bracings by cross bracing elements, which can be obtained through the contraction of stiffness matrices describing the cross bracings as plane frame structures. In cases where lateral bracings exist, lateral bracing elements are similarly introduced.

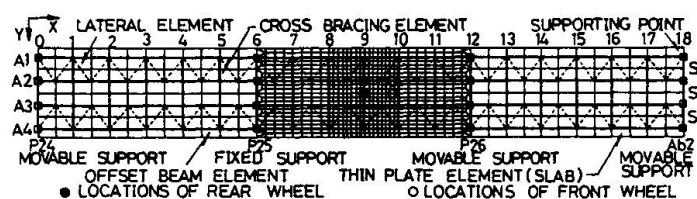


Fig. 11 Modelling of the whole bridge superstructure

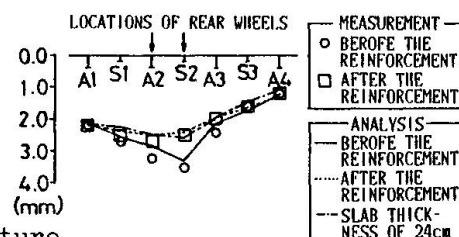


Fig. 12 Comparison of concrete slab deflections

6.2 Influences of Additional Stringers with Cross Bracing Reinforcement

Here, the object of analysis is the Muramatsu Viaduct with four main girders. The moments of inertia of supplemented stringers are about one-tenth of main girders. Additional diagonals and reinforcement of lower struts are provided for cross bracings. The element mesh division diagram for this object of analysis is illustrated in Fig. 11. The Ai in the diagram indicates the number of the main girder, the numerals the numbers of cross bracings, Pij and Ab2 the numbers of piers and abutment, respectively.

The load applied are rear wheels of T-20 load as specified in the Japanese Highway Bridge Specifications [6] (each 8 tf (78.4 kN)) totaling 16 tf (156.8 kN) on the cross bracing location at the center of the middle span (the location indicated by dark circle marks in the diagram; hereafter called "center section") and front wheels (each 2 tf (19.6 kN)) totaling 4 tf (39.2 kN) at locations of the circle marks in the diagram.

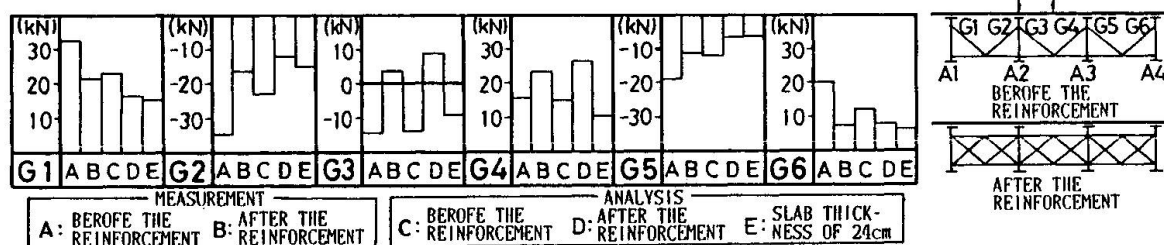


Fig. 13 Comparison of axial force in diagonal members of a cross bracing

The floor slab deflections and axial forces of diagonals in cross bracings at the center section before and after reinforcing are given in Figs. 12 and 13, respectively. Measured values are also given therein. The ratios of axial forces of cross bracing members before and after reinforcing for measured and analytical values are very close to each other. Floor slab deflection is reduced on the whole by the reinforcement, and it can be seen that the original purpose of this slab reinforcement is achieved. However, although the axial forces of diagonals of cross bracings are reduced 30 to 50 percent in almost all diagonals, at the diagonal G4 the axial force increases by about 80 percent and an axial force (2.68 tf (26.3 kN)) greater than the maximum axial force (2.38 tf (23.3 kN)) before reinforcing is produced. This tendency was observed in .lh12 measurements also.

6.3 Influence of Floor Slab Thickness on Forces in Cross Bracing Members

Since cracking damage occurred frequently in slabs of thickness 17 cm made based on the standard design up to the latter half of the 1960s, the specifications were subsequently revised and since 1978 a slab thickness of 24 cm has been adopted.

The results of analyses based on the current specification as for slab thickness are also illustrated in Figs. 12 and 13.

It may be understood from this that slab thickness of 24 cm which coincides with the current specification and aforementioned reinforcing by addition of stringers and cross bracing reinforcement as measures for reinforcing existing bridges have effects that are roughly equal from the point of view of reducing deflection of floor slabs. But it may be judged that increasing floor slab thickness is more effective in the sense that it reduces forces in cross bracing members on the whole, although this procedure may not necessarily be applicable to all existing bridges.

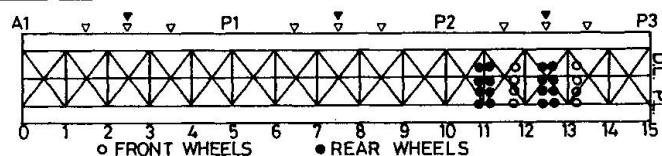
6.4 Effects of Introduction of Cross Beams and Additional Cross Bracings

Toyoda Viaduct with three main girders is concerned here. Calculated cases of structural changes and the results are illustrated in Table 1 and Figs. 14 and 15, respectively. Loading conditions are similar to the ones described previously, but here, the subject of the study is a side span instead of the main span.

Table 1 Considered structural changes and loading conditions

CASE	LOCATION OF REAR WHEELS	SUPPLEMENTED MEMBER			LOCATION	REMOVAL OF CROSS-BRACING MEMBER
		FORM	NUMBER PER SPAN	BENDING STIFFNESS*		
F/G	11/SPAN CENTER	CROSS BEAM	1	1/4	SPAN CENTER	NONE
H/I	11/SPAN CENTER	CROSS BEAM	1	1/4	SPAN CENTER	NONE
J/K	11/SPAN CENTER	CROSS BRACING	1	1/8	SPAN CENTER	NONE
L/M	11/SPAN CENTER	CROSS BRACING	3	1/8	**	NONE
N/O	11/SPAN CENTER	CROSS BEAM	1	1/4	SPAN CENTER	***

* RATIO WITH THAT OF A MAIN GIRDER
 ** INDICATED BY IN THE FIGURE AT BOTTOM
 *** THOSE MEMBERS AS SHOWN IN Fig.14 BY DOTTED LINE



The results can be summarized as in the following subsections:

6.4.1. Effects of additional cross beams or cross bracings on member forces of existing cross bracings

When rear wheels are placed on the center of a side span, induced member forces in the cross bracings at locations 12 and 13 adjacent to the span-center are reduced 40 to 50 percent for the case where cross beams, whose bending stiffness are about one-fourth of the main girders, are introduced at the center of each span. For the cases where one and three-per-span additional cross bracings having equivalent bending stiffness of one-eighth of main girders are introduced, reductions of member forces in the same cross bracings at locations 12 and 13 are 20 to 30 percent and 30 to 40 percent, respectively.

6.4.2 Effects of removal of cross bracing members on remaining cross bracing member forces

When the load is applied at the span center, the largest member force existing at location 13 is reduced by the removal from 2.5 tf (24.5 kN) to 1 to 2 tf (9.8 to 19.6 kN) according to the lane loaded. When the load is applied at location 11, on the other hand, the largest member force existing at location 11 is further increased by several percent, if the removals have taken place.

6.4.3 Effects of additional cross beams or cross bracings and removal of cross bracing members on floor slab deflections

For any of the previously-mentioned cases deflection of the floor slab at the loaded location does not show considerable change from the present situation.

Considering the effects both on member forces and floor slab deflections, the method of adding three-per-span cross bracings may be the best one among the



methods listed here, for the purpose of countering fatigue of girder-cross bracing connections.

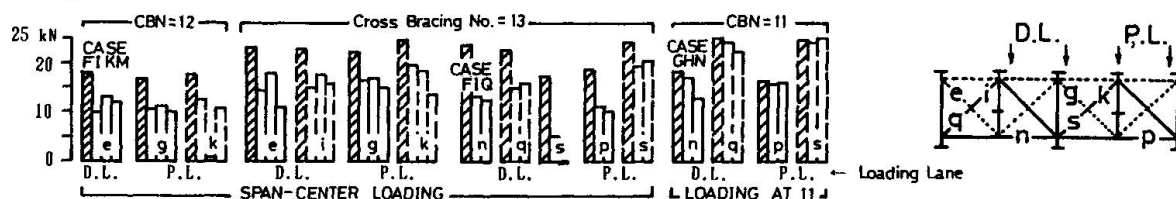


Fig. 14 Effects of structural changes on axial forces in bracing members

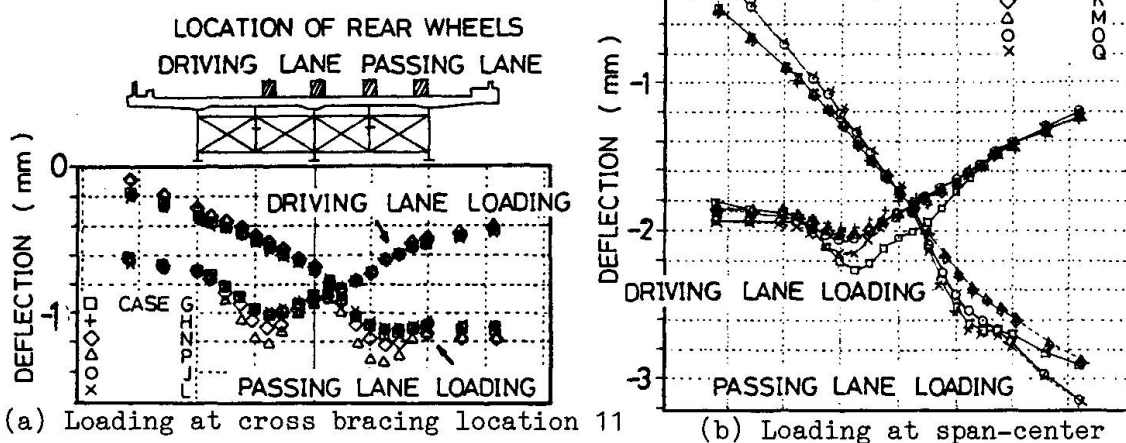


Fig. 15 Effects of structural changes on floor slab deflections

7. CURRENT STUDY ON LIFE EXTENSION PROGRAMS

Based on the results of this study, a repair manual for the fatigue cracks in cross bracing connections has been prepared by the Japan Highway Public Corporation, and it is now beginning to be used. At the same time, the following two main items are being studied concerning the repair manual.

- (1) Education and training for proper use of the repairing manual
- (2) Long-term observations of repaired portions

Various studies for life extension of highway bridges are being conducted at Toyoda Viaduct, where damage were first reported and stress measurements described in this report were carried out. Presently, experimental works of thickness incrementation on top of reinforced concrete slab and adding cross bracings to the present framework are being done and stress measurements to investigate the effects of these works are being performed.

REFERENCES

1. MIKI C., et al, Computer Simulation Studies on the Fatigue Load and Fatigue Design of Highway Bridge. St. Eng./EQ Eng., JSCE, Vol.2, No.1, 1985-4.
2. TAKENOUCHI H., et al, Stress Measurement of Highway Bridges under Actual Traffic Load. St. Eng., JSCE, Vol.32A, 1986-3, (in Japanese).
3. MIKI C., et al, Repair of Fatigue Damage in Cross Bracing Connections in Steel Girder Bridges. St. Eng./EQ Eng., JSCE, Vol.6, No.1, 1989-4.
4. JSCE, The Design Specifications for Steel Railway Bridges. 1974.
5. MASUDA N., et al, Analyses of Sway Bracing Members in Composite-girder Bridges. St. Eng./EQ Eng., JSCE, Vol.4, No.2, 1987-10.
6. Japan Road Association, Specification for Highway Bridges. 1980-2.

Crack Control: Decision Making Aided by Knowledge Processing Technology

Aide à la décision grâce aux systèmes de traitement de la connaissance

Entscheidungsfindung unterstützt durch Datenverarbeitungssysteme

Ian F.C. SMITH

Research Associate
Swiss Fed. Inst. of Tech.
Lausanne, Switzerland



Dr. Smith received engineering degrees from Cambridge University, U.K. and the University of Waterloo, Canada. Over the past fifteen years, he has worked in research, design and construction in several countries. Presently at ICOM, he is performing research into engineering applications of knowledge processing technology and fatigue of metal structures.

SUMMARY

Issues associated with remaining fatigue life are well suited to applications of knowledge processing technology since critical information can be badly organized and poorly distributed. This paper describes a small system called CRACK CONTROL developed in order to help engineers make decisions when a crack is discovered in a steel structure. Incomplete and inexact information is accommodated through approximately sixty questions asked by the system during a typical session. The system helps determine the causes of cracking and then provides recommendations for action – including proposals for subsequent management of the structure. This system could serve as one module in a set of decision aids which are made available to engineers and maintenance staff.

RÉSUMÉ

Les conclusions relatives à la durée de vie restante s'appliquent bien aux techniques de traitement de la connaissance, parce que l'information nécessaire est mal structurée et encore peu répartie. Cet article traite d'un système appelé CRACK CONTROL développé dans le but d'aider les ingénieurs à prendre des décisions quand une fissure est découverte dans une structure en acier. L'information, incomplète et inexacte, est acceptée par une soixantaine de questions qui sont posées par le système pendant une session. Le système aide à déterminer les causes de la fissuration et propose des recommandations – y compris des propositions quant à la gestion de l'ouvrage. Ce système pourrait servir de module dans un ensemble d'aides à la décision qui seraient disponibles aux ingénieurs et aux responsables de la maintenance.

ZUSAMMENFASSUNG

Da Informationen zu Fragen der Restlebensdauer bestehender Bauwerke nur schwer erhältlich sind, ist die Anwendung von Datenverarbeitungssystemen für diesen Problemkreis besonders geeignet. Der vorliegende Artikel beschreibt ein System namens CRACK CONTROL, welches Ingenieuren helfen soll Entscheidungen zu treffen, falls in einer Stahlkonstruktion Risse entdeckt werden. Unvollständige und ungenaue Informationen werden mit Hilfe von etwa sechzig Fragen, die durch das System an den Benutzer gerichtet werden, ergänzt. Das System hilft die Ursachen zu bestimmen, die zu einem Riss geführt haben, und liefert Empfehlungen für Gegenmassnahmen und Vorschläge für den Unterhalt der Konstruktion. Es ist ein Hilfsmittel, das Ingenieuren und Unterhaltspersonal zur Entscheidungsfindung dient.



1. INTRODUCTION

Determination of remaining fatigue life is complex. Although more work is needed to obtain new information and to develop better models, an additional effort - taking advantage of existing knowledge - is justified. Currently, much relevant information is concentrated among a small group of experts. For the most part, written knowledge is available through scattered comments within documents devoted primarily to other themes. As the average age of structures increases, the need for understandable, organized and widely distributed knowledge grows.

Applications of knowledge-processing (expert system) technology are developed in order to improve representation and distribution of knowledge. Operating systems, especially those assisting diagnostic tasks, in other fields have been successful. For example, a system in the car manufacturing industry is credited with saving one company over ten million dollars each year [1].

Civil engineers have been slow to accept such new possibilities. This is understandable since civil engineering is a fragmented and necessarily conservative field where new techniques are not embraced blindly. Also, practical applications have necessitated processing speeds and memory requirements that were possible only using machines and software which are not compatible with the activities of civil engineers.

Recently, this situation has changed. Improvements in personal-computer capacity and less expensive software has created a situation where sufficient speed and memory is available in small offices and on site at reasonable cost. As a result, civil-engineering interest in this technology is growing, for example see [2-5]. Tasks associated with remaining fatigue life of steel structures stand to benefit from such trends, especially since such activities involve problem solving procedures akin to diagnosis.

This paper examines the potential of knowledge systems for remaining fatigue life and presents a system called CRACK CONTROL - created in order to help engineers make decisions when a crack is discovered in a steel structure. Representation, implementation and verification aspects are discussed. Finally, the development of a large system for activities related to managing structures in service is explored.

2. KNOWLEDGE SYSTEMS FOR REMAINING FATIGUE LIFE

It is of interest to examine the difference between knowledge development and knowledge management within the context of remaining fatigue life. Knowledge development includes activities such as analysis, modelling, parametric studies, laboratory testing and site measurements. Knowledge development generates new facts and identifies causal relationships. On the other hand, knowledge management concentrates on improving the way existing knowledge is used. Elements of knowledge management include acquisition, organization or representation, knowledge distribution, default knowledge and revision. A summary of these elements is given in Table 1.

TABLE 1 Difference between knowledge development and knowledge management

IMPORTANT ELEMENTS OF	
KNOWLEDGE DEVELOPMENT	KNOWLEDGE MANAGEMENT
Analysis	Acquisition
Modelling	Organization
Parametric studies	Distribution
Laboratory testing	Defaults
Site measurements	Revision
...	...

For example, load modelling, dynamic analyses, corrosion studies, crack growth measurements, fracture mechanics analyses, fracture and fatigue testing, field measurements, numerical simulation, development of crack detection technology, and life improvement studies are knowledge-development activities. Assimilation of new research, code writing, record keeping, communication, co-ordination, planning, knowledge structuring, updating and learning are concerned with knowledge management.

In a recent study of over 600 structural failures in the United States from 1975 to 1986, a large majority of cases could be attributed to poor knowledge management [6]. Cases of lack of fundamental knowledge, classified as "unknown situations", made up only one third of all failures. This is probably an over-estimate of failures caused by a lack of fundamental knowledge since the term "unknown situations" was not defined and consequently, it is conceivable that other factors such as inadequate records had some influence. Similar studies have reached the same conclusions, for example [7] [8].

Therefore, improvements in knowledge management may have a greater impact on structural engineering than additional knowledge development. In addition, explicit organization of knowledge may identify previously un-noticed shortcomings in existing knowledge and thus initiate useful research [9]. Another advantage of explicit knowledge representation is that it is more resistant to what is termed "knowledge erosion" due to transfers, retirements and resignations of personnel.

Many opportunities for creating knowledge-processing systems exist, and work in progress, for example [2][10] represents a small proportion of possible systems. For any development effort, a prerequisite for good solutions is a complete definition of the problem. Often, the original definition is inaccurate because relevant knowledge and user needs were not defined accurately. Therefore, an attempt should be made to develop a small prototype as soon as possible in order to begin testing the system at an early stage. An example of such a system is presented next.

3. A CRACK IN A STEEL STRUCTURE

A system called CRACK CONTROL was developed to help engineers decide what to do if a crack is discovered in a steel structure. Intuitive repair solutions such as filling the crack with weld metal may not be effective. Good decisions require a combination of scientific knowledge and experience gained through examining cracks in structures. Generally, if a crack is found in a steel structure, more careful inspection will reveal additional cracks in similar elements. If no action is taken to eliminate the cause of cracking, more cracks usually appear at other locations. These heuristics have an influence upon the knowledge structure described below.

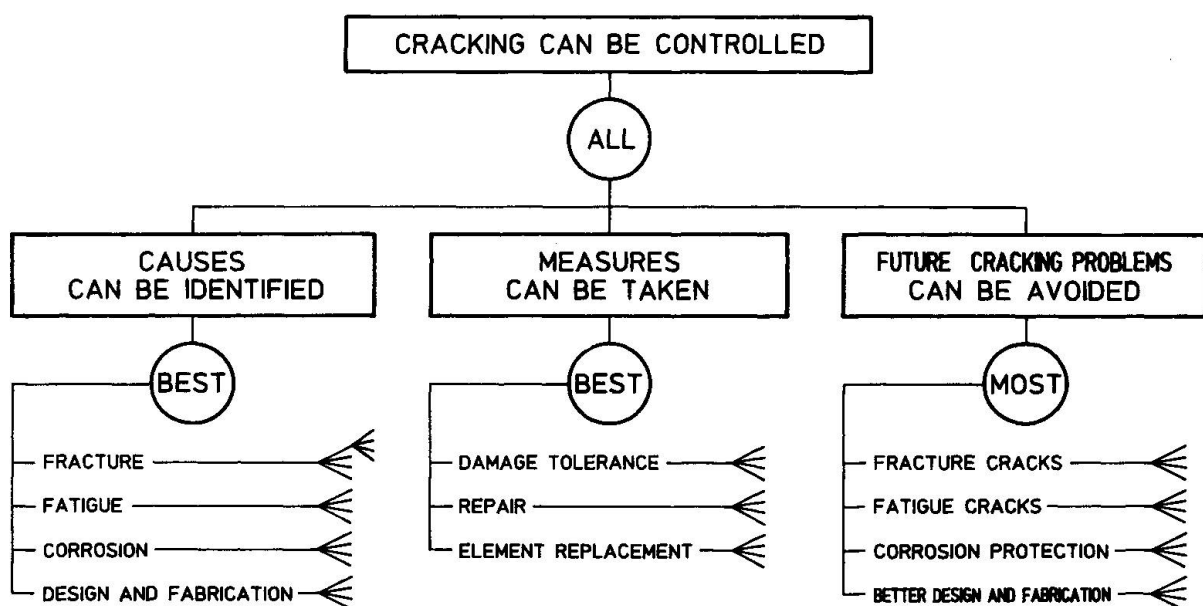


FIGURE 1 Partial inference net of CRACK CONTROL



The knowledge necessary to solve this problem is split into three parts, as shown in Figure 1. The first part concentrates on parameters which cause cracks in steel structures and thus, it contains the majority of the diagnostic knowledge in the system. This knowledge is split into categories which reflect the origins of cracking. Cracking may be due to fracture, fatigue, corrosion or design and fabrication practices, or most often, a combination of these factors.

The second part of the knowledge focuses on the most appropriate action, given a cracked element. Measures to be taken are subdivided into damage tolerance, repair and element replacement. Damage tolerance involves no immediate repair but an increased inspection effort. This solution is only explored under certain conditions since it is not appropriate if, for example, further crack growth could cause catastrophic collapse. Repair measures are dependent upon the causes determined in the first part. Element replacement is a valid measure when damage tolerance and repair are not practicable.

The third part of the knowledge concentrates on identifying a maintenance strategy for the rest of the structure. Once cracking has been discovered in a steel structure, the maintenance effort needs to be modified since more cracking is likely. While these considerations do not depend greatly upon the measures chosen for the cracked element, they are closely linked to the causes determined in the first part. Also, several general precautions are needed regardless of the cause of cracking.

This knowledge was implemented rapidly into a small system using a development tool specifically designed for diagnostic applications - THE DECIDING FACTOR (TDF) [11]. This tool was developed using experience gained during the PROSPECTOR project [12] and it has already been employed for diagnostic applications in civil engineering, e.g. [13].

Rather than require direct input of production rules, TDF processes knowledge organized in inference nets, see, for example, Figure 1. The user expresses opinions related to ideas low down on the net. These opinions are transferred into a belief value and multiplied by a factor to contribute to the hypothesis represented as the parent of a set of ideas. In turn, sub-hypotheses contribute to hypotheses further up on the net. Belief values are combined using special logical relationships provided by TDF. In Figure 1, ALL, BEST and MOST are three of eight possible relationships. ALL and MOST pass weighted averages of belief values, whereas BEST passes the highest belief value. Thus, BEST is analogous to OR logic. The system, CRACK CONTROL, employs six relationships in all.

One of the strong points of TDF is the user interface, see Figure 2. Typically, a question screen is composed of an introductory explanation, a question, an answer box and a scale of possible answers. The user manipulates the cursor in order to adjust his answer. A definite reply of yes or no is not needed.

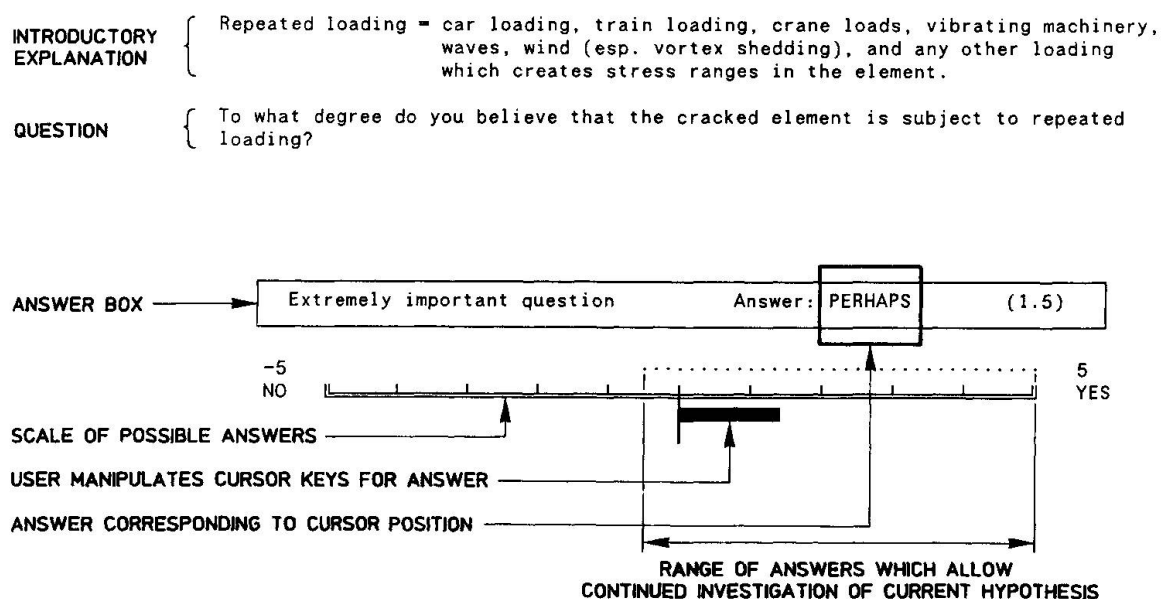


FIGURE 2 CRACK CONTROL User interface

Intermediate answers such as MAYBE SO and THINK NOT are possible. The middle of the scale is the reply, DON'T KNOW. This feature is very useful for applications to structures in service since information is rarely complete and never certain. This interface has been well accepted by users during tests.

Questioning proceeds from left to right in the inference net (Figure 1). It is possible to fix a range of answers, thereby allowing continued investigation of the ideas which contribute to the current hypothesis. If the user replies outside this range, questioning relating to the current hypothesis is terminated, and the system goes on to the next part of the net. For example if damage tolerance was the current hypothesis and the user had any doubt whether further cracking would lead to catastrophic failure, the system would not pursue this possibility further. Therefore, questions which would have followed, relating to the safety and economy of a damage tolerance philosophy, would not be asked, and repair would be investigated.

A final step in the system involves a review of the recommendations provided for the particular case. Note that heuristic information is used only to identify the most appropriate recommendations. Once these are identified, the user is asked to what extent he believes that the recommendations can be carried out. This belief determines which recommendations are reviewed and ultimately used by the system to evaluate the hypothesis that cracking can be controlled. Note that this system performs no calculations; the focus is placed entirely on prior qualitative reasoning.

Due to the ease of development, a working prototype was ready for testing two weeks after development began. Many changes were introduced after initial tests. Indeed, it was discovered that the problem was not completely defined from the start. Some measures for dealing with cracked structures were overlooked. Users employ a different language than experts and sometimes prefer that questions are raised in a different order. A small system developed rapidly using a simple tool created a situation where these differences were identified as quickly as possible.

4. LARGE SYSTEMS FOR MANAGEMENT OF STRUCTURES IN SERVICE

Activities associated with the management of structures in service are shown in Figure 3. Over their lifetimes, structures are subjected to monitoring, evaluation, maintenance and perhaps, modification. All of these activities could benefit from better organized and more widely distributed knowledge.

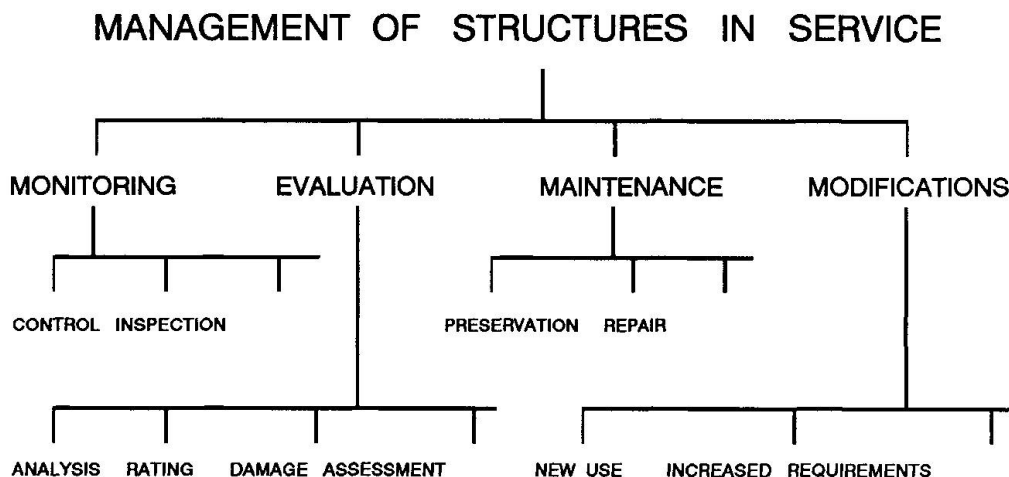


FIGURE 3 Activities associated with management of structures in service

Each activity in Figure 3 requires diagnostic or classification procedures to be most effective. These procedures are important for identifying good solutions and areas where more information would be most helpful. Nevertheless, a distinct focus is required for each activity since the user wishes to proceed differently for each case. Therefore, each activity has a unique set of rules which make up and control the methods employed during solution formulation. However, much of the information used by these methods



is similar. Also, solutions implemented during different activities can affect each other. Common information requirements and possible interaction can be well accommodated by an integrated system. A proposal for such a system is presented next.

Small systems developed rapidly for testing help to ensure that effort is not wasted solving the wrong problem. Knowledge is verified at an early stage and the requirements of the user become well defined. However, as the size of the problem grows, the number of assertions increases rapidly. Interaction between these assertions becomes difficult to manage and verification of all possible solutions is increasingly arduous. Well organized knowledge becomes essential.

Models and more abstract reasoning provide effective ways to organize knowledge. Generally, two types of models could be used to simulate structures in service. The first type is a mathematical description of the behaviour of the structure. Examples of models of this type include structural-analysis algorithms, fracture-mechanics simulations and fatigue-damage-accumulation techniques.

The second type is a representation where the design and function of the structure is described. Figure 4 gives an outline of such a model of a structure. In this figure, actions, such as gravity loads and wind, act on the structure. The structure is described in terms of the material employed, elements and their connections to each other, details at connections and attachments, built-in stresses, etc. The structure acts on the foundations, which for the purposes of this outline, include surrounding soil and geological properties. External factors, such as salt-water exposure, atmospheric pollution and changing ground-water levels also act on the structure and foundations. Also, changes in the behaviour of the foundations over time may in turn affect the behaviour of the structure.

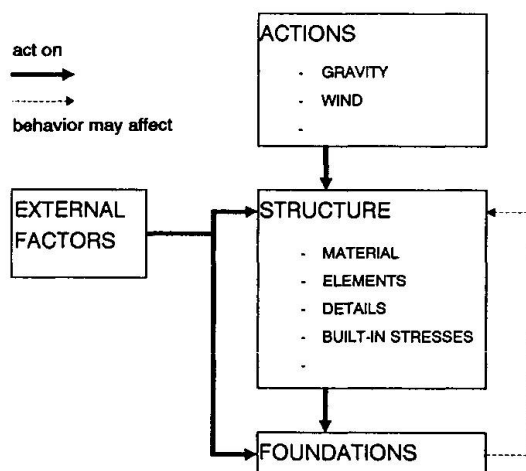


FIGURE 4 An outline of a functional model of a structure

Recent work in artificial intelligence has examined the advantages of domain-independent reasoning for diagnostic activities, e.g. [14]. Using models such as the one outlined in Figure 4, domain-independent theories provide methods for diagnosis from first principles. Given a state which is observed to be outside the limits of expected behaviour, models can help identify the origin of faults. They provide a means of representing knowledge for large quantities of information and complicated relationships. Therefore, models are important to the future of large diagnostic systems [15].

A further advantage of models is that they are useful for a range of activities. For example, the model in Figure 4 could be employed for many of the activities shown in Figure 3. On the other hand, systems using only heuristic pattern matching are typically constructed to do a specific task.

However, first-principle models [14] are not useful for many types of practical problems. An exact model of the system is required, and uncertain information cannot be treated. As the number of possible faults increases, computation time rises exponentially. If multiple faults are considered, models are especially

sensitive to problem size. Therefore, first-principle diagnostic models are most useful for medium sized "closed-world" problems such as small electrical circuits.

Problems associated with structures in service are very different from small electrical circuits. Important information may have a high degree of uncertainty. Relationships between objects may be poorly defined. A structure may have thousands of elements and details, and tens of load cases. In addition, critical measurements may be very difficult to carry out and external factors may include social and political considerations. These factors mean that structures in service have "open-world" characteristics.

Research into artificial intelligence has developed new techniques which are very useful for representing activities associated with structures in service. For example, specialized strategies used with inexact models may help reduce the difficulties associated with existing structures. Rather than attempting to construct complete models, inexact models contain only knowledge relevant to a group of activities [16]. Other developments in non-monotonic reasoning and machine learning have created many opportunities for applications involving ill-defined problems such as those typical of structures in service. These techniques are often implemented within a system which employs various reasoning methods.

A hybrid approach for activities associated with structures in service is proposed. The user would start the system by providing information which identifies modules that are appropriate to the problem. The majority of these modules would be activity-dependent. However, some modules, such as those used to estimate behaviour, would be used for several activities. For example, modules such as CRACK CONTROL would be chosen from a library of available small systems. At this point, the system would carry out reasoning using heuristic knowledge which is independent of the structure in question.

The findings of the system would then be assessed by the user. If an acceptable solution was identified, the system would not invoke methods of more abstract reasoning. This step is comparable to traditional engineering methods since engineers typically employ more sophisticated methods when acceptable solutions are unavailable through simpler approaches. Also, if models of the structure do not exist, this step enables the advantages of model creation to be assessed. The complexity of some structures in service could require a substantial investment in order to produce useful models.

If an acceptable solution is not identified, the system would envoke reasoning using structure-dependent models and more abstract heuristics. For example, if a crack is discovered in a steel structure, reasoning could help identify candidate causes of the cracking by backtracking and examining all factors which affect the element. Optimal locations for additional measurements could be identified and when new information is received, the candidate list would be updated. Most likely causes, learned from previous experience with this structure and others like it, could be placed in default slots; reasoning with such information would proceed until evidence disqualified the assumption. Similar procedures could be employed for identifying other areas at risk in the structure and for evaluation of repairs. As stated already, new research in artificial intelligence has created conditions where these capabilities are applicable to activities associated with structures in service.

The models used would be independent of activities such as those in Figure 3. In this way, information would be shared as required by the particular task. However, many heuristics would be activity dependent, especially those which control how the model is examined. Also, information obtained in the structure-independent reasoning stage would be used for pruning search.

CONCLUSIONS

1. Improvements in knowledge management through applications of knowledge-processing technology could have an important impact on decisions relating to remaining fatigue life. New and current work should improve capabilities to manage knowledge, thereby reducing costly repairs and unnecessary replacement of steel structures.
2. Since the factors which influence existing structures are complex, it is essential that knowledge-base development begins with a rapidly developed prototype for testing with the expert and the user.



3. Models help organize the knowledge necessary for large diagnostic systems. However, for problems encountered by structures in service, a purely model-based system, controlled by domain-independent heuristics, is not appropriate.
4. A hybrid system which combines heuristic reasoning with model-based reasoning is a feasible and effective approach for structures in service.

ACKNOWLEDGEMENTS

Research at ICOM in the area of knowledge processing is funded by the Swiss National Science Foundation. Also, the staff at ICOM are thanked for their help in the preparation of this document.

REFERENCES

- [1] Bajpai, A. and Marczewski, R. "CHARLEY : An expert system for diagnostics of manufacturing equipment" Innovative Applications of Artificial Intelligence, AAAI, 1989, p. 178-185.
- [2] Chen S.S., Wilson, J.L. and Mikroudis, G.K. "Knowledge-based expert systems in civil engineering at Lehigh University" ATLSS Report No. 87-01, Lehigh University, 1987.
- [3] "Expert systems in civil engineering" Proceedings ASCE, 1986.
- [4] Maher, M.L. ed. "Expert systems for civil engineers" TCCP, ASCE, 1987.
- [5] "Expert systems in civil engineering" IABSE Reports, Vol 58, Zurich, 1989.
- [6] Ayyub, B.M. and Eldukair, Z.A. "Statistical analysis of recent United States construction failures" Symposium on reliability-based design in civil engineering, EPFL, Lausanne, 1988.
- [7] Matousek, M. and Schneider, J. "Untersuchungen zur Struktur des Sicherheitsproblems bei Bauwerken" ETH-Zurich, 1976.
- [8] Pfang, E.O. et al "Building structural failures - Their cause and prevention" IABSE Surveys S-35/86, Zurich, 1986.
- [9] Fisher, J.W. Private communication, 1988.
- [10] Roddis, W.M.K., and Connor, J. "Qualitative/quantitative reasoning for fatigue and fracture in bridges" Coupling symbolic and numerical computing in expert systems, North Holland, Amsterdam, 1988, p. 249-257.
- [11] Campbell, A.N. and Fitzgerrell, S.T. "The Deciding Factor" User's Manual, Channelmark Corp. 1985.
- [12] Campbell, A.N., Hollister, V.F., Duda, R.O. and Hart, P.E. "Recognition of a hidden mineral deposit by an artificial intelligence program" Science, 217, 1982.
- [13] Levitt, R.E. "Howsafe : A microcomputer-based expert system to evaluate the safety of a construction firm" (in [3], p. 55-66).
- [14] Reiter, R. "A theory of diagnosis from first principles" Artificial Intelligence, 32, 1987, p. 57-95.
- [15] Milne, R. "Strategies for diagnosis" IEEE Transactions on systems, man and cybernetics, 17, 1987, p. 333-339.
- [16] Reed, N.E., Stuck, E.R. and Moen, J.B. "Specialized strategies : An alternative to first principles in diagnostic problem solving" Proceedings of AAAI-88, St. Paul MN, 1988, p. 364-368.